CERN–2012–004
24 May 2012

ORGANISATION EUROPÉENNE POUR LA RECHERCHE NUCLÉAIRE
CERN EUROPEAN ORGANIZATION FOR NUCLEAR RESEARCH

40th Anniversary of the First Proton-Proton Collisions in the CERN Intersecting Storage Rings (ISR)

Authors: U. Amaldi
P. J. Bryant
P. Darriulat
K. Hübner

GENEVA
2012

ISBN 978–92–9083–375–8
ISSN 0007–8328

This report should be cited as:

40th Anniversary of the First Proton-Proton Collisions in the CERN Intersecting Storage Rings (ISR)
U. Amaldi, P. J. Bryant, P. Darriulat and K. Hübner, CERN-2012-004 (CERN, Geneva, 2012)

A contribution in this report should be cited as:

[Author name(s)], in Report of the 40th Anniversary of the First Proton-Proton Collisions in the CERN Intersecting Storage Rings (ISR), U. Amaldi, P. J. Bryant, P. Darriulat and K. Hübner, CERN–2012–004 (CERN, Geneva, 2012), pp. [first page]–[last page]

Foreword

The Intersecting Storage Rings (ISR) was the world's first proton collider and formed a bridge between the fixed-target experiments at the relatively low energies prior to the 1970s and the high-energy frontier at the colliders of today. The machine, which worked with protons, deuterons, alpha particles and anti-protons, was at the forefront of technology in many fields and catalysed a rapid advance in accelerator technologies and techniques, including vacuum systems, precision power converters, superconducting quadrupoles, and especially the renowned stochastic cooling. These developments have resulted in the ISR having had a profound legacy to its successor machines – the Super Proton Synchrotron, the first proton-antiproton collider, and the LHC, CERN's current flagship accelerator at the forefront of particle physics research at the highest energies.

Moreover, owing to the challenges posed by the environment of the proton collisions for the physics under study, there were also many developments for particle detector techniques at the ISR. In particular, the use of 'Roman pots' for the positioning of detectors close to the circulating beams was demonstrated, as was the widespread use of multi-wire proportional chambers, cylindrical drift chambers and the use of liquid argon in calorimeters.

Last but not least, the ISR made contributions to the understanding of fundamental particle physics processes. In particular, the study of hadronic interactions advanced QCD as the theory of strong interactions. The experiments also showed that the proton-proton total cross-section was not constant with energy. These results are still the subject of research today at the LHC.

We are privileged to have had contributions at this colloquium from some of the key people of the ISR, 40 years after the first proton-proton collisions. We heard directly from them how the achievements at the ISR were realised, insight that will be of assistance in discovering new aspects relevant to the future of research in particle physics.

Rolf-Dieter Heuer

CERN Director-General

Contents

Foreword
R.-D. Heuer iii

Design and construction of the ISR
K. Hübner 1

The impact of the ISR on accelerator physics and technology
P.J. Bryant 15

Small-angle physics at the intersecting storage rings forty years later
U. Amaldi 33

Large-transverse-momentum processes: the ISR as a gluon collider
P. Darriulat 63

Design and construction of the ISR

Kurt Hübner

Introduction

The emergence of the ISR project at CERN is described in the light of the situation at CERN at the end of the 1950s when the CERN Proton Synchrotron (PS) was still under construction. The discussions leading to the project are put into context with world-wide efforts to build larger and more powerful accelerators at that time; the evolution of the project before approval is sketched. The basic design considerations and the most significant technological choices are explained. The construction period is summarized by highlighting important milestones and the performance achieved during commissioning in 1971, the first year of running, is given.

1 On the early history of colliders

First ideas

The first proposal for colliding beams was made by Rolf Wideröe in a German patent of 1943 which was published only in 1953 due to the circumstances of that time [1]. Figure 1 shows the first page of the patent taken from the scientific biography of Wideröe by Pedro Waloschek [2]. Figure 2 is taken from the patent showing injector and collider. All essential features are described: the counter-rotating particle beams (protons or deuterons) to reach a high reaction energy in the centre-of-mass, a ring-shaped vacuum tube and a magnetic guide field. Even electron-proton reactions were considered. Wideröe discussed the idea with Bruno Touschek who was not very impressed saying that the idea was obvious and trivial [3]. Nobody could see an application of the idea since the reaction rate was simply too low to be of any practical use and, at that time, no scheme for accumulating intense beams was known.


Erteilt auf Grund des Ersten Überleitungsgesetzes vom 8. Juli 1949
(WiGBl. S. 175)

BUNDESREPUBLIK DEUTSCHLAND

AUSGEGEBEN AM
11. MAI 1953

DEUTSCHES PATENTAMT

PATENTSCHRIFT

Nr. 876 279

KLASSE 21g GRUPPE 36

W 687 VIIIc / 21g

Dr.-Ing. Rolf Wideröe, Oslo
ist als Erfinder genannt worden

Aktiengesellschaft Brown, Boveri & Cie, Baden (Schweiz)

Anordnung zur Herbeiführung von Kernreaktionen

Patentiert im Gebiet der Bundesrepublik Deutschland vom 8. September 1943 an
Patentanmeldung bekanntgemacht am 18. September 1952
Patenterteilung bekanntgemacht am 26. März 1953

Fig. 1: The patent of R.Wideröe introducing colliding beams

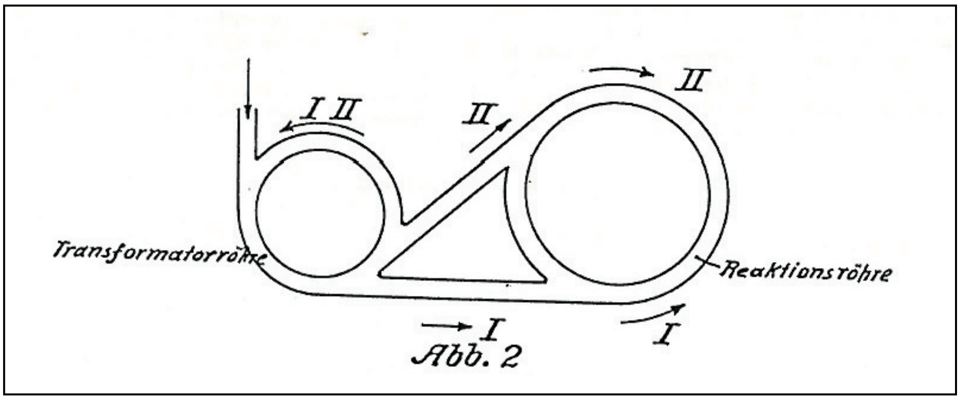

Fig. 2: The layout of a collider with injector by R.Wideröe

Practical ideas

A breakthrough came with the invention of the so-called radio-frequency (rf) stacking by the MURA Group in the US in 1956 [4] which showed a way to accumulate proton beams of sufficient intensity so that reasonable interaction rates could be hoped for. Based on this technique, this group led by Donald W. Kerst worked out in detail a technical proposal for collisions based on two Fixed-Field Alternating Gradient (FFAG) rings with a common straight section where the beams could collide. The layout is sketched in Fig. 3 [5]. At the same time, Gerard K. O'Neill presented a layout (Fig. 4) with tangential rings having a synchrotron-type magnet structure operating at 3 GeV [6, 7]. Similar ideas occurred to Lichtenberg, Newton, and Ross of MURA [8] and Brobeck [9]. Concentric, intersecting storage rings were suggested later [10], a topology finally adopted for the ISR. The ideas of the MURA Group and of O'Neill were not followed up in the US as cascaded synchrotrons appeared more attractive, leading eventually to the 200 GeV main ring of FNAL. MURA was eventually dissolved [11] and O'Neill became interested in electron-electron collisions.

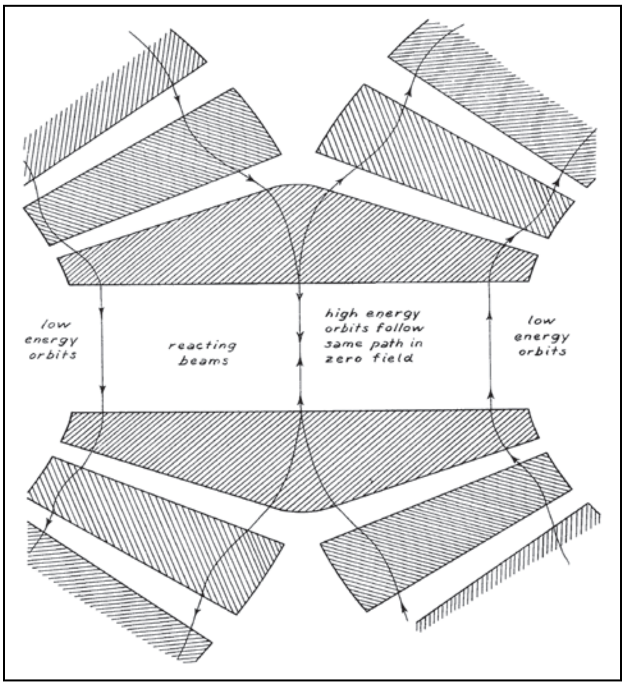

Fig. 3: Layout of a collider proposed by the MURA Group [5]

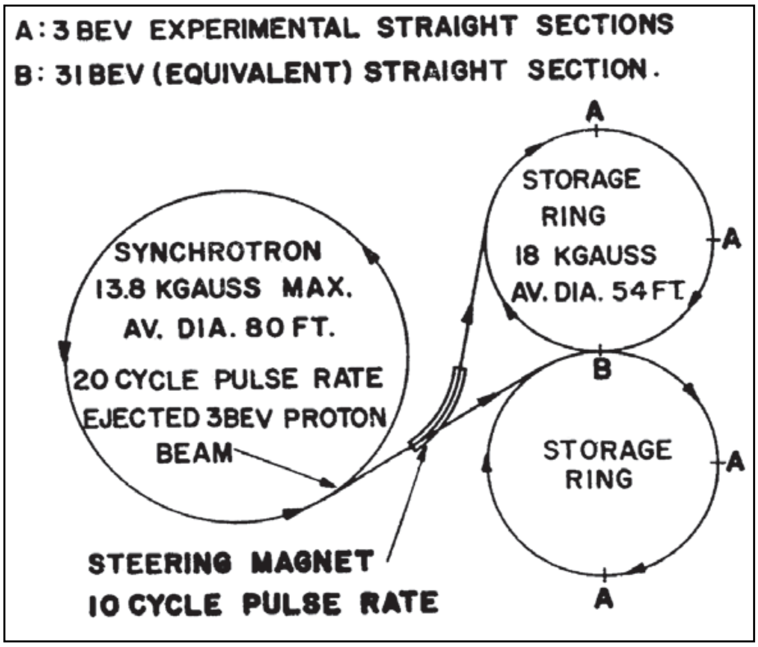

Fig. 4: Proton storage rings fed by a synchrotron [6]

Electron–electron and electron–positron colliders

In order to illustrate the general context of the CERN ISR studies, it is useful to recall the parallel activities in the field of $e^- e^-$ and the $e^- e^+$ colliders. The design of the Princeton–Stanford $e^- e^-$ rings with a beam energy of 500 MeV started in 1957 and the rings operated from 1961 onwards in Stanford. Their operation revealed the strong effect of synchrotron radiation on the vacuum system which has been an important issue for electron and positron rings ever since [12]. Also in 1957 the design of the $e^- e^-$ VEP-1 with 160 MeV per beam started at the Kurchatov Institute in Moscow under the leadership of Gersh Budker. VEP-1 operated from 1965 at BINP in Novosibirsk [13].

The lineage of single rings for counter-rotating $e^- e^+$ beams, which culminated in LEP at CERN, was initiated at Frascati by Touschek with ADA [14] designed for beams with an energy of 200 MeV. Amazingly, it took less than a year from proposal to first operation in 1961. Since the beam power of the Frascati 1 GeV electron synchrotron turned out to be insufficient for adequate positron production, ADA was moved in 1962 to the more powerful 1 GeV electron linac of LAL at Orsay where real physics experimentation started. ADA was followed by VEPP-2 in 1964 at BINP and by ACO in 1965 at LAL. Their beam energies were already much higher, 0.7 GeV and 0.5 GeV, respectively.

2 The emergence of the ISR

In 1956, still during the construction of the CERN Proton Synchrotron (PS), the CERN Council established the Accelerator Research (AR) Group to be led by Arnold Schoch following a proposal of John Adams. This group was expanded in 1959 with manpower that became available after the PS construction had been terminated. It initially studied plasma acceleration and an electron collider with 100 MeV beam energy in a FFAG ring, but in 1960 interest swung to proton–proton storage rings fed by the PS. A proposal of tangential rings was made in December 1960 and, in 1961, it was decided that the AR Division, formed at the beginning of 1961, should study the proton storage rings and a large 300 GeV synchrotron. In 1962, Intersecting Storage Rings were proposed, thus considerably simplifying the project.

In order to obtain a reasonable luminosity in the ISR, accumulation of the beam injected from the PS was imperative. The method of choice was rf stacking invented and promoted by MURA [4, 11]. Given the importance of the performance of this new method, an experimental proof was indispensable. Hence the idea of constructing a small electron ring to test this method came up in 1960 and the ring, the CERN Electron Storage and Accumulation Ring (CESAR), was ready in 1964 (Fig. 5). It had a circumference of 24 m. To mimic the proton behaviour at 25 GeV in the ISR correctly, synchrotron radiation had to be negligible but v/c close to 1. This led to the choice of an electron energy of 2 MeV and a low magnetic bending field of 130 G. This low field led to trouble in operation as, in addition, solid bending magnets had been chosen. Their substantial residual magnet field compared to the nominal field of 130 G was difficult to control. Nevertheless CESAR quickly demonstrated rf stacking [15] (Fig. 6) giving welcome momentum to the ISR project.

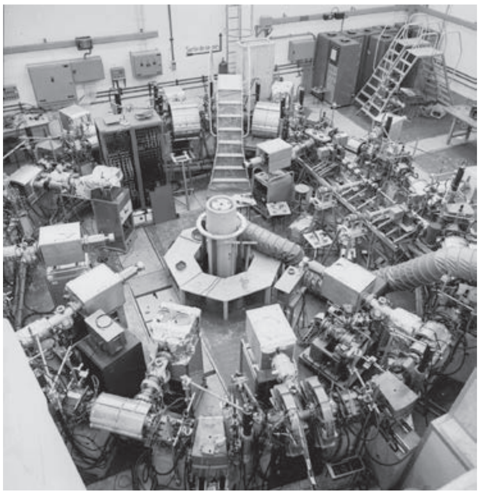

Fig.5: The CERN Electron Storage and Accumulation Ring (CESAR)

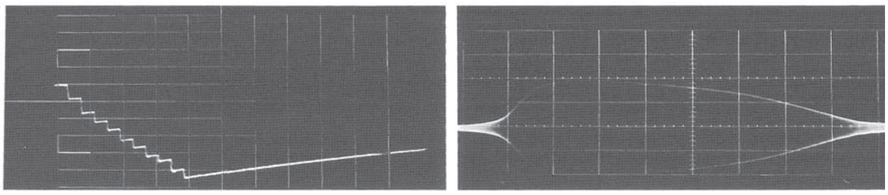

Fig. 6: a) Accumulated electron beam current as a function of time in CESAR; b) Particle density of the stack versus particle momentum

In order to channel the discussions, an ECFA Working Group chaired by E. Amaldi was formed in 1963 which recommended the ISR and the 300 GeV synchrotron. However, the Homeric debate went on between those who favoured a facility to peep at interactions at the highest energies and those who preferred intense secondary beams with energies higher than the PS could provide. Those against the ISR were also afraid of the leap in accelerator physics and technology required by this venture, which appeared to them as a shot in the dark. In May 1964, the AR Division presented the ISR design report [16] and in November the design report of the 300 GeV accelerator [17]. The following year, CERN Council approved the ISR as a supplementary programme in June and then approved the project in December with K. Johnson as project leader after the financing had been clarified. The prevailing argument had been “to remain competitive for as low a cost as possible” given that the ISR was estimated to be much cheaper than a 300 GeV synchrotron. The cost of the former was estimated to be 312 MCHF [16] compared to 1556 MCHF [17] for the latter. A very detailed account of the period up to the decision can be found elsewhere [18].

3 ISR design

No small-scale proton collider had ever been built before, hence no extrapolation was possible. The only experience at CERN with an accelerator of that size was the PS. A number of leading team members had indeed acquired their expertise during PS design, construction and running-in, which turned out to be very beneficial for the project, in particular for its rapid and uneventful construction, though one might argue today that this stifled somewhat the quest for new solutions.

Magnet lattice

The magnet lattice requirements were different from the PS: long straight sections were needed at the crossing points to make space for the experiments and the horizontal aperture for the beam had to be larger as the rf stacking required a large momentum bite. The long straight sections were inserted between two focusing magnets in order to minimize the disturbance to the beta-functions and to provide a small vertical beam size at the crossing point as the luminosity is inversely proportional to the vertical beam size. Matched low-beta insertions with vanishing dispersion, common today in all colliders, had not yet been invented.

Three alternative types of magnet lattice had been considered: a separated-function lattice where the magnets have either bending or focusing function; combined-function lattices either of FODO or FOFDOD type consisting of magnets with dipole and quadrupole fields providing both bending and focusing. Since elaborate poleface-windings were foreseen because they are easier to implement in combined-function magnets, this type of magnet was preferred but also for easier access to the very demanding vacuum system. The latter argument led also to the choice of FODO because the access to the FD junction in FOFDOD is not so easy, as experience in the PS had shown. An additional argument for the combined-function lattice was the claim that a separated-function lattice would increase the cost up to 1.7 MCHF. Table 1 gives a synopsis of the parameter ranges considered, the final choice and the consideration leading to the decision.

Table 1: Considerations and choices for the ISR lattice

	Range	Chosen	Consideration
Interaction regions (No.)	6–8	8	Avoid betatron stop-bands
Betatron oscillations per turn Q (h/v)	6–9	8.8/8.7	$nQ = p(N/2)$, $N/2$ – number superperiods
Lattice periods	45–60	48	Betatron phase advance between $\pi/4$ to $\pi/3$
Half-periods in outer arc	14–24	16	Limit on circumference
Half-periods in inner arc	4–12	8	Geometry
Full crossing angle	9–32°	14.77°	Numerology relative to PS

The resulting topology with the transfer lines relative to the PS is shown in Fig. 7. The ISR circumference was chosen to be 1.5 times that of the PS resulting in 942.64 m (300 π m). Inspection of Fig. 8 showing one octant reveals indeed a clear FODO structure in the outer arc but it is harder to clearly determine the type of lattice in the inner arc.

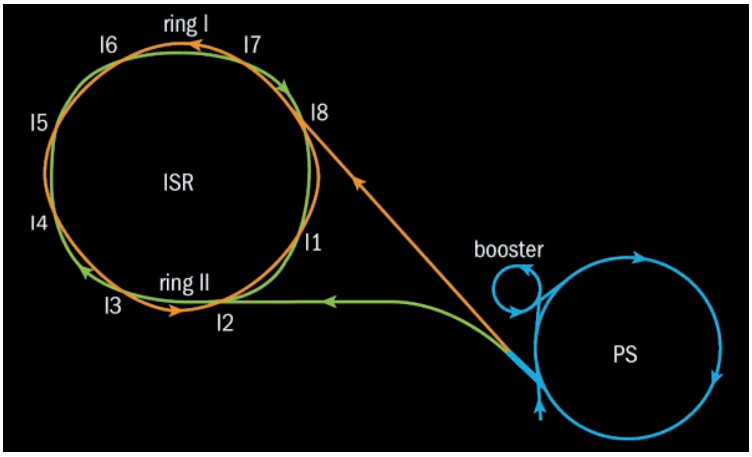

Fig.7: Schematic layout of the ISR, its transfer lines and its injector, the PS

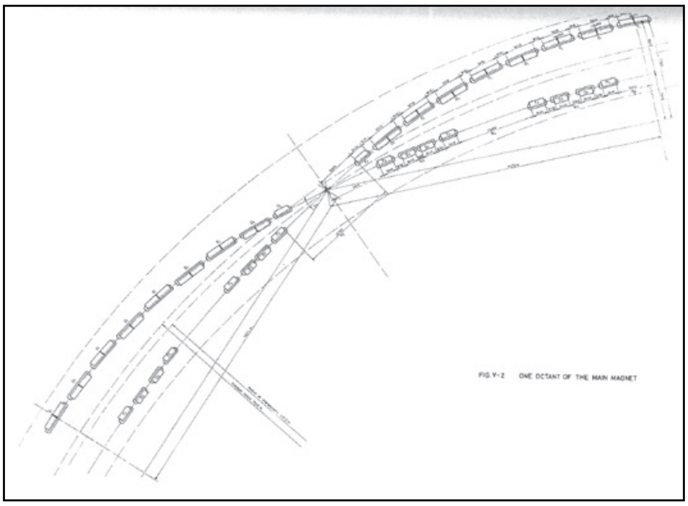

Fig.8: One octant of the ISR magnet lattice [16]

The ISR were argued for initially as an improved facility for the CPS also providing additional fixed-target beams of high-intensity but low duty cycle. A token of this is the layout shown in the design report [16] (see Fig.1 of P. Bryant's contribution) which still features a hall for fixed-target experiments in the lower right corner but this hall disappeared very quickly from the drawings during the construction stage. The extraction channel towards the West Hall, however, was constructed but never equipped.

Magnets

The magnets were designed for protons of 28 GeV/*c*, the maximum the PS could supply. The nominal bending field was 1.2 T implying a bending radius of 78.6 m. Each ring contained 60 long magnet units and 72 short units. The long units (L= 5.03 m) were made up of two blocks and the short units (L = 2.44 m) of one block. The 32-turn coil was made of copper. Figure 9 gives the magnet cross-section displaying also the pole-face windings and vacuum chamber which can be accessed easily including its heating elements (not shown) for the bake-out in situ. A photo of a magnet is shown in Fig. 3 of P. Bryant's contribution. In the best tradition of CERN, where key elements of an earlier accelerator are often used for mundane purposes by the next accelerator, the bending magnets are still in service but as elements of the beam dump of the LHC as can be seen in Fig. 10. A number of auxiliary magnets completed the magnet system.

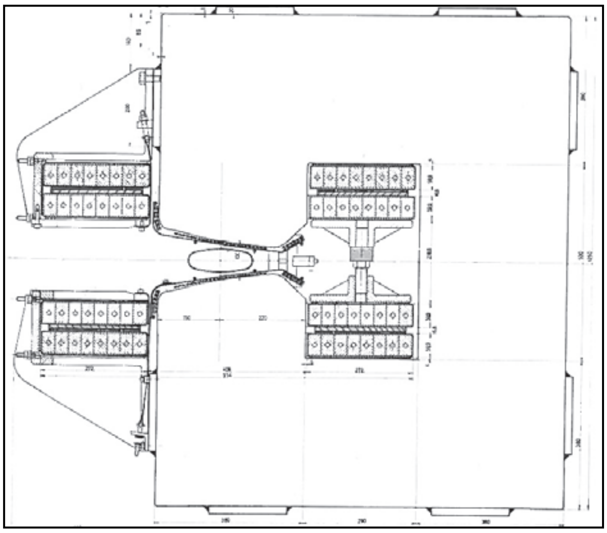

Fig.9: Cross-section of an ISR combined-function magnet [19]

Fig.10: Cores of ISR bending magnets as component of the LHC beam dump

Given the bending radius, the energy loss per turn by synchrotron radiation can be calculated. It was $6 \cdot 10^{-14}$ GeV, which is indeed very small compared to 28 GeV. Hence, no radiation damping would fight the beam blow-up by non-linear resonances and by the beam-beam effect as in electron accelerators. Since this was new territory, it fired the fear that the ISR might never work. However, this eventually turned out to be a chimera.

Vacuum system

The ISR key performance parameter, the integrated luminosity, is proportional to

$$\int (I_1 \cdot I_2 / h_{\text{eff}})\, \mathrm{d}t$$

with all three variables depending on time t. The currents I_i of the counter-rotating beams decay due to nuclear and single-Coulomb scattering, and the effective beam height h_{eff} gets blown up by multiple-Coulomb scattering of the protons on the residual gas. Hence, an ultra-high vacuum system was imperative for the performance of the ISR, in order to achieve a reasonable beam lifetime and to limit the beam blow-up as a function of time. Imposing a beam loss of less than 50% and a growth of h_{eff} of less than 40% in 12 h, implying a drop to not less than 18% in luminosity after 12 h, leads to a requirement that the pressure be less than 10^{-9} Torr (N_2 equivalent) averaged around the circumference. The pressure in the interaction regions had to be less than 10^{-11} Torr to limit the background for the experiments. To produce such an ultra-high vacuum system extending over a total length of nearly 2 km was one of the biggest technological challenges of the project.

CESAR had been a valuable test bed to guide the choice of the vacuum technology: a stainless-steel vacuum chamber of low magnetic permeability and bakeable in situ to 300°C (initially baked only to 200°C); flanges with metal seals; sputter ion pumps (350 l/s) complemented with Ti-sublimation pumps (2000 l/s) in critical places. Figure 9 indicates the position of the vacuum chamber in the bending magnet. The long vacuum chambers in the interaction points were particularly challenging as they had to be designed with a minimum of mechanical support and with very thin walls to reduce the loss and scattering of secondary particles produced in the collision point. Engineering highlights were the self-supporting chambers with 0.3 mm wall-thickness made from Ti and with 0.2 mm thickness made from stainless steel. INCONEL of 0.2 mm thickness was also used [20]. Figure 11 shows an example.

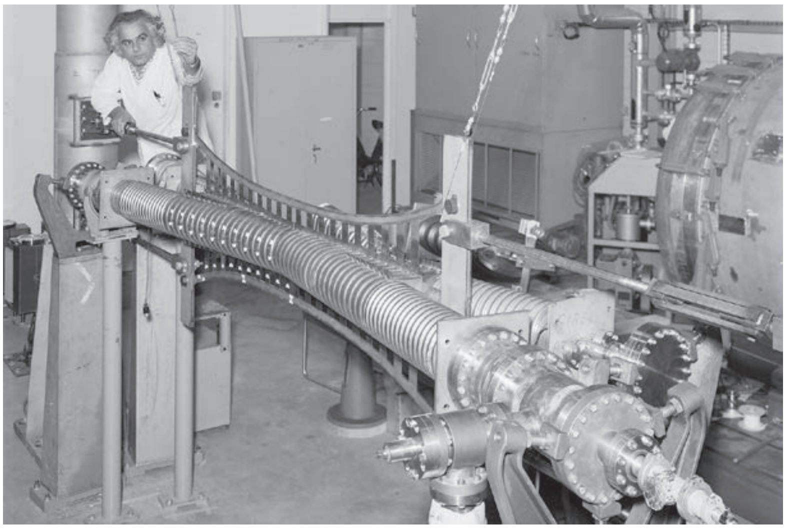

Fig.11: A thin-wall ISR vacuum chamber for an intersection region

Clearing electrodes inside the vacuum chambers were foreseen to remove the electrons created by ionization of the residual gas and accumulating in the potential well of the d.c. proton beam. Damping resistors reduced the quality factor of the electromagnetic eigen-modes in all cavity-like chambers to prevent collective instabilities of the beams.

4 ISR construction and commissioning [21]

ISR tunnel

The tunnel was built using the cut-and-fill method implying excavation and removal of more than one million cubic metres, mainly moraine material, since the tunnel was 15 m wide and it had to be put on competent rock, i.e., molasse in the Geneva basin. Figure 12 illustrates this point. The tunnel floor was

12 m above the level of the PS to reduce the amount of material to be removed. The erection of the tunnel proceeded so as to protect the foundations of the magnets as much as possible. First, two concentric concrete footings (1 m deep, 1.5 m wide) were laid. The floor in between was left 20 cm higher than the final general level. The footings formed the base for the mobile crane and, then, for the foundations for the pre-fabricated concrete main walls of the tunnel. Once a section of the tunnel had been completed, the remaining molasse was excavated to the general level and trenches were prepared for the concrete beams supporting the magnets [19].The cross-section of the ring tunnel is shown in Fig. 13. Its height was 6.5 m and 4.0 m under the hook of the crane. The finished tunnel and the concrete support beams for the magnets can be seen in Fig. 14 showing also the first magnet in the tunnel used for a positioning trial.

Fig.12: The excavation of the ISR tunnel

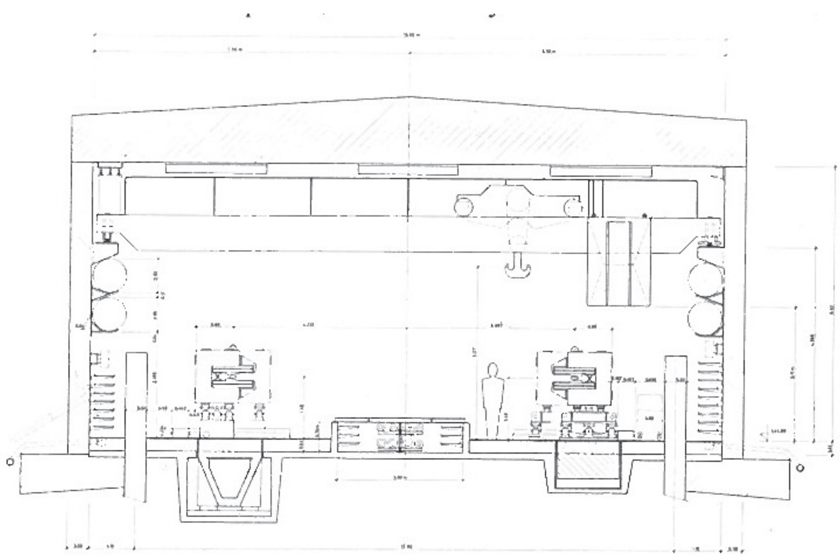

Fig.13: The cross-section of the ISR tunnel [21]

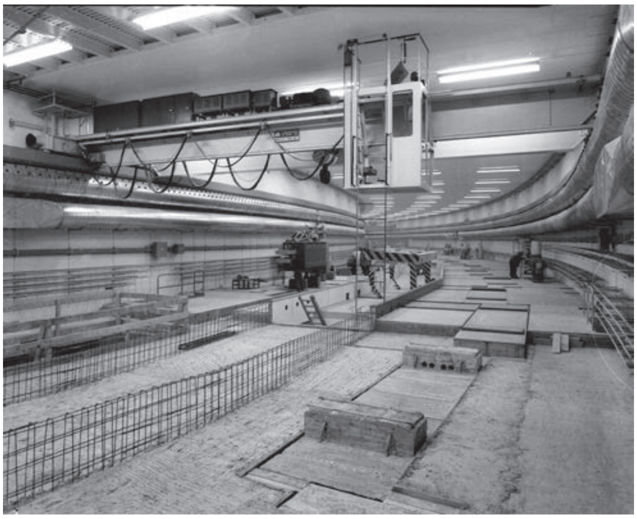

Fig.14: A view of the ISR tunnel

Construction milestones

The ISR construction got off to a flying start. Excavation started in November 1966, less than 12 months after approval. The pre-fabricated structure of the tunnel was in place in 1969 and installation in six octants had started. By 1967, all major magnets had been ordered. Two prototype magnets were delivered in early 1968 and measured. The bulk production of magnet steel started at the beginning of 1968 and the whole order (11 kt) was delivered by October. The West Hall became available for the assembly, testing, and storage of the magnets in 1969 (Fig. 15). The final race started in 1970. In April, the transfer lines from the PS were ready for tests with beam and the last ring magnet was installed in May. The earth shielding was complete in July and ring 1 was ready for injection in October.

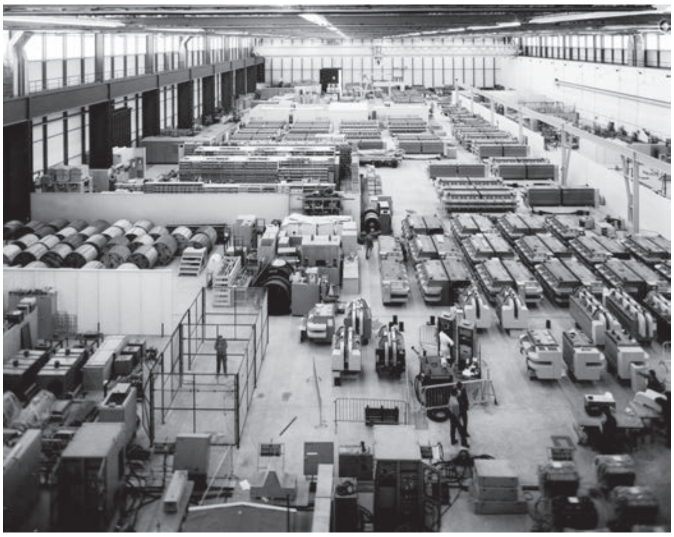

Fig. 15: Assembly, testing and storage of ISR magnets in the West Hall

Commissioning

The first 15 GeV/*c* proton beam was injected into ring 1 on 29 October 1970 and a circulating beam was quickly obtained. The uncorrected closed-orbit distortions were about 20 mm peak-to-peak in the horizontal plane and 8 mm in the vertical plane, which could easily be corrected. The number of betatron oscillations per turn was as expected indicating correct focusing of the ring. A first trial of beam accumulation by rf stacking led to 0.65 A showing a satisfactory efficiency of 70% (longitudinal phase space density of the stored beam over that of the injected beam) and confirming the findings in CESAR. An example of early stacking is shown in Fig. 16.

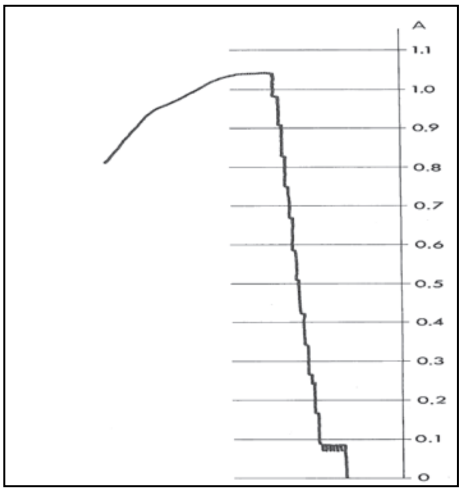

Fig.16: Build-up of proton current as a function of time (going to the left) during rf-stacking

In January 1971, the second ring became available and first proton–proton collisions were recorded on 27 January, anxiously observed by the team to see whether the beam–beam effect would quickly destroy the beams as some simulations had predicted. However, nothing catastrophic happened and, to general relief, the beam decay was as expected from the measured vacuum pressure. Regular physics runs started in February with 15 GeV/*c* beams, and collisions at 26.5 GeV/*c*, the maximum scheduled for the PS, were obtained in May, providing a centre-of-mass energy equivalent to a 1500 GeV proton beam on a fixed target. The beam currents were gradually increased during the year reaching 10 A at the end as illustrated on Fig. 17. The maximum luminosity obtained in 1971 was $3 \cdot 10^{29}$ cm^{-2} s^{-1}, a quite respectable performance when compared with the design luminosity of $4 \cdot 10^{30}$ cm^{-2} s^{-1}. The beam decay rate was less than 1% per hour at currents of 6 A in both rings, much better than the design value of less than 6% per hour. The ISR operated 1800 h in its first year (800 h for colliding beam physics) with a remarkable availability of 95%.

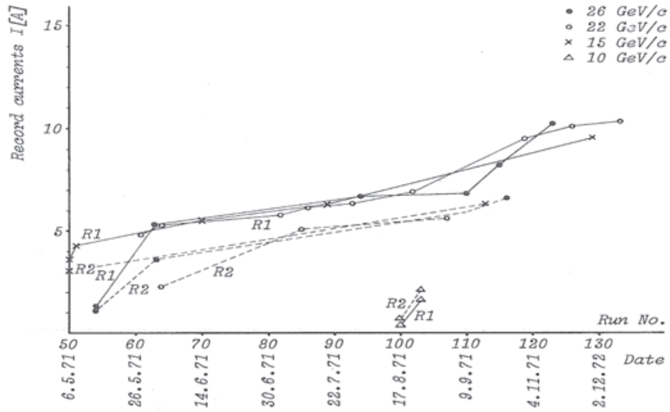

Fig.17: The evolution of the stacked proton beam current in the first year of operation for ring 1 and 2 with beam momentum as parameter

The successful completion of the project, terminated officially on 1 March 1971 within budget (332 MCHF in 1965 prices), was duly celebrated in an inauguration ceremony on 16 October where the photograph (Fig. 18) of two of the main-players, Eduardo Amaldi and Kjell Johnsen, was taken. The third one was Viktor Weisskopf who had the stamina to push their vision until it was accepted by the funding authorities catapulting CERN to the very high-energy front. It would turn out that it was not quite enough to be at this frontier since this state was eventually not fully exploited by CERN.

Fig.18: Eduardo Amaldi and Kjell Johnsen at the ISR inauguration ceremony in October 1971

5 Conclusions

The ISR construction went very smoothly due to a careful and meticulous preparation by a competent, dedicated team which designed and constructed the conventional components as well as possible, knowing that this provides the best basis for dealing later with unknowns which might appear. Some accused the team of overdesign and waste of resources. However, this careful approach provided the potential for the later gradual, but spectacular improvement in performance until the ISR were decommissioned as a collider in 1983. A token of this is the fact, that the ISR luminosity record was not broken until 1991 when an $e^- e^+$ collider, CESR in Cornell, took over.

The ISR was a solid basis for the development of all the hadron colliders to come such as the proton–antiproton collider in the CERN SPS and at FNAL, the p–p and ion–ion collider at BNL and, eventually, LHC at CERN. It was a fine and unique instrument, or as Weisskopf put it at the closure ceremony in 1984: "*First considered a window into the future, it turned out to be more"*.

References

[1] R. Wideröe, *Anordnung zu Herbeiführung von Kernreaktionen*, Bundesrepublik Deutschland, Deutsches Patentamt (1953) Patenschrift Nr. 876279.

[2] P. Waloschek, *The Infancy of Particle Accelerators: Life and Work of Rolf Wideröe* (Vieweg, Braunschweig, 1994).

[3] E. Amaldi, *The Bruno Touschek Legacy,* CERN Report 81-19 (1981), p. 29.

[4] K. R. Symon and A. M. Sessler, *Methods of radio frequency acceleration in fixed-field accelerators with applications to high-current and intersecting beam accelerators,* Symposium on High-Energy Accelerators and Pion Physics, Geneva/CERN, Report CERN 56–26 (1956), p. 44.

[5] D. W. Kerst, *Properties of an intersecting-beam accelerating system,* ibid. p. 36.

[6] G. K.O'Neill, *Storage-ring synchrotron,* ibid. p. 64.

[7] G. K. O'Neill, *Storage-ring synchrotron: device for high-energy physics research,* Phys. Rev. **102** (1956) 1418.

[8] D. B. Lichtenberg, R. G. Newton, and H. M. Ross, *Intersecting beam accelerator with storage ring,* MURA Report 110 (1956).

[9] W. M. Brobeck, *The design of high-energy accelerators,* Symposium on High-Energy Accelerators and Pion Physics, Geneva/CERN, 1956, Report CERN 56-26 (1956), p. 60.

[10] E. J. Woods and G. K. O'Neill, *Concentric storage rings,* Bull. Amer. Phys. Soc., Ser. II, **3** (1958) 169.

[11] L. W. Jones, F. E. Mills, A. M. Sessler, K. R. Symon, and D. E. Young, *Innovation Was Not Enough; A History of the Midwestern Universities Research Association (MURA)* (World Scientific, Singapore, 2009).

[12] G. K. O'Neill, *Storage-ring work at Stanford,* Summer Study on Storage Rings, Accelerators and Experimentation at Super High-Energies, Upton, NY, 1963, BNL 7534 (Brookhaven Nat. Lab., Upton, NY, 1963), p. 209.

[13] G. I. Budker et al., *Check of quantum electrodynamics by electron–electron scattering,* Sov. J. Nucl. Phys. **6** (1968) 889.

[14] J. Haissinski, *Expériences sur l'anneau de collisons ADA,* Thèse, Orsay, Série A, No. 81 (1965).

[15] S. Hansen, E. Jones, H. Koziol, and M. J. Pentz, *Some Results of Stacking Experiments with the CERN Electron Storage and Accumulation Ring (CESAR),* CERN Report 65-8 (1965).

[16] The CERN Study Group on New Accelerators, *Report on the Design Study of Intersecting Storage Rings (ISR) for the CERN Proton Synchrotron,* Report to Council, CERN/542 and AR/Int.SG/64-9.

[17] The CERN Study Group on New Accelerators, *Report on the Design Study of a 300 GeV Proton Synchrotron,* Report to Council, CERN/563 and AR/Int.SG/64-15.

[18] D. Pestre, *The second generation of accelerators for CERN, 1956–1965: the decision process,* Chapter 12 in *History of CERN, Vol. II, Building and Running the Laboratory,* by A. Hermann, G. J. Krige, U. Mersits, D. Pestre, and L. Weiss (North-Holland, Amsterdam, 1990), pp. 679–782.

[19] Public Information Office, *ISR,* CERN Technical Notebook No. 5, 1969.

[20] J. C. Brunet et al., *The design and construction of transparent vacuum chambers for interaction areas of colliding beam machines,* 1979 Particle Accelerator Conference, San Francisco, IEEE Trans. Nucl. Sci. **NS-26** (1979) 4063.

[21] CERN Annual Reports1966–1971, *ISR Construction Department*,
See http://library.web.cern.ch/library/Library/AnnualReport.html.

The impact of the ISR on accelerator physics and technology

P.J. Bryant

Abstract
The ISR (Intersecting Storage Rings) were two intersecting proton synchrotron rings each with a circumference of 942 m and eight-fold symmetry that were operational for 13 years from 1971 to 1984. The CERN PS injected 26 GeV/*c* proton beams into the two rings that could accelerate up to 31.4 GeV/*c*. The ISR worked for physics with beams of 30–40 A over 40–60 hours with luminosities in its superconducting low-β insertion of 10^{31}–10^{32} cm^{-2} s^{-1}. The ISR demonstrated the practicality of collider beam physics while catalysing a rapid advance in accelerator technologies and techniques.

Introduction

To appreciate the role played by the CERN Intersecting Storage Rings (ISR) in accelerator physics let us try to imagine ourselves back in the 1960s. In an atmosphere of close collaboration and friendly competition, Europe and America had just commissioned the first generation of strong-focusing machines, the CERN PS (1959) and the BNL AGS (1960). With the PS working, CERN embarked on the study of a proton–proton collider leading to the approval of the ISR in 1965. The ISR [1] was an exciting concept that offered a giant leap in the centre-of-mass energy over the fixed-target configuration, but it was clouded by doubts as to its practicality, and support was far from unanimous. On the one hand, the CERN team was highly experienced by 1960 standards and well connected to the other leading laboratories, but on the other hand there were voices saying that the residual gas and non-linear resonances would destroy the beams, since there was no stabilizing influence from synchrotron radiation. These were not empty fears. The vacuum problem was very real and there is indeed an infinite web of non-linear resonances [2], [3]. The deleterious effect of electrons trapped in the potential well of the beam following ionization of the residual gas was also foreseen by the early designers [4]. With hindsight we know these effects were not going to be fatal, but could one be sure in 1965? We also know that the CERN team was standing at the foot of a steep and exciting learning curve in accelerator technology, techniques, and diagnostics. By the time the ISR closes in 1984, our concepts of accelerator engineering and diagnostics and the way experimental physics is conducted will have changed radically and will look very much as they do today. The aim of this paper is to illustrate the rapid change that took place, mainly in the years 1965 to 1977, and to underline the role played by the ISR.

1 Advances in lattice design

The '1965' lattice

Figure 1 shows the layout of the two rings with their injection lines and Fig. 2 shows the original ISR lattice functions from the centre of an outer arc to the centre of an inner arc. The underlying lattice is a FFDD structure, but in the crossing regions and inner arcs the lattice is opened between the F units to form FDDF cells. The longer drift spaces are a welcome innovation compared to the tightly-packed FD–DF cells of the PS. The ISR magnets are, however, still combined-function of the open 'C' type (see Fig. 3), a legacy from the days of weak focusing. Note that the betatron amplitude functions are very rounded. This is due to the spread-out gradients of the combined-function magnets. The lattice has been manipulated globally to fit the interlaced geometry and to provide space for physics equipment in the interaction regions. The 'split-F' structure provides local betatron minima at the crossing points, although these are not as low as would have been liked. There are no dispersion-free regions or low-β insertions as the local customization of a lattice (i.e. insertions) had still to be developed.

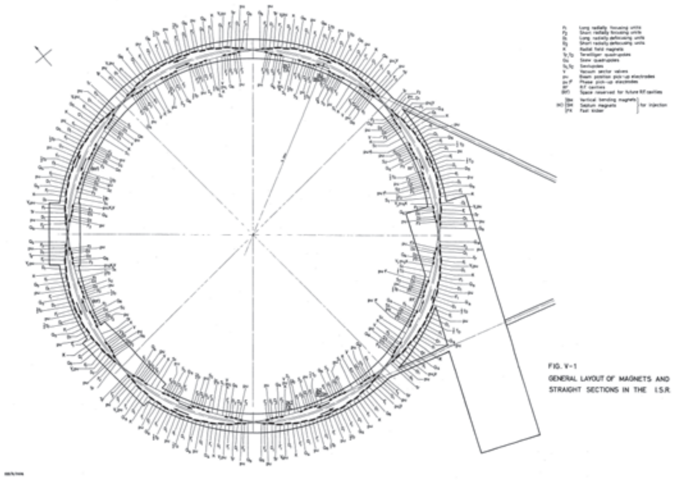

Fig. 1: Layout of the CERN ISR with transfer lines (Design Study 1964)

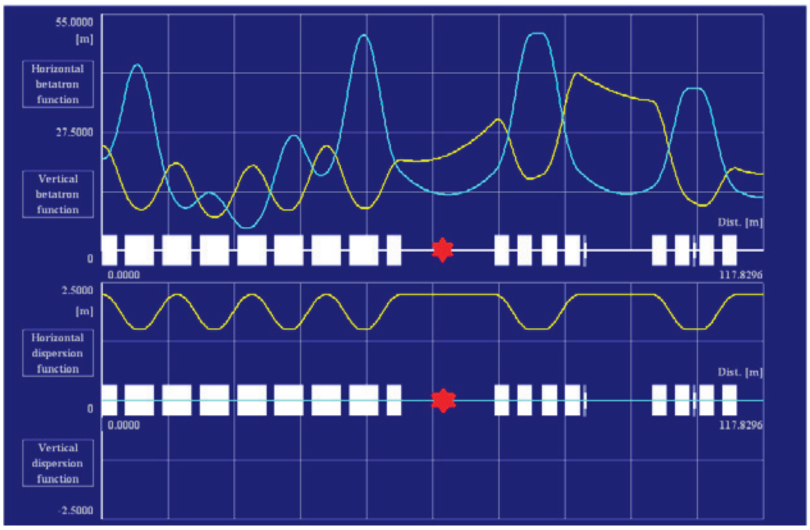

Fig. 2: Design lattice functions of the ISR (based on ISR Parameter List Rev. 5 CERN/ISR-GS/76-4)

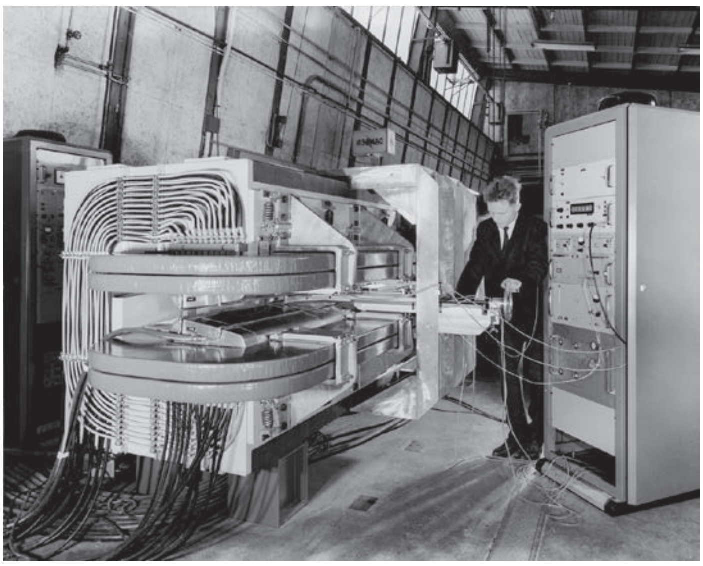

Fig. 3: ISR main magnet model (December 1965)

The '1977' SCISR upgrade lattice

Some years later in 1977, a project was published to convert the ISR to the SCISR, a superconducting machine [5]. Figure 4 shows the lattice functions in the outer arc for this conversion and Fig. 5 shows the cross-section of the new quadrupole. Immediately, one sees the advances that have taken place. The arc is a tightly-packed FODO structure, terminated by a dispersion suppressor and matched into a low-β insertion, which is exactly how the job would be done today. The use of separated-function magnets provides a more efficient focusing with clearer features in the shapes of the lattice functions, and the superconducting quadrupole using the Roman arch principle to support the coils is right up to date. This is just one illustration of the rapid changes mentioned in the introduction that were to take place during the brief 13-year life of the ISR. Eberhard Keil [6] had proposed the elegant method used for the dispersion suppressor and, although low-β insertions were not an ISR invention, the matching was based on an analytical solution for a variable-geometry triplet published by Bruno Zotter [7] in 1973. This is perhaps the most useful of all the analytical matching modules ever published.

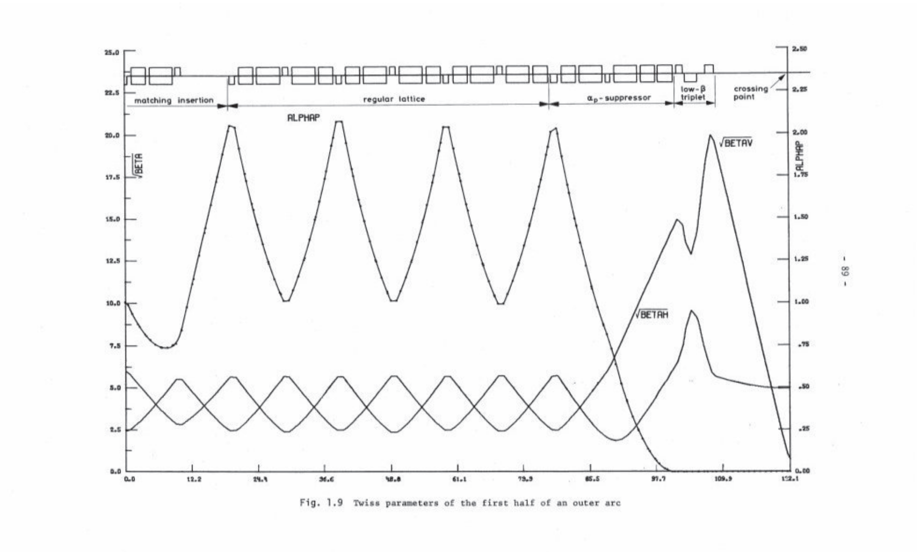

Fig. 4: Lattice functions of the proposed superconducting ISR upgrade (1977)

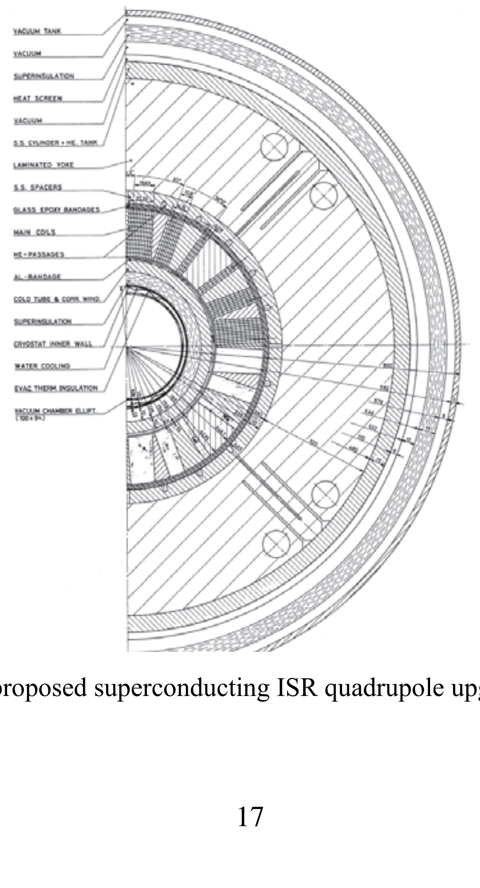

Fig. 5: The proposed superconducting ISR quadrupole upgrade (1977)

2 From ‘global fitting’ to insertions

Terwilliger scheme

One example of ‘global fitting’ with the 1965 lattice is the so-called Terwilliger Scheme [8], which creates small interaction diamonds by driving the dispersion function to zero at regularly-spaced positions in betatron phase using a superimposed gradient with a suitable azimuthal harmonic. In the ISR, which is the only machine to have demonstrated this now obsolete principle [9], only four of the eight minima fell on interaction regions (see Fig. 6).

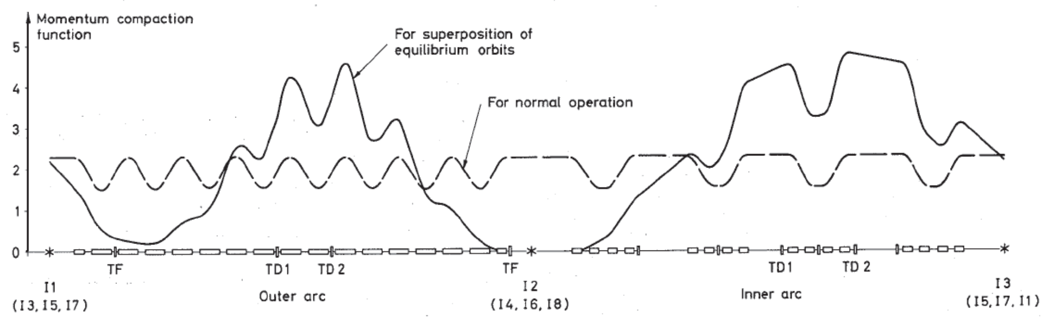

Fig. 6: The unperturbed and perturbed momentum compaction functions through one superperiod of the ISR showing how the small interaction diamonds are formed (1973)

Conventional steel low-β insertion

The concept of ‘global fitting’ is to be compared to the more modern idea of ‘insertions’ that tailor the lattice locally for a particular task. By 1974, the concept of a local insertion had been demonstrated in the ISR by a conventional steel low-β insertion built in Intersection 7 using largely borrowed quadrupoles from the CERN PS, DESY, and the Rutherford Appleton Laboratory. Since the ISR had no dispersion-free regions and the lattice functions were far from regular, matching the low-β was a significant challenge, but the result was highly successful and increased the luminosity by a factor of 2.3 [10]. The steel low-β insertion was initially an ‘experiment’ to test the fear that the very marked super-periodicity of unity would cause the high-intensity ISR beams to be unstable or noisy. In reality, this did not prove to be an issue and two years later in 1976, the insertion was demounted and moved to Intersection 1, where it was used in conjunction with a superconducting solenoid, see Fig. 7. It remained operational until the closure of colliding beams.

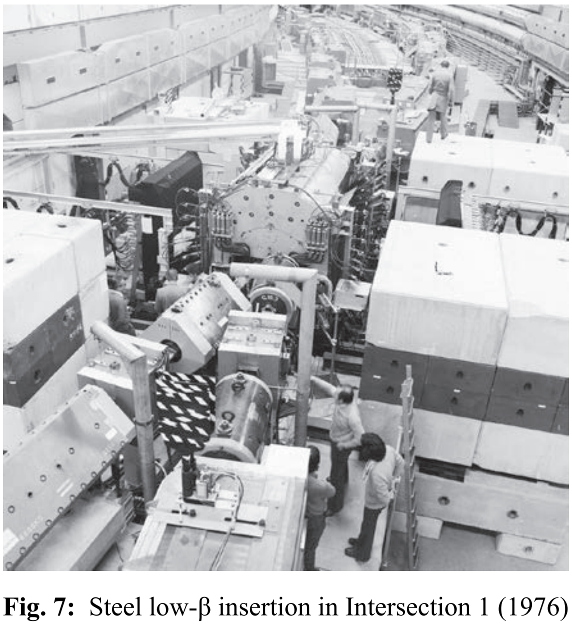

Fig. 7: Steel low-β insertion in Intersection 1 (1976)

3 Lattice programs

During the construction of the ISR, lattice computations were made with the programs SYNCH [11] (LBL), AGS [12] and BEATCH [13] (CERN). By the time the ISR closed in 1984, the ISR Theory Group had replaced the CERN AGS code by MAD (Methodical Accelerator Design) [14], which is now a de facto world standard for the study and design of large synchrotrons like LHC. Lattice programs are the essential tools behind lattice design and beam simulations. The effort devoted to these tools during the ISR years was very important to CERN, since CERN now holds the 'gold standard' software for one of the core competences of accelerator building. Similarly, at the start of the ISR, Romeo Perin, Simon van der Meer and Steve Caeymaex were working on computer codes for 2D [15] and 3D [16] magnet design, but these topics were not carried to the same level.

4 Coupling

The ISR also contributed strongly to the theory and design of coupling compensation schemes. A complete Hamiltonian theory for sum and difference resonances was published in 1976 by Gilbert Guignard [17], in which, amongst other things, the driving terms and coupling coefficients are defined. It later turned out that Phil Morton from SLAC had reached many of the same results in an unpublished and unfinished note [18]. A story that is similar to those of Rolf Wideröe and his betatron and Lee Teng who did not publish his theory for the rotator for medical gantries. As the operation of the ISR progressed, there were practical applications of the theoretical work. Since there were no dispersion-free regions in the ISR, the compensation scheme for the global coupling was of a special and unique design [19]. Similarly, the physics solenoid in Intersection 1 had horizontal slots in its end plates to accommodate the beams that crossed at an angle. This new feature was described analytically and compensated. The ISR was also first to be equipped with an electronic coupling meter that directly gave the modulus of the coupling coefficient defined in the theory [20].

5 Advances in magnet technology

Poleface windings

Figure 3 shows the ISR model magnet that clearly has a close affinity to the CERN PS magnet. Although the combined-function and C-type construction of the ISR main magnet was not according to modern tastes, it did have an extremely versatile set of poleface windings set into a thick epoxy cover (Fig. 8) placed over the pole under a copper heat shield*. The F-blocks and D-blocks were each equipped with 12 circuits and a 13th circuit in each case to compensate the stray field from the cable bundle. Probably no other machine has ever had such complete control over higher-order field components. The field shaping was applied using a 'practical' system of so-called 'half-multipoles' that acted independently on the inner and outer halves of the aperture. I will return to the use of this system under space-charge loading corrections in the section on beam–chamber interactions.

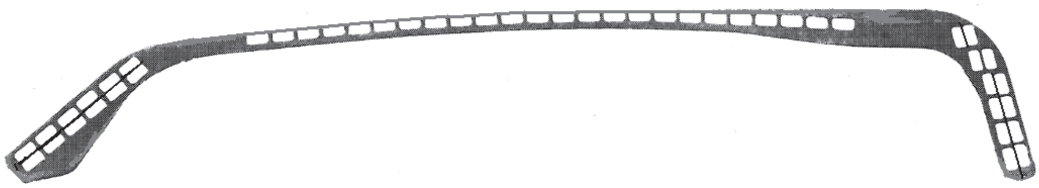

Fig. 8: Cross-section of the poleface windings sheath that was mounted on each pole of the ISR main magnet under the heat shield

* Eddy currents in the heat shield played a significant role in the stability of the fields against ripple when coasting.

Superconducting quadrupoles for a low-β insertion

It has already been mentioned that a superconducting upgrade for ISR was published in 1977. This upgrade was not approved, but another project to build a superconducting low-β insertion [21] had already been accepted. At that time, CERN made an important decision not to outsource the work to a Member State laboratory such as Rutherford, UK, but rather to start accumulating in-house expertise in magnet building and cryogenics, which was later to be immensely important for LEP and LHC. A number of superconducting magnets already existed in transfer lines in various laboratories, but nobody had operated superconducting quadrupoles in the lattice of a synchrotron. CERN then made a second important decision to build the models and prototypes in-house in order to reduce the new technology to a detailed engineering specification. On the basis of this specification, tenders were then invited from industry for the series production. This was a middle-of-the-road approach between the extremes of building everything in-house, as is usually done in US laboratories, or requesting industry to do the R&D as well as the series production, as some Member States wanted CERN to do. In the ISR approach, it is made clear to the manufacturer that the magnetic design is the responsibility of CERN and that he, the manufacturer, is only responsible for respecting the tolerances, choices of materials, and adherence to the various qualified procedures. The superconducting low-β, see Fig. 9, was a great success, increasing the luminosity in Intersection 8 by a factor of 6.5 [22] and laying the foundations for the LHC magnets and cryogenics. This was the first time that industrially-built superconducting quadrupoles had been operated in the lattice of a synchrotron for regular operation. In a typical run, the magnets would operate at top energy for 60 hours.

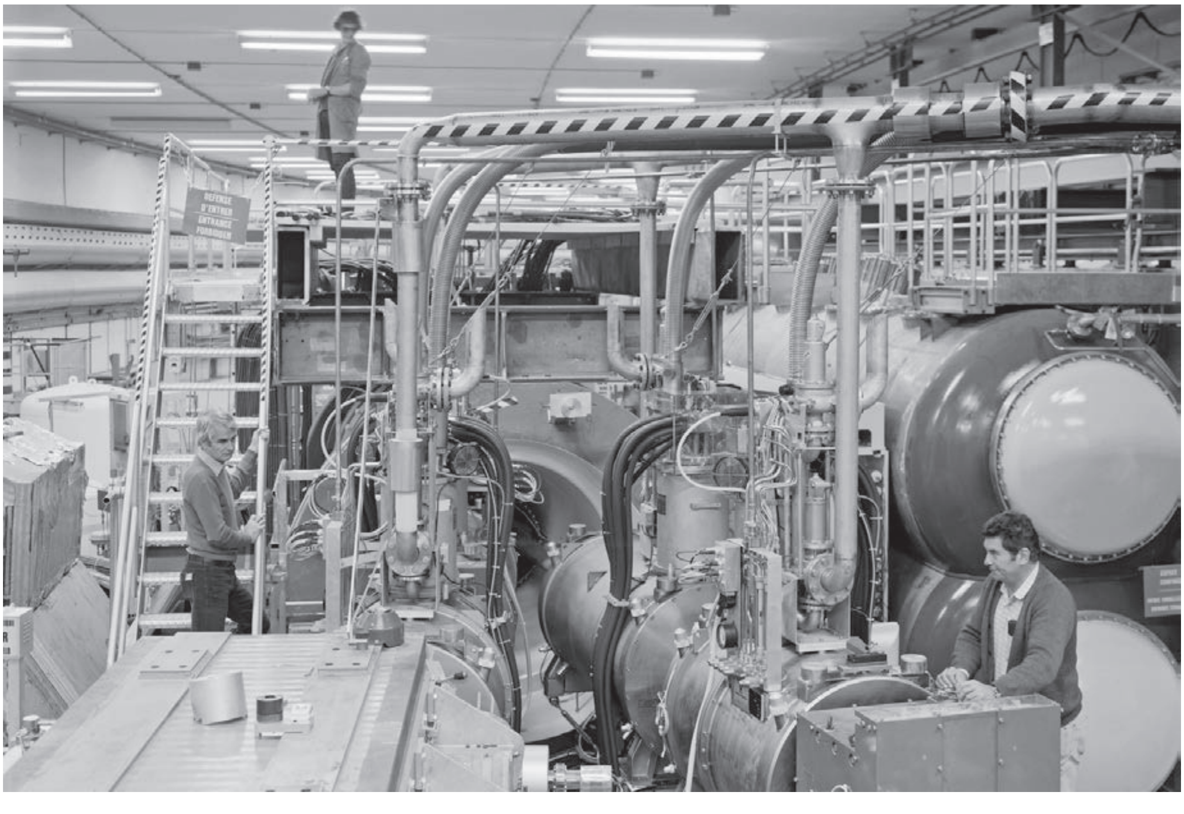

Fig. 9: Superconducting low-β insertion in Intersection 8 (1980)

At the start of a physics run in December 1982, the record luminosity of 1.4×10^{32} cm^{-2} s^{-1} was measured in the superconducting low-β insertion. This record was not beaten until 1991 by CESR at Cornell with 1.7×10^{32} cm^{-2} s^{-1}. Figure 10 shows the history of the maximum luminosity in the ISR over its working life. It is interesting to note that the design luminosity of 4×10^{30} cm^{-2} s^{-1} was reached within the first 2 years and thereafter rose by nearly 2 orders of magnitude.

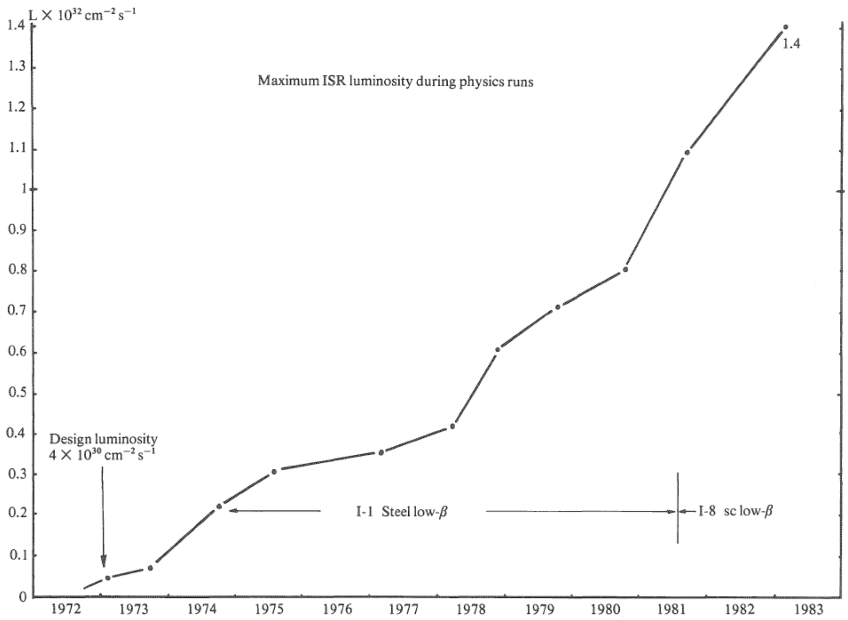

Fig. 10: History of the maximum luminosity in the ISR

Physics detector magnets

In 1965, colliding beam physics was more or less a blank page. In the official history of CERN, it was said that ISR was regarded by some as "an expensive small-angle scattering experiment for the PS". By the late 1970s, detector magnets with 4π acceptance were standard equipment for the ISR. The Superconducting Solenoid was installed in Intersection 1, the Open Axial Field Magnet was installed in Intersection 8 and an Air-cored Toroid in Intersection 6. This was effectively a single jump to today's technologies in just a few years. The principles had been established and only the scale of the equipment would increase further. The Open Axial Field Magnet (OAFM) is shown in Fig. 11 because it is perhaps the least well known of the examples.

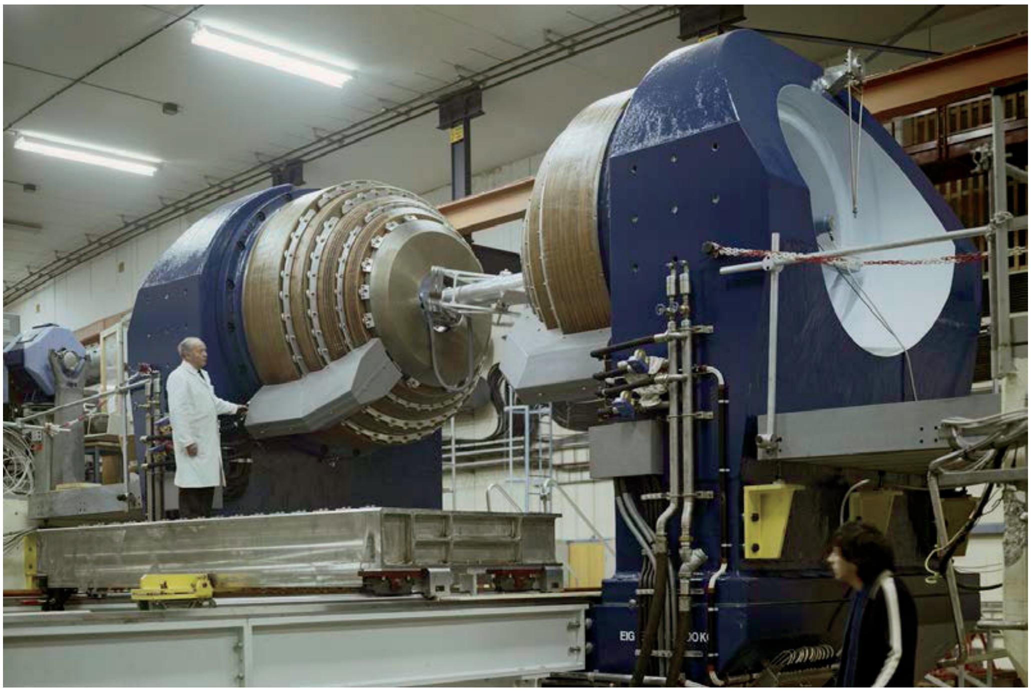

Fig. 11: The Open Axial Field Magnet in Intersection 8 (1979)

6 Vacuum

Base vacuum

The original design criterion stated that the lifetime imposed by gas scattering should be at least one order of magnitude longer than the time needed to fill the rings. This was interpreted as 10^{-9} torr in the arcs (using ion pumps) and 10^{-10} torr in the crossing regions (using cryo-pumps), although it was noted that 10^{-11} torr would be more desirable. The chamber itself was to be stainless steel bakeable to 300°C to 350°C, although initially it was only baked to 200°C. This made the ISR the world's largest ultra-high vacuum (UHV) system, which was an enormous challenge for the technology of the time. In fact, the pressure in the arcs was 10^{-10} torr (beams < 2 A) for the first run in January 1971, and 10^{-11} torr (beams < 2 A) was quickly reached in the crossing regions in 1972. In subsequent years, the pressure fell further to an average around the machine close to 10^{-12} torr. Figure 12 shows the evolution of the average pressure over the lifetime of the machine. This improvement meant that the principal source of background in the experiments became the beam losses from non-linear resonances. This led to hundreds of hours of machine development investigating working lines in the tune diagram, halo scraping exercises (called beam cleaning) and tests with cooling.

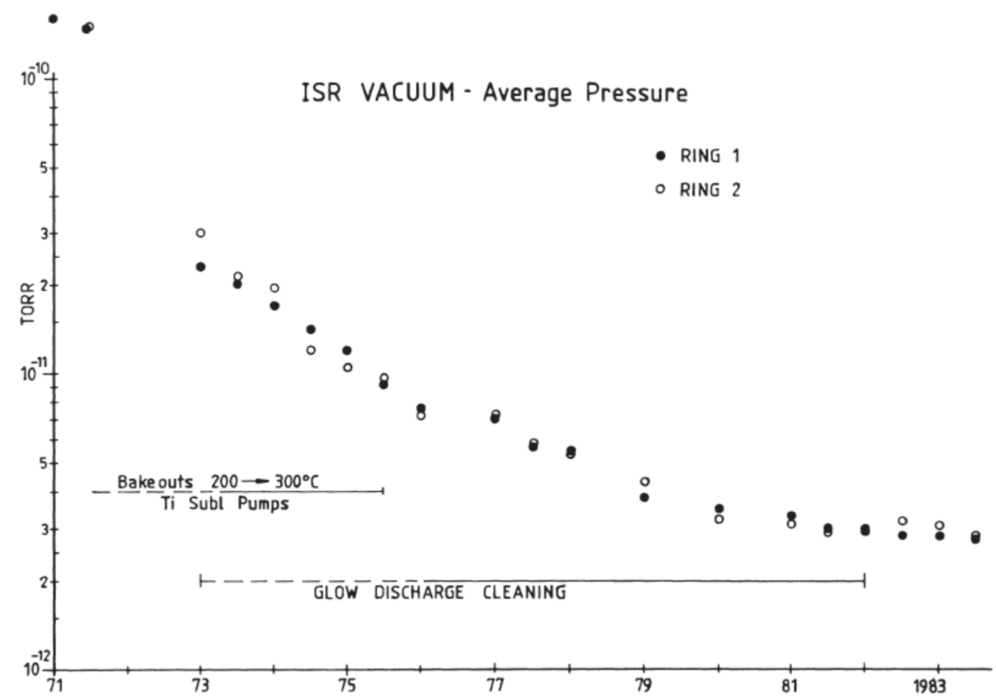

Fig. 12: Evolution of the average pressure in the ISR over its lifetime

Beam-induced vacuum instability

It was quickly discovered, however, that the beam and the vacuum could mutually destroy themselves in more ways than one. As the beam current increased, the residual gas was ionized and positive ions were repelled by the beam (the beam potential was typically 1 kV–2 kV) to crash into the chamber walls only to release adhered gas molecules that were in turn ionized by the beam to create a runaway effect that caused catastrophic beam loss. A staged programme to improve the vacuum system was started in 1971 and progressed over several years. Baking at 300°C and later at 350°C, instead of the initial 200°C helped and some 500 additional titanium sublimation pumps were added. The vacuum system was demounted arc by arc during shutdowns and cleaned using a new technique called glow-discharge cleaning. Later this was done in situ during bakeout by using the clearing electrodes to excite an argon discharge. Incredibly, a glow-discharged chamber could be opened to the air and left for many hours and still recover its ultra clean condition when pumped. This was the first demonstration of the efficiency of glow-discharge cleaning on a large scale [23].

Neutralization from ionization of residual gas

The unwanted neutralization caused by electrons trapped in the potential well of the beam following ionization of the residual gas was already mentioned in the introduction. The trapped charge would cause tune shifts and eventually beam instability. Bunched beams could, under the right circumstances, flush out such regions, but the only sure way was to install clearing electrodes. Although the ISR design had foreseen hundreds of these, the inadequacy of the clearing system was already evident in 1971 and many more electrodes had to be added. When the ISR became operational, it provided the perfect test bed for measurements and many papers were published on neutralization tune shifts, e–p instabilities, electron removal by RF clearing, and ion clearing in antiproton beams. A good pedagogic account is to be found in Ref. [24] which contains a large number of references to the ISR.

Vacuum system design philosophy

The ISR years saw another marked change in philosophy concerning vacuum systems. The '1965' design was based on ease of access with 'C' shaped magnets and bolted flanges for all sections of the vacuum system. When the TT6 transfer line was installed in the early 1980s to bring antiprotons into the ISR, the vacuum system was practically all welded. Changing a magnet meant cutting the chamber and re-welding; a philosophy that has been largely adopted by the LHC.

Thin-walled chambers

Another pioneering activity in the ISR was the design and production of large, thin-walled vacuum chambers for the intersection regions. Typically the chamber walls were 0.28 mm to 0.4 mm thick and the materials used were stainless steel and titanium. Figure 13 shows the example of a thin-walled chamber being installed in Intersection 7 in 1974. Beryllium was considered, but never used in the ISR; LHC has beryllium chambers in the physics intersections.

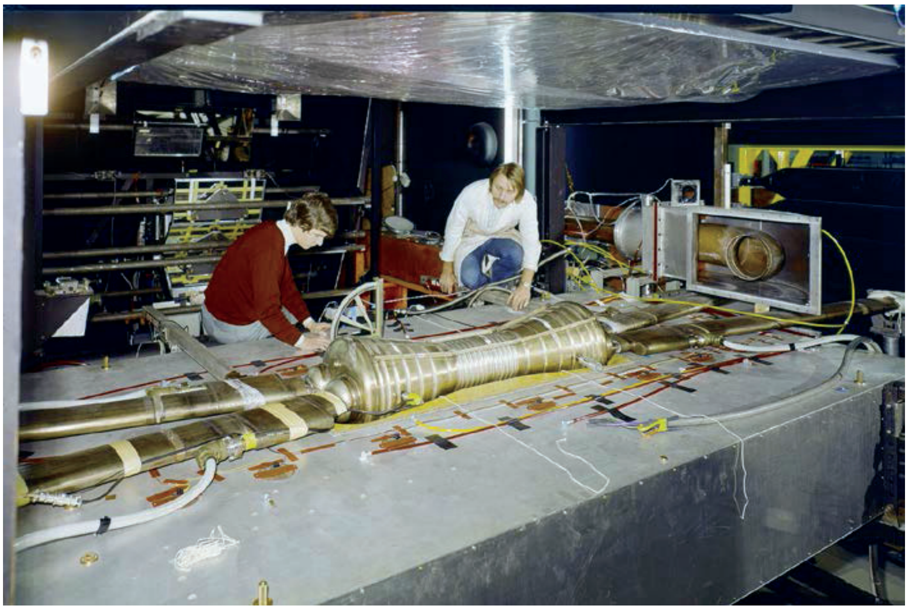

Fig. 13: Installing a thin-walled vacuum chamber in Intersection 7 (January 1974)

Vacuum accidents

By 1973 the ISR had suffered two catastrophic events caused by the beam burning holes in the vacuum chamber, see Fig. 14. Bellows were particularly vulnerable because each convolution would radiate onto its neighbour so the heat could only escape by conduction through the thin metal. This led to collimation rings being inserted in the flanges to protect the adjacent bellows. The thin-walled intersection chambers were also vulnerable to mechanical accidents as they were designed with small safety margins. The occasional collapse of such a chamber would leave a twisted sculpture and weeks of work to clean the contaminated arcs, see Fig. 15.

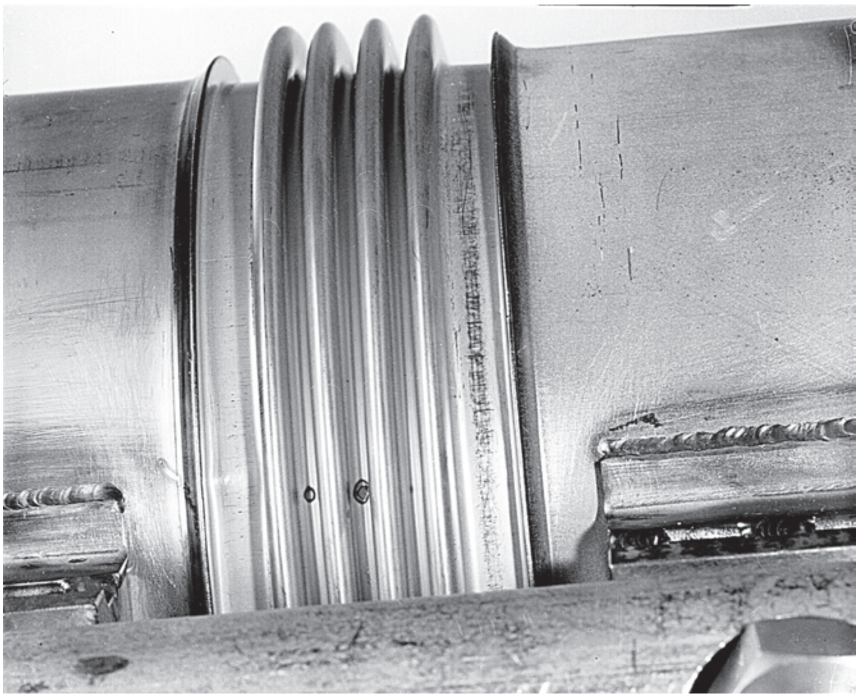

Fig. 14: Holes burnt by the beam in a bellows

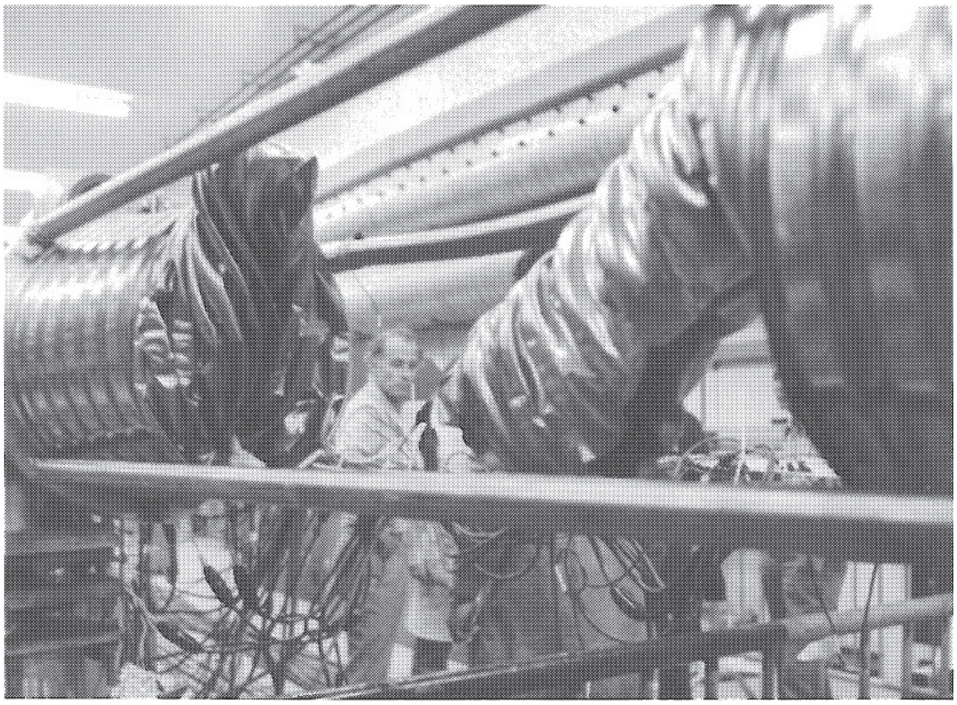

Fig. 15: The thin-walled (0.3 mm) titanium chamber in Intersection 7 implodes (1975)

7 Operation

Computer control

In 1965, the new dual Ferranti-Argus computers with a 16k core store of 24-bit words and a 1 μs store cycle time to a 640k disk store was not fully trusted and the control room was equipped with manual control panels some of which were physically locked by key to prevent unauthorized access. By the mid-term of the ISR attitudes had completely changed and a highly sophisticated control system was in place. Manual interventions were discouraged and automated procedures dominated physics operation, and for machine development high-level functions were used to control the machine.

Closed-orbit correction

One of the first operations to be carried out in any machine is the correction of the closed orbit. Two methods were developed for the ISR, out of which the algorithm MICADO [25] written by Bruno Autin was by far the more practical and efficient. MICADO was written into the COCO program [26] and after some years of development this became a de facto standard for many laboratories. The most advanced versions now have feedback loops and can be found in synchrotron light machines. A subject closely related to closed-orbit correction is injection optimization. After some years of development the ISR also had a sophisticated automatic injection procedure [27].

Luminosity calibration method

Luminosity calibration runs for the physics experiments were run as a semi-automatic procedure under computer control (LUMS program). The measurement method, which is still used today in the LHC, was invented in 1968 by Simon van der Meer, especially for the ISR colliding beam configuration [28]. The two beams are moved relative to each other in the vertical plane so that one beam effectively sweeps through the other while the interaction rate is monitored. The closed-orbit bumps used to move the beams were corrected for the coherent beam tune shift [29] and hysteresis in the so-called radial field magnets [30].

Stacking

Stacking in momentum space was an essential technique for accumulating the beam intensities needed to get a useful luminosity. In this scheme, proposed by MURA and tested in CESAR, the beam from the PS was slightly accelerated by the RF system in the ISR and the first pulse deposited at the highest acceptable momentum on an outer orbit in the relatively wide vacuum chamber. Subsequent pulses were added until the vacuum chamber was filled up to an orbit close to the injection orbit, which was on the inside of the chamber.

Phase displacement acceleration

Much of the operating life of the ISR was at 31.4 GeV/*c*, the maximum energy the magnet system could reach. After stacking at 26 GeV/*c* the coasting beams were accelerated by the novel method of phase-displacement acceleration first suggested by MURA, but first extensively used in the ISR. The technique consisted of moving empty buckets repeatedly through the stacked beam from high to low energy. In accordance with longitudinal phase-space conservation, the whole stack was accelerated while the magnet field was simultaneously increased to keep the stack centred in the vacuum chamber. It was necessary to make many hundreds of sweeps with the empty buckets, which required a low-noise RF system operating at a low voltage with a fine control of the high-stability, magnet power supplies to prevent excessive beam blow-up. One amusing feature of this system was that the current would increase slightly as a beam was accelerated, a testimony to the extremely low losses that occurred during this operation.

Other particles

The ISR was also able to store deuterons and alpha particles as soon as they became available from the PS, leading to a number of runs with p–d, d–d, p–α and α–α collisions from 1976 onwards. For CERN’s antiproton programme, a new beam line (TT6) was built from the PS to Ring 2 for antiproton injection. The first p–pbar runs took place in 1981. The ISR’s final runs in 1984 were dedicated to a 3.5 GeV/*c* antiproton beam colliding with a gas-jet target.

8 Diagnostics

Schottky noise and stochastic damping

If just one key discovery in the field of accelerator physics has to be singled out, then it would be Schottky noise — a statistical signal generated by the finite number of randomly distributed particles in a beam — which is well known to designers of electronic tubes. Simon van der Meer had worked on stochastic damping in 1968, but his ideas had seemed too far-fetched at that time. This changed in

1972 when Wolfgang Schnell actively looked for and found the longitudinal and transverse Schottky signals at the ISR [31], see Fig. 16. This prompted van der Meer to publish his work from 1968 about Schottky noise and the possibility of stochastic damping [32], opening new vistas for non-invasive beam diagnostics and active cooling systems for reducing the size and momentum-spread of a beam.

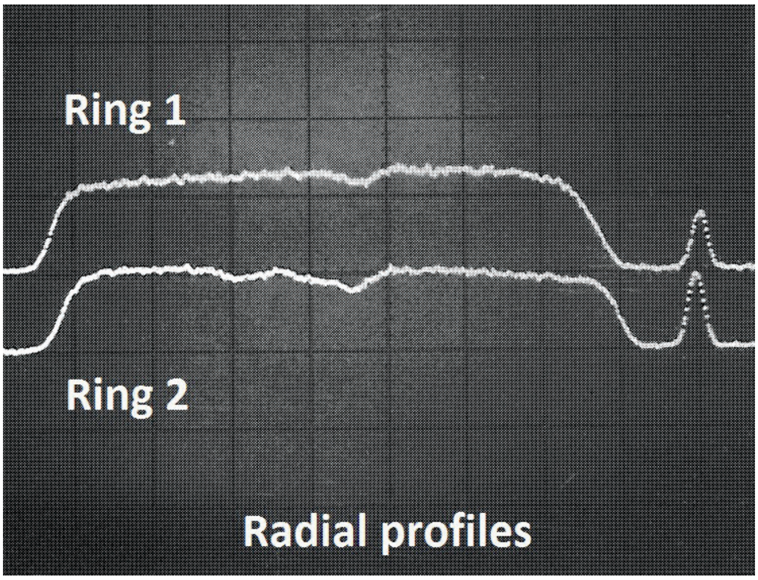

Fig. 16: First longitudinal Schottky results from the ISR (CERN Annual Report 1972, p. 109)

The longitudinal Schottky signal made it possible to measure the current density in the stack, without perturbing it, as a function of the momentum (transverse position), while the transverse Schottky signals gave information about how the density of the stack varied with the betatron frequency, or 'tune'. The combination of the two types of scan yielded a complete picture of the beam in the tune diagram, see Fig. 17, and the current density through the stack. These scans clearly show the beam edges and any markers. A marker could be created by using phase-displacement to accelerate part of the stack to create a narrow region of low current density, or by losses on resonances.

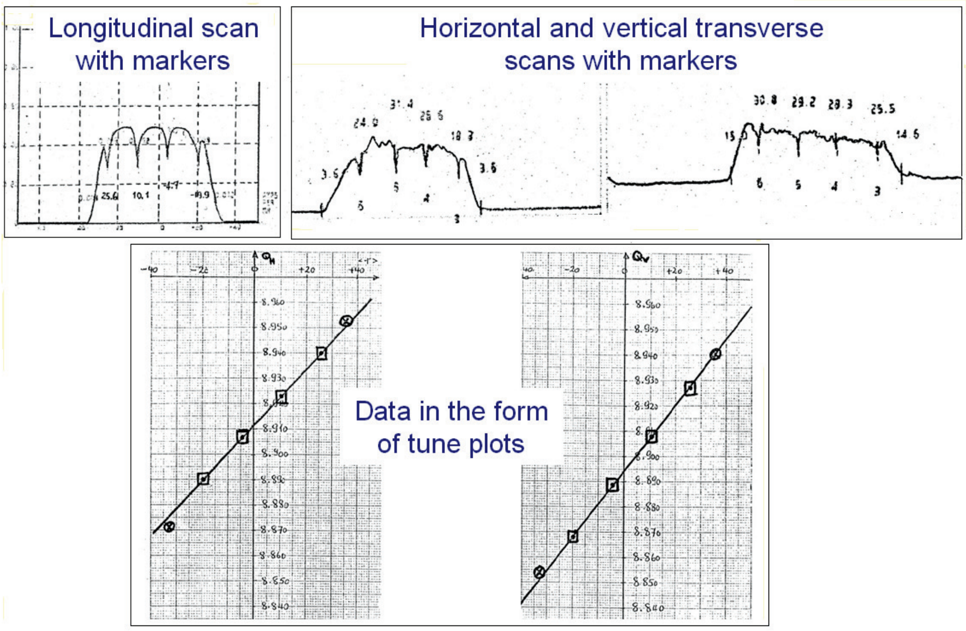

Fig. 17: Longitudinal and transverse Schottky scans used for beam diagnostics (ISR Performance report, S. Myers, 1977)

Stochastic cooling (damping)

The possibility of damping the betatron oscillations was experimentally demonstrated in the ISR in 1974 [33], see Fig. 18. Towards the end of the ISR's life, stochastic cooling was routinely used to cool antiproton beams in order to increase the luminosity in antiproton–proton collisions by counteracting the gradual blow-up of the antiproton beam through scattering with residual gas as well as resonances. Furthermore, stochastic cooling was the decisive factor in the conversion of the SPS to a p–pbar collider and hence in the discovery in 1983 of the long-sought-after W and Z bosons. Simon van der Meer and Carlo Rubbia shared the Nobel Prize in Physics in 1984.

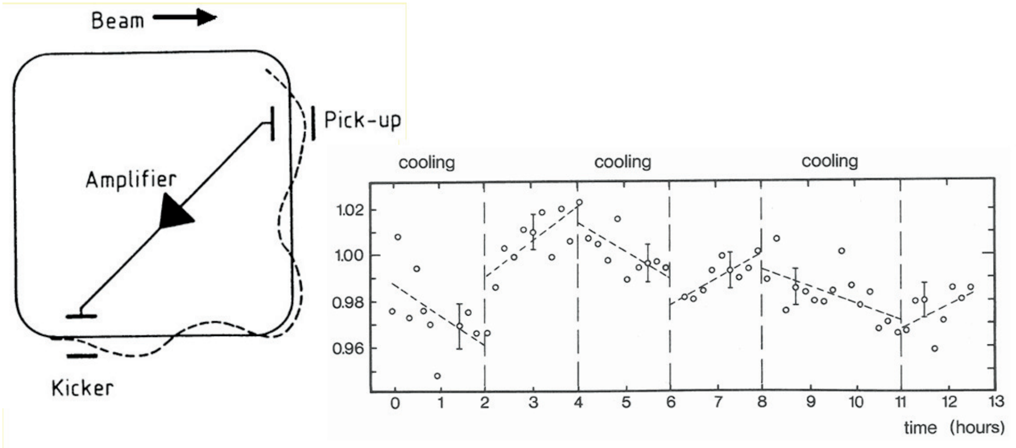

Fig. 18: Early results showing cooling in the ISR (CERN Annual Report 1974, p. 97)

Stochastic cooling became the cornerstone for the success, not only of the p–pbar collider in the SPS, but also for the more powerful Tevatron at Fermilab. CERN's low-energy antiproton programmes in the Low Energy Antiproton Ring and the Antiproton Decelerator, as well as similar programmes at GSI in Germany and at Brookhaven in the US, also owe their existence to stochastic cooling. The extension to bunched beams and to optical frequencies makes stochastic cooling today a basic accelerator technology.

Direct-current beam transformer

The ISR was also the home of the zero-flux, direct-current transformer (DCCT) [34], see Fig. 19. This device became another de facto world standard. Beam current monitors of this type developed at CERN in 1981 and 1990 became national primary standards in Germany, certified and operated by the PTB (Physikalisch-Technische Bundesanstalt) in Berlin.

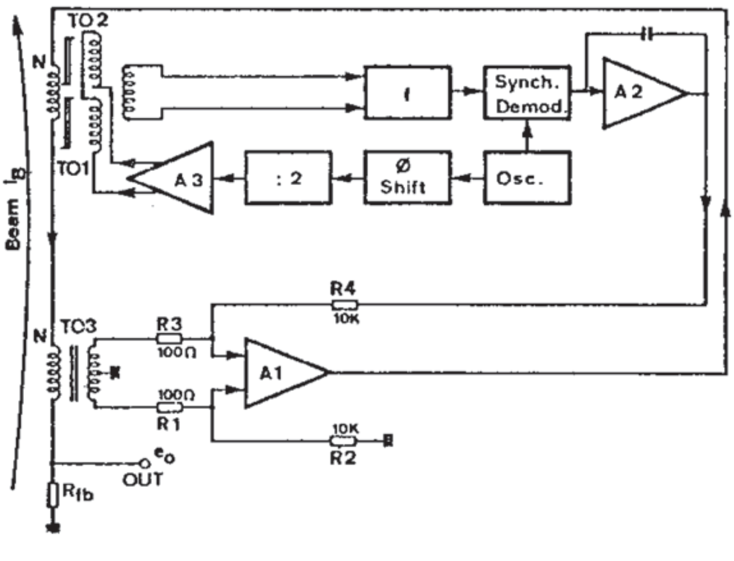

Fig. 19: Original zero-flux DCCT

9 Beam–chamber interaction

'Brick wall' instability

Shortly after the start of the ISR a coherent transverse instability was observed that limited the beam intensity. This phenomenon was dubbed the 'brick wall' instability [35], Fig. 20. The intensity would increase while stacking to around 3 A where there would be a sudden loss of 10% to 15% of the beam after which stacking would resume only to have a repeat beam loss at around the 3 A level. This gave a sawtooth pattern on the accumulated current that appeared to be knocking against a 'brick wall'. The phenomenon was due to the resistive wall instability [36] and it had been correctly predicted that a tune spread of 2 would stabilise the beams [37]. The additional tune spread was applied and the effect disappeared. Studies of the shape of the working line in the tune diagram revealed how the action of tune shifts induced by space-charge loading could destroy the tune spread and hence the stability of the beam (see insert in Fig. 20). From these beginnings, the ISR spawned tens of papers on incoherent and coherent space-charge tune shifts on central and off-axis orbits in variously shaped chambers and the correction of these effects.

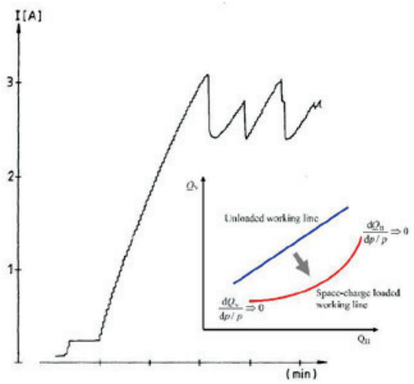

Fig. 20: Brick wall instability

Pre-calculated and on-line space-charge corrections

The first space-charge corrections to the working line in the tune diagram used the nominal beam density in momentum space to build a set of 'pre-stressed' working lines that when loaded with space charge would have the ideal shape and tune spreads for stability [38], see Fig. 21, but once longitudinal Schottky scans became operational the true current density could be measured at any time, the tune shifts with radial position calculated and the necessary poleface winding currents calculated and applied. Typically, these corrections would be performed every 3 A by a semi-automated procedure called QCOM [39]. This procedure was unique and so successful that currents of many tens of amperes could be safely accumulated. The maximum current recorded in a single ring was 57 A at 26 GeV/*c* and physics beams were typically 30–40 A at 31.4 GeV/*c*.

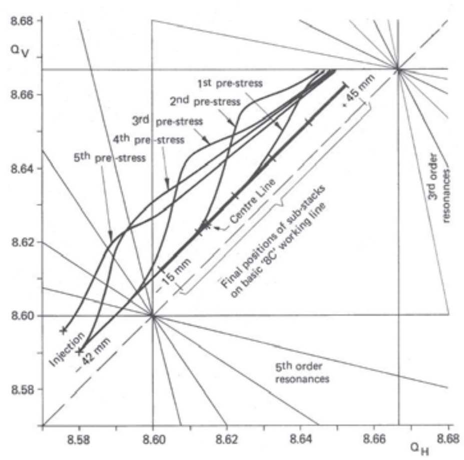

Fig. 21: Pre-calculated, pre-stressed working lines

Impedance and stability criteria

The ISR was the ideal machine for studies on beam impedance and stability. There were many publications, but some notable topics were the now widely-used longitudinal Keil–Schnell criterion [40], the Schnell–Zotter criterion for the transverse plane [41], and Landau damping.

10 Beam–beam interaction

In 1973, Eberhard Keil wrote a short note entitled "Why be afraid of magnet imperfection resonances in high luminosity storage rings?" [42]. He was referring to the beam itself being, in most cases, a stronger source of resonance excitation and one that excites all orders since a Gaussian distribution can be expressed as an infinite power series. The ISR was an ideal and unique test bed for the study of coasting and bunched beams colliding at a small angle. These results were compared at length with those from electron–positron machines and helped to guide the design of future colliders. A large number of papers were published and a useful introduction is given in Ref. [43]. As part of the beam-beam studies the ISR was also equipped with a non–linear lens [44].

11 Others topics

The above is far from an exhaustive list. The ISR was also used for the study of intra-beam scattering and overlap knockout resonances. Other examples of special beam equipment are the transverse feedback systems and the scrapers for beam cleaning. Moving more to the physics, there was the development of the Roman pots. Today there is a strong emphasis on technology transfer and the ISR also has examples of this such as the Digital Teslameter designed by Klaus Brand and commercialized by a company in Geneva [45].

12 Conclusion

The ISR was a major project with a large experienced staff that had the critical mass to spontaneously generate new ideas and the capacity to follow them up. It attracted visitors, students, fellows, experts on sabbatical leave and many others all of whom helped to catalyse progress. The timing of the project was such that the world-wide community was poised to advance to what we would now recognise as 'modern' accelerators. One could argue that many of the topics described would have occurred whether the ISR was a collider or just a plain synchrotron, but much of what has been described depends rather strongly on the particular attributes of the ISR. Schottky noise exists in a bunched beam, but it is less likely to be discovered. The exceptionally large momentum spread of the ISR pushed the studies of tune shifts, coupling and chromaticity schemes into more detail. The colliding beam geometry was essential for beam–beam studies. Colliding beam physics would certainly have been seriously held back without this full-scale test stand for experimentation. In short, the ISR looked into the part of parameter space that would be needed for the next step in high-energy physics. It was the right machine at the right time. This appears logical now, but it was a brave decision at the time.

References

[1] The CERN Study Group on New Accelerators, Report on the Design Study of Intersecting Storage Rings (ISR) for the CERN proton synchrotron, CERN AR/Int. SG/64–9 (May 1964).

[2] R. Hagedorn, Stability and amplitude ranges of two dimensional non-linear oscillations with periodical Hamiltonians, CERN 57–1 (March 1957).

[3] A. Schoch, Theory of linear and non-linear perturbations of betatron oscillations in alternating gradient synchrotrons, CERN 57–23 (February 1958).

[4] B. Angerth, Review of studies on beam neutralisation in storage rings, CERN AR/Int. SG/65–1 (1965).

[5] SCISR Study Group, Superconducting Conversion of the Intersecting Storage Rings, CERN 77–20 (December 1977).

[6] E. Keil, *Single particle dynamics – linear machine lattices*, *in* Theoretical Aspects of the Behaviour of Beams in Accelerators and Storage Rings, CERN 77–13 (July 1977), pp. 22–31.

[7] B. Zotter, Calculations of the parameters of a quadrupole triplet from the transfer matrices, CERN/ISR-TH/73–43 (September 1973).

[8] K. M. Terwilliger, *Achieving higher beam densities by superposing equilibrium orbits*, Proc. 2nd Int. Conf on High-Energy Accelerators and Instrumentation, CERN, Geneva,1959, L. Kowarski (ed.) (CERN, Geneva, 1959), pp. 53–57.

[9] P. J. Bryant, The creation of small interaction diamonds in the CERN Intersecting Storage Rings (ISR*)*, CERN/ISR-MA-73–5 (1973).

[10] J.-P. Gourber, E. Keil, and S. Pichler, The first high-luminosity insertion in the ISR, ISR-MA-75–8 (1975).

[11] A. Garren and J. W. Eusebio, SYNCH: A computer system for synchrotron design and orbit analysis, UCID-10153, AS/Theoretical/03 (April 1965).

[12] E. Keil and P. Strolin, AGS: The ISR Computer System for Synchrotron Design and Orbit Analysis, CERN 69–5 (March 1969).

[13] G. Burton, M. Hanney, and P. Strolin, BEATCH: a Fortran programme for the particle optics of beam transfer channels, CERN-ISR-BT-TH-69–27 (1969).

[14] C. Iselin, The MAD program, CERN-LEP/TH/83–20 (August 1983).

[15] R. Perin and S. van der Meer, The Program MARE for the Computation of Two-Dimensional Static Magnetic Fields, CERN 67–7 (1967).

[16] S. Caeymaex, MIMI: a computer program for three-dimensional magnetic field problems, CERN-ISR-MA-70–19 (1970).

[17] G. Guignard, The General Theory of all Sum and Difference Resonances in a Three-Dimensional Magnetic Field in a Synchrotron, CERN 76–06 (1976).

[18] P. L. Morton, Unpublished addendum to Internal SLAC report SR-11 (July 1966).

[19] P. J. Bryant, The revised skew quadrupole system for coupling compensation in the CERN Intersecting Storage Rings, CERN-ISR-BOM-79–16 (1976).

[20] P. J. Bryant, P. Galbraith, J. P. Gourber, G. Guignard, and K.Takikawa, Measurement of the excitation of the coupling resonance $Q_h - Q_v = 0$, CERN/ISR-BOM-77–4 (1974).

[21] L. Resegotti, Superconducting low-beta insertion and high luminosity prospects at ISR, CERN ISR-BOM/77–58 (1977).

[22] J. Billan, K. N. Henrichsen, H. Laeger, P. Lebrun, R. Perin, S. Pichler, P. Pugin, L. Resegotti, P. Rohmig, T. Tortschanoff *et al.*, *A superconducting high-luminosity insertion in the Intersecting Storage Rings (ISR)*, Proc. 11th Int. Conf. on High-Energy Accelerators, Geneva, Switzerland, 1980, W. S. Newman (ed.) (Birkhäuser, Basel, 1980), pp. 848–52.

[23] A. W. Jones, E. Jones, and E. M. Williams, *Investigation by techniques of electron stimulated desorption of the merits of glow discharge cleaning of the surfaces of vacuum chambers at the CERN intersecting storage rings*, Vacuum, 23 (1973) 227–30.

[24] Y. Baconnier, *Neutralisation of accelerator beams by ionization of the residual gas*, Proc. CERN Accelerator School: General Accelerator Physics, Gif-sur-Yvette, 1984, CERN 85–19 (1985), pp. 267–300.

[25] B. Autin and Y. Marti, Closed orbit correction of AG machines using a small number of magnets, CERN ISR-MA/73–17 (March 1973).
[26] B. Autin, Run 711 - 27 April 1976, Ring 1 - 11.776 GeV/*c* - 8C working line, Test of COCO program, ISR-MA/BA/rh (April 1976).
[27] L. Vos, *Automated injection procedure for the CERN Intersecting Storage Rings (ISR)*, Proc. 9th Particle Accelerator Conf., Washington, DC, USA, 1981, IEEE Trans. Nucl. Sci. 28 (1981) 3031–3.
[28] S. van der Meer, Calibration of the effective beam height in the ISR, CERN-ISR-PO-68–31 (1968).
[29] P. J. Bryant, Space charge corrections for LUMS, ISR-MA/PJB/cd (August 1973).
[30] T. Taylor, Run 246 - Tests of the importance of hysteresis in the radial field magnets for luminosity measurements, ISR-MA/TMT/rh (November 1972).
[31] J. Borer, P. Bramham, H. G. Hereward, K. Hübner, W. Schnell, and L. Thorndahl, *Non-destructive diagnostics of coasting beams with Schottky noise*, Proc. 9th Int. Conf. on High-Energy Accelerators, Stanford, SLAC, 1974 (A.E.C., Washington, DC, 1974), pp. 53–6.
[32] S. van der Meer, Stochastic damping of betatron oscillations in the ISR, CERN/ISR-PO/72–31 (August 1972).
[33] P. Bramham, G. Carron, H. G. Hereward, K. Hübner, W. Schnell and L. Thorndahl, Stochastic cooling of a stored proton beam, NIM 125 (1975), pp. 201.
[34] K. Unser, Beam current transformer with DC to 200 MHz range, ISR-CO/69–6 (March 1969).
[35] K. Johnsen, *The ISR and accelerator physics*, Part. Accel. 18 (1986), 167–182.
[36] L. J. Laslett, V. K. Neil, A.M. Sessler, *Transverse resistive instabilities of intense coasting beams in particle accelerators*, Rev. Sci. Instr., 36 (1965), pp. 436.
[37] K. Hübner, P. Strolin, V. G. Vaccaro, and B. Zotter, Concerning the stability of the ISR beam against coherent dipole oscillations, CERN/ISR-RF-TH/70-2 (1970).
[38] P. J. Bryant, Dynamic compensation during stacking of the de-tuning caused by space charge effects, CERN/ISR-MA-74-17 (1974).
[39] P. J. Bryant, D. M. Lewis, B. Nielsen, and B. Zotter, On-line correction of the incoherent tune shifts due to space charge, CERN/ISR-MA-75-54 (1975).
[40] E. Keil and W. Schnell, Concerning longitudinal stability in the ISR, CERN/ISR-TH-RF/69–48 (July 1969).
[41] W. Schnell and B. Zotter, A simplified criterion for transverse stability of a coasting beam and its application to the ISR, CERN ISR-GS-RF/76–26 (July 1976).
[42] E. Keil, Why be afraid of magnet imperfection resonances in high luminosity stage rings, CERN/ISR-TH/73–25 (1973).
[43] E. Keil, *Beam-beam interactions in p-p storage rings*, 1st Int. School of Particle Accelerators, 'Ettore Majorana', Erice, Italy, 1976. M. H. Blewett (ed.), CERN 77–13, pp. 314–40.
[44] E. Keil, Effects of a non-linear lens on the stored proton beam in the ISR, CERN-ISR-TH-GE-75–178 (1975).
[45] K. Brand and G. Brun, A Digital Teslameter, CERN 79–02 (1979).

Small-angle physics at the intersecting storage rings forty years later

Ugo Amaldi

University Milano Bicocca and TERA Foundation

1 Hadron–hadron cross-sections at the beginning of the 1970s

The first surprising 'small-angle physics' result produced at the Intersecting Storage Rings (ISR) was the announcement that the proton–proton total cross-section was not constant over the newly opened energy range. Since the present report is not a review paper but a personal recollection on the beginnings of ISR physics, I start by underlining that, forty years later, it is difficult to describe and explain the surprise and scepticism with which the news of the 'rising total cross-section' was received by all knowledgeable physicists. Among the many episodes, I vividly recall what Daniele Amati told me while walking out of the CERN Auditorium after the seminar of March 1973 in which I had described the results obtained independently by the CERN–Rome and Pisa–Stony Brook Collaborations: 'Ugo, you must be wrong, otherwise the pomeron trajectory would have to cut the axis above 1!'

Nowadays, all those who still care about the pomeron know the phenomenon, find it normal and accept the explanations of this fact given by the experts. But at that time the reggeon description of all small-angle hadronic phenomena was the only accepted dogma since it could explain the main experimental results in hadronic physics: (i) the tendency of the total cross-sections of all hadron–hadron collisions to become energy independent; and (ii) the 'shrinking' of the forward differential cross-sections when the collision energy was increasing.

The second phenomenon was discovered in 1962 by Bert Diddens, Alan Wetherell *et al.*, who were studying proton–proton collisions at the CERN Proton Synchrotron (PS) [1]. They found that the forward proton–proton differential elastic cross-section at small centre-of-mass angles $\theta_{\rm cm}$ (i.e., at small momentum transfers $q = cp_{\rm cm} \sin \theta_{\rm cm}$ usually measured in GeV) is proportional to $\exp(-Bq^2)$, with a slope parameter B that *increases* with the centre-of-mass energy, indicating, through the uncertainty principle, that the proton–proton interaction radius *increases* as $\sqrt{B}$.

As far as the first point is concerned, it was later said that the results shown in Fig. 1 – which had been obtained in the early 1970s at the Protvino 70 GeV synchrotron [2] – were already showing that the Regge model could not describe the rise of the K^+–proton cross-section with energy.

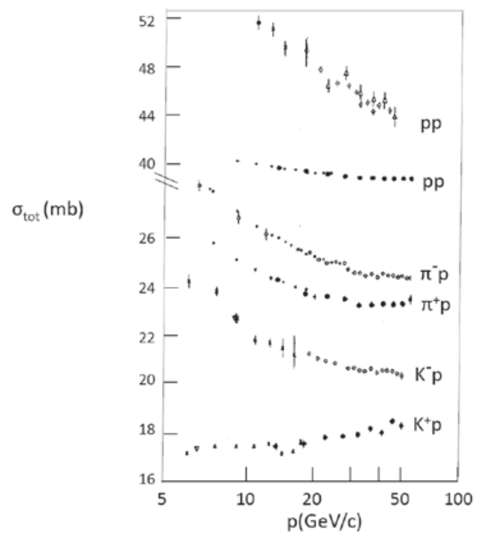

Fig. 1: The total cross-sections $\sigma_{\rm tot}$ (measured in the early 1970s at the Serpukhov 70 GeV synchrotron and at lower-energy accelerators) plotted versus the laboratory proton momentum p [2]

However, these experimental results were immediately interpreted in the framework of the Regge model, and even the authors did not conclude that there was an indication of an anomaly in the energy dependence of the cross-section of this particular channel. With reference to Fig. 1, in the paper by Denisov *et al.* [2], which was also signed by Jim Allaby and Giorgio Giacomelli and was received by *Physics Letters* in July 1971 – three months after the ISR start-up – one can read: 'This figure suggests that the total cross-section for K^+–p will approach the asymptotic value from below … unless the cross-section oscillates in value.'

The regime in which all the total cross-sections would become energy independent was called 'asymptopia', and theorists and experimentalists alike were convinced that the ISR would demonstrate that the total proton–proton cross-section, which slightly decreases in the Serpukhov energy range (Fig. 1), would tend to a constant of about 40×10^{-26} cm^2 (40 mb), thus confirming the mainstream interpretation of all hadronic phenomena, the Regge model, to be discussed in the next section.

2 The theoretical framework

As far as the hadronic forward differential cross-sections were concerned, they had found a universally accepted interpretation in terms of the collective effect of the exchanges of all the particles, which, in the mass^2–spin plane, lay on a Regge 'trajectory'. In Fig. 2, the present knowledge of the ρ trajectory is reported [3].

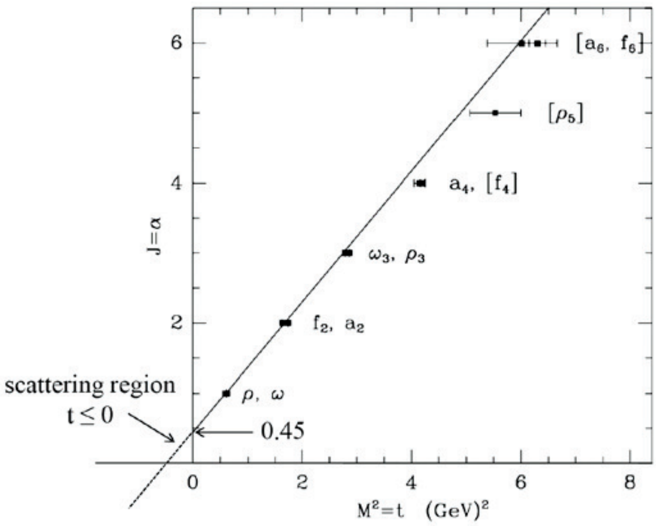

Fig. 2: The present situation of the Chew–Frautschi plot shows that the Regge trajectory containing the ρ meson (mass = 770 MeV) is practically linear up to very large masses

The exchange of the ρ trajectory dominates the charge-exchange cross-section of Fig. 3a. By using the usual parameter $s = E_{\mathrm{cm}}^2$, where E_{cm} is the centre-of-mass energy, the recipes of the Regge model give a cross-section that varies as $s^{\alpha(t=0)-1}$.

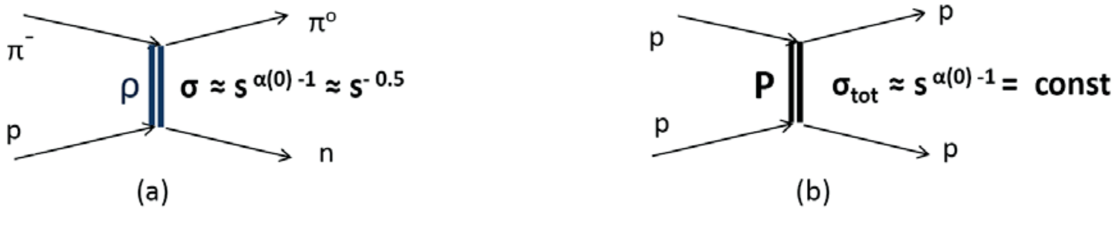

Fig. 3: (a) The main contribution to the pion charge-exchange phenomenon is the exchange of the ρ trajectory. (b) In the Regge model, the exchange of a pomeron trajectory is the dominant phenomenon in all high-energy elastic collisions.

Since, in Fig. 3a, $\alpha(0) \approx 0.5$, the charge-exchange cross-section was predicted to vary roughly as $s^{-0.5} = 1/E_{\mathrm{cm}}$. In the 1960s the experimental confirmation of this prediction was one of the strongest arguments in favour of the Regge description of the scattering of two hadrons. Such a description is still used because these phenomena cannot be computed with quantum chromodynamics – the strong interacting theory of the fundamental components of all hadrons.

A second argument concerned the differential cross-sections $\mathrm{d}\sigma/\mathrm{d}|t|$, which defines the behaviour of the trajectory in the region of the plot in Fig. 2 indicated as 'scattering region', where the variable m^2 becomes $t = -q^2$.

At the time that the rising cross-section was reported, accurate preliminary data on the charge-exchange differential cross-section were coming once again from Yuri Prokoshkin's group working at the Serpukhov accelerator [4]. Figure 4 shows how well the data in the 'scattering region' of Fig. 2 join the slope value of the ρ trajectory in the positive m^2 region.

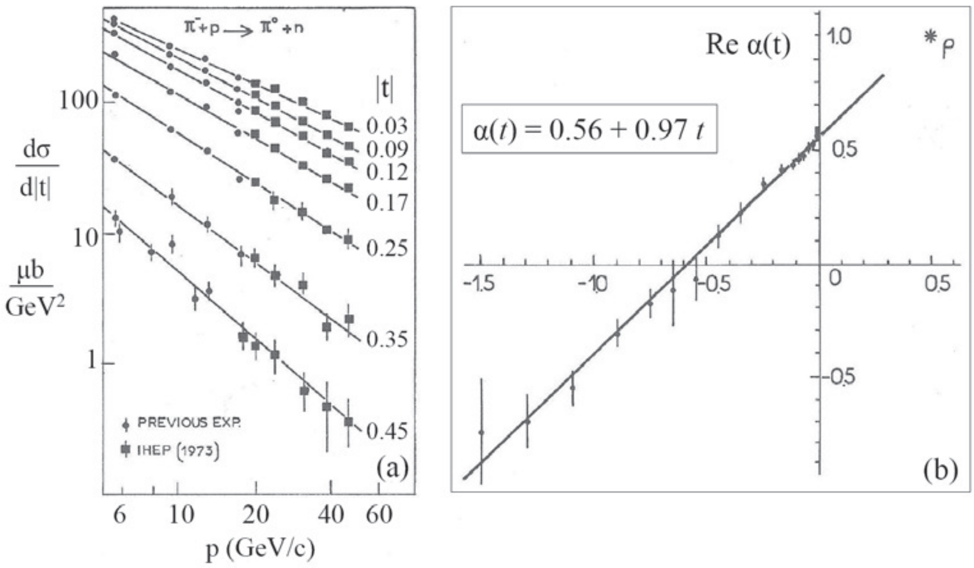

Fig. 4: (a) The exchange of a linear ρ trajectory fits the experimental data very well [4]. (b) In this experiment, the trajectory was found to be linear in the range $-1.5 \leq t \leq 0$ GeV^2 and the derivative of $\alpha(t)$ was measured to be $\alpha'(0) = 1$ GeV^{-2} at $t = 0$.

As shown in Fig. 3b, in the Regge approach, the proton–proton scattering process was also described by the exchange of a trajectory, the pomeron, which, given the proportionality of σ_{tot} to $s^{\alpha(t=0)-1}$, had to have the value $\alpha_{\mathrm{p}}(t = 0) = 1$ to be consistent with an energy-independent total cross-section. For this reason, at the beginning of the 1970s, the so often heard 'asymptopia' and 'the pomeron intercept is equal to 1' were used as different ways of saying the same thing.

Since there were no particles belonging to the pomeron trajectory, its slope could be fixed only by measuring the t dependence of the forward elastic proton–proton cross-section, as done for the exchange cross-section with the data of Fig. 4. Here we meet the already quoted argument in favour of the reggeon model: the forward proton–proton elastic cross-section could be described by the simple exponential $\exp^{-B|t|}$ and that the 'slope' B *increases* with the centre-of-mass energy. This is described by saying that 'the forward peak shrinks with energy', a statement that we now know applies to most high-energy differential cross-sections.

The shrinking of the forward peak measured at Serpukhov confirmed earlier data and indicated that the slope of the pomeron trajectory is about three times smaller than that of the ρ trajectory, which is about 1 GeV^{-2} (Fig. 4b). At the time the ISR was constructed, the determination of the slope B – easy to measure in a new and large energy range – was considered a very important issue.

In parallel with this 't-channel' description, other theorists, working on the 's-channel description', were deriving rigorous mathematical consequences from the fundamental properties of the S-matrix, which describes the scattering processes: unitarity, analyticity and crossing. Unitarity of the S-matrix implies that one can compute the imaginary part of the forward scattering amplitude $\mathrm{Im}\, f(t)$ by taking the product of a scattering amplitude and its conjugate and summing them over all possible intermediate states, as graphically depicted in Fig. 5.

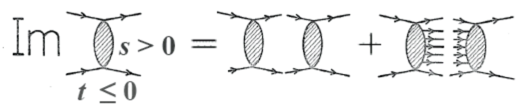

$$4\pi\, \mathrm{Im}\, f(t)/k = G_{\mathrm{el}}(t) + G_{\mathrm{in}}(t).$$

$$\textbf{For } t = 0\textbf{:}\ 4\pi\, \mathrm{Im}\, f(0)/k = \sigma_{el}(s) + \sigma_{inel}(s) = \sigma_{tot}(s)$$

Fig. 5: The graphical representation of the unitarity relation, at a given s and for $t \leq 0$, explains the definition of the elastic and inelastic overlap integrals $G_{\mathrm{el}}(t)$ and $G_{\mathrm{in}}(t)$. In the equations, $k = p/\hbar$.

The sum is made up of two contributions, which are called 'elastic and inelastic overlap integrals' $G_{\mathrm{el}}(t)$ and $G_{\mathrm{in}}(t)$. In the forward direction, i.e., for $t = 0$, the overlap integrals reduce to the elastic and inelastic cross-sections, and the unitarity relation gives the 'optical theorem', which states that the imaginary part of the forward scattering amplitude equals the total cross-section σ_{tot}, except for a factor $4\pi/k$, which depends on the definition chosen for the amplitude itself.

The figure and the formulae indicate that hadron–hadron forward elastic scattering is determined by the amplitudes of both elastic and inelastic reactions. When the collision energy is large, there are many opened inelastic channels, the incoming wave is absorbed and the elastic scattering amplitude is dominated by its imaginary part, which is the 'shadow' of the elastic and inelastic processes. In such a *diffraction phenomenon*, the ratio $\rho = \mathrm{Re}(f)/\mathrm{Im}(f)$ between the real and imaginary parts of the elastic amplitude is expected to be small, so that, in the expression for the forward elastic cross-section deduced from the optical theorem,

$$\left(\frac{d\sigma_{\mathrm{el}}}{d|t|}\right)_{t=0} = \frac{(1+\rho^2)\,\sigma_{\mathrm{tot}}^2}{16\pi} \qquad \text{with} \quad \rho = \frac{\mathrm{Re}\, f(0)}{\mathrm{Im}\, f(0)}\,,$$

the term ρ^2 is of the order of a few per cent.

Combining unitarity with analyticity and crossing, in the 1960s three important theorems had been demonstrated.

- The *Pomeranchuk theorem* [5] states that, in the limit $s \to \infty$, the hadron–hadron and the antihadron–hadron cross-sections become equal.
- According to the *Froissart–Martin theorem* [6, 7] the total cross-section should satisfy the bound

  $$\sigma_{\mathrm{tot}} \leq C \ln^2(s/s_0) \approx 60 \text{ mb} \ln^2(s/s_0)$$

  where the numerical value $C = \pi(\hbar/m_\pi)^2$ is determined by the mass of the pion, which is the lightest particle that can be exchanged between the two colliding hadrons, and s_0 is usually taken equal to 1 GeV^2.
- Finally, the *Khuri–Kinoshita theorem* [8] relates the energy dependence of ρ with the energy dependence of the total cross-section by stating that, if σ_{tot} increases with energy, ρ passes from small negative values to positive values. This is a consequence of the 'dispersion relations', which connect the real part of the forward elastic amplitude with some appropriate energy integrals of the total cross-section. Khuri and Kinoshita showed that, if σ_{tot} follows the Froissart–Martin bound and increases proportionally to $\ln^2 s$, for $s \to \infty$, the ratio ρ is *positive* and tends to zero from above towards the horizontal axis proportionally to $\pi/\ln s$.

In summary, the reggeon (t-channel) description of hadron–hadron collisions and the theorems derived from the properties of the S-matrix were the theoretical tools available at the end of the 1960s to experimental physicists interested in total cross-sections and small-angle physics.

3 Three proposals

In March 1969 the ISR Committee received three proposals that are relevant to the subjects discussed in this paper.

The title of the proposal by the Pisa group (signed by G. Bellettini, P.L. Braccini, R.R. Castaldi, C. Cerri, T. Del Prete, L. Foà, A. Menzione and G. Sanguinetti) was ‘Measurements of the p–p total cross section’ [9]. Two of their figures are reproduced in Fig. 6. The very large scintillator hodoscopes would detect the outgoing particles and count the total number of events. Moreover, the small-angle telescope, not shown in the figure, would detect forward elastic events and extrapolate to zero scattering angle the differential cross-section to estimate the number of elastic events not recorded because the protons, scattered at small angles, would be lost in the ISR vacuum chamber.

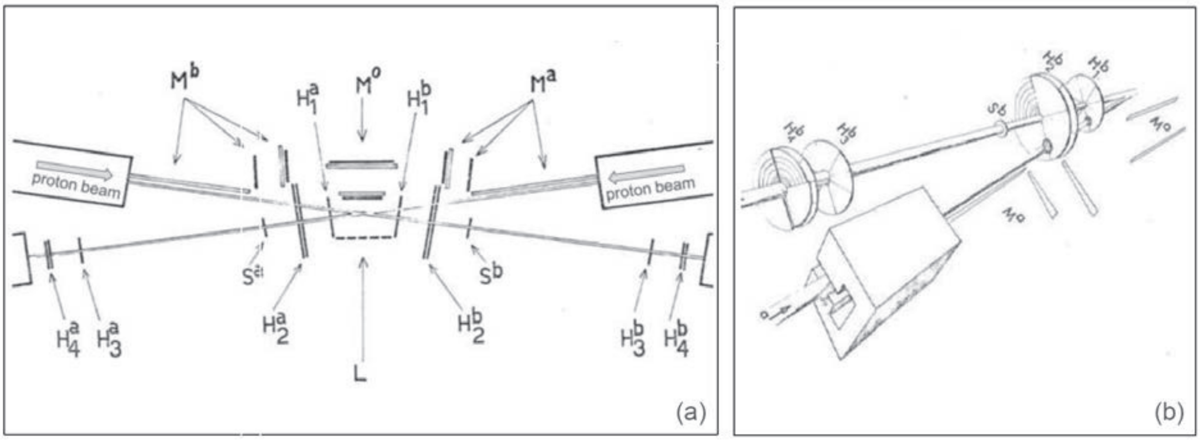

Fig. 6: The initial proposal by the Pisa group to measure the proton–proton total cross-section

To compute any cross-section, one needs a measurement of the ‘luminosity’ L. In the case of a beam of parallel particles that cross at an angle, the only important spatial variable is the vertical one y. Given the normalized vertical distributions of the two beams, $\rho_1(y - y_o)$ and $\rho_2(y)$, which are displaced vertically by y_o, the luminosity is proportional to the two currents and depends upon the crossing angle of the beams according to the formula:

$$L(y_o) = \underbrace{\frac{I_1 I_2}{c\, e^2 \tan(\phi/2)}} \underbrace{\int \rho_1(y - y_o)\, \rho_2(y)\, dy}$$

$$R(y_o) = \sigma \cdot K \cdot \textit{(overlap integral)}$$

To obtain the luminosity, the Pisa group proposed to measure ρ_1 and ρ_2 separately, with the two sets of spark chambers indicated in Fig. 6 with the letters M^o and M^a, and then to compute the beam overlap integral numerically.

The problem of measuring the ISR luminosity was amply debated during 1968 and various proposals to do so by *separated measurements* of the vertical distributions were put forward by Darriulat and Rubbia [10], Rubbia [11], Schnell [12], Steinberger [13] and Onuchin [14].

Another method proposed in different forms by Cocconi [15], Di Lella [16] and Rubbia and Darriulat [17] was based on the detection of the two protons scattered at angles smaller than about 1 mrad, where the *known* Coulomb elastic scattering cross-section dominates.

All the proposals requiring the separate measurements of the vertical distributions of the two beams were superseded by a very simple observation made by Simon Van der Meer [18]. He remarked that the cross-section σ_M of a particular type of event (detected by a set of monitor counters surrounding the interaction region) can be obtained by measuring the rate of the monitor events $R_M(y_o)$ as a function of the distance y_o between the centres of the two beams, which are moved vertically in small and precisely known steps.

In the integral $I_{VdM} = \int R_M(y_o)\, dy_o$ the double integral over dy_o and dy equals 1, because ρ_1 and ρ_2 are normalized, the cross-section of the monitor counters is given by $\sigma_M = I_{VdM}/K$ and the cross-section σ corresponding to any other rate R is simply obtained as

$$\sigma = \frac{R}{R_M}\sigma_M = \frac{I_{VdM}}{K}\frac{R}{R_M}$$

The magnets needed to precisely displace the two beams vertically were installed in the ISR, and since then the Van der Meer method has been used to measure proton–proton luminosities. A typical distribution obtained at the ISR is shown in Fig. 7 [19].

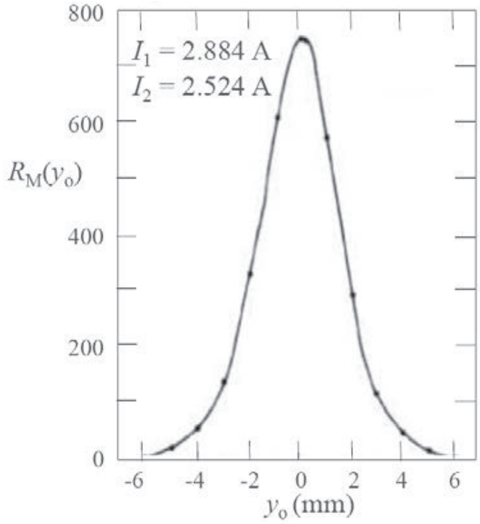

Fig. 7: Distribution of a monitor rate versus the vertical distances between two ISR beams

Figure 8 shows the apparatus built by what became the Pisa–Stony Brook Collaboration after joining with the Stony Brook Group led by Guido Finocchiaro and Paul Grannis.

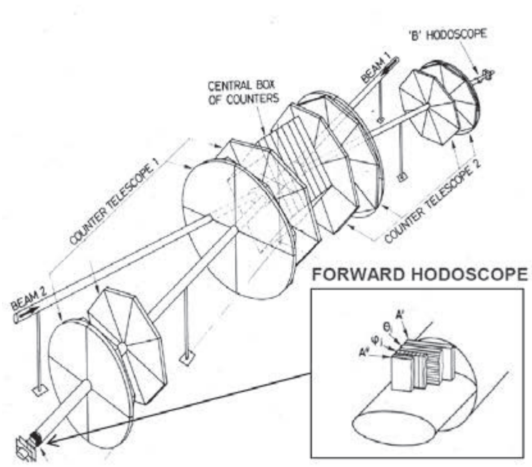

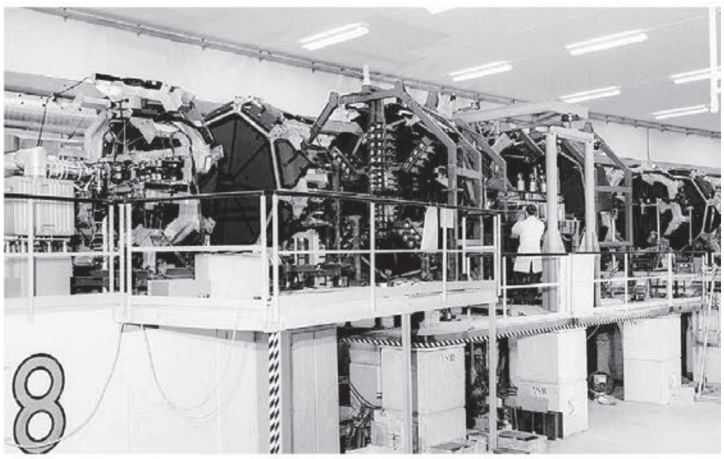

Fig. 8: In the final detector built by the Pisa–Stony Brook Collaboration, forward telescopes were used to measure elastic scattering events at small angles

Coulomb scattering was the focus of the proposal 'The measurement of proton–proton differential cross-section in the angular region of Coulomb scattering at the ISR' [20] by the Rome–Sanità group and Paolo Strolin, who at the time was an ISR engineer (signed by U. Amaldi, R. Biancastelli, C. Bosio, G. Matthiae and P. Strolin). The apparatus (shown in Fig. 9) required a modification of the ISR vacuum pipe, and two quadrupoles and one bending magnet had to be installed on each beam.

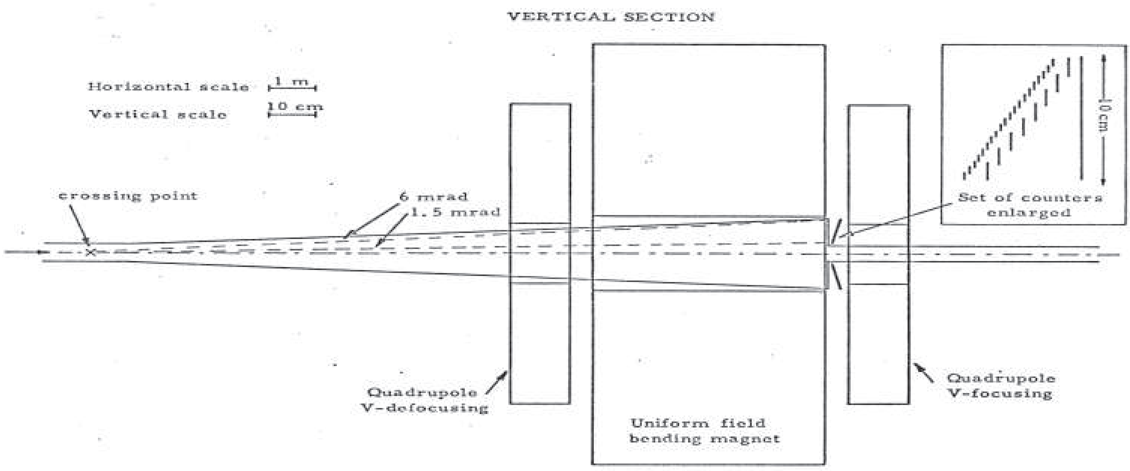

Fig. 9: In the first proposal, two quadrupoles and one magnet focused the protons and bent them so as to measure protons scattered down to 1.5 mrad

A few months later, in an addendum to the proposal, the authors wrote: 'In discussions with the specialists of the machine (R. Calder and E. Fischer) we found a simple way for allocating the detectors near the beam, which does not imply a modification of the standard parts of the vacuum chamber.'

The proposal (Fig. 10) foresaw getting as close as 10 mm to the beam with the bottom of the movable sections, as proposed many years before by Larry Jones [21]. This was a daring operation and many people worried so much that, in an ISR meeting, Carlo Rubbia said: 'Your scintillators will give light as bulbs!'

To counter the criticisms, in 1970 a test was performed at the CERN PS to check whether one could install scintillation counters very close to a circulating proton beam. Previously Hyams and Agoritsas had performed similar measurements [22].

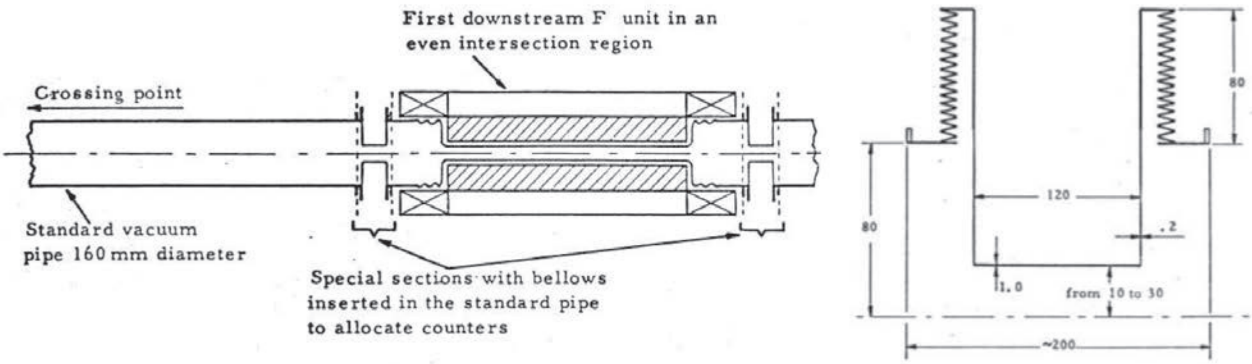

Fig. 10: In the 1969 proposal there were four movable sections on each beam and the forward-scattered protons were detected by a coincidence between counters located upstream and downstream of the first ISR magnet

Eifion Jones participated in the planning and in the tests – in which the PS beam was moved towards the scintillators – and a memorandum was sent to the ISR Committee [23], which concluded that, down to a few millimetres from the beam, the rate to be found at the ISR would have been sufficiently low to allow the Coulomb experiment (Fig. 11).

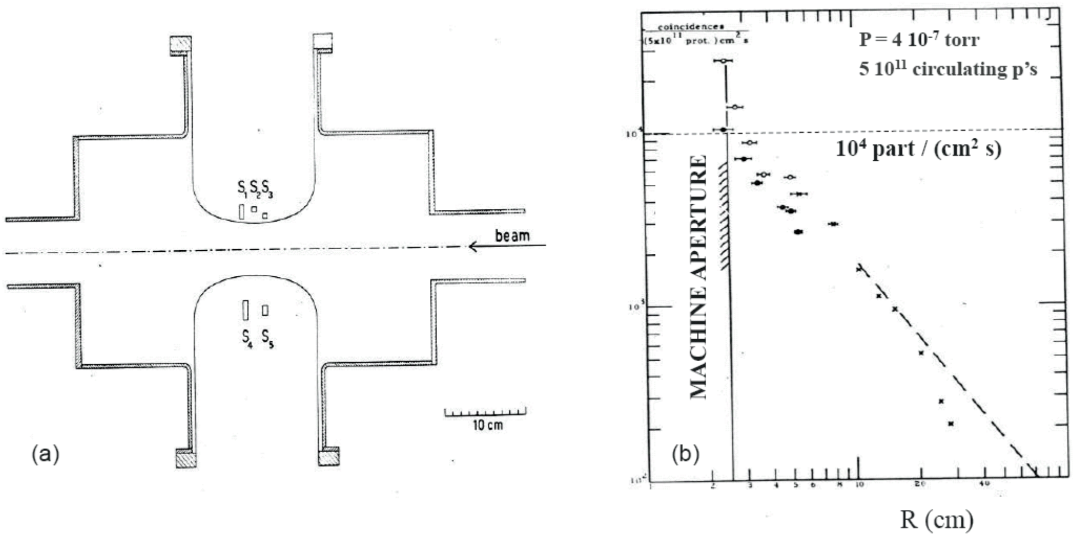

Fig. 11: Special section of the PS that allowed the measurement of the rate detected by scintillators placed very close to a circulating beam formed by 5×10^{11} protons

The ISR movable sections of the vacuum chamber soon became known as 'Roman pots', which was the translation of the expression '*les pots de Rome*' invented by the French draftsman whom we visited regularly travelling from Rome to Geneva and who, under the direction of Franco Bonaudi, transformed our rough sketches into construction drawings.

In October 1970 the ISR Committee took various decisions on pending experiments. Following it, the CERN group of Giuseppe Cocconi, Alan Wetherell, Bert Diddens and Jim Allaby wrote the Committee a memo, which said: 'At the meeting of the ISRC on 14 October it was concluded that there is no way to fit the proposed experiment on deep inelastic scattering into the present ISR experimental program. As a result we have decided, on their invitation, to collaborate with the Rome group (U. Amaldi *et al.*) on the small-angle scattering experiment.'

For the final experiment, the newly formed CERN–Rome Collaboration decided to retain only the four movable sections located in front of the first ISR magnet, a decision that simplified the experiment and its interactions with the accelerator.

The title of the proposal by the CERN–Genoa–Torino group (P. Darriulat, C. Rubbia, P. Strolin, K. Tittel, G. Diambrini, I. Giannini, P. Ottonello, A Santroni, G. Sette, V. Bisi, A Germak, C. Grosso and M.I. Ferrero) was 'Measurement of the elastic scattering cross-section at the ISR' [24]. The apparatus of Fig. 12 was made of two parts such that 'the whole angular range from 1 mrad to about 100 mrad can be covered. The very small-angle events (in the Coulomb region) are detected by a two-arm spectrometer sharing the first four magnets with the storage ring system. The larger-angle events are momentum-analysed with a pair of magnets that do not perturb the circulating beams.

After many discussions, the ISR Committee decided to approve only the system made of two septum magnets installed in the intersection regions and to leave the detection of elastic scattering in the Coulomb region to the scintillators mounted in the Roman pots. Since then, Carlo Rubbia has described the ISR experimental program as 'key-hole physics'. After the approval, the Collaboration was joined by the Aachen and Harvard groups and became the Aachen–CERN–Harvard–Genoa–Torino (ACHGT) Collaboration.

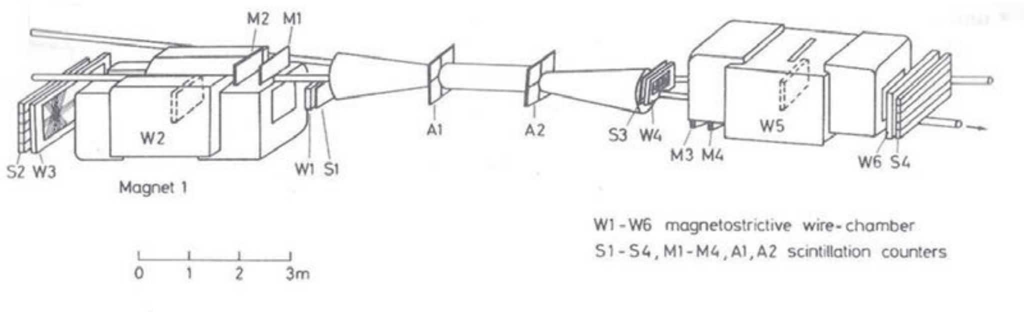

Fig. 12: The septum magnets of the ACHGT Collaboration, which have been used to measure the forward elastic cross-section

These three experiments were mounted in interaction regions I2 and I6 of the ISR, as shown in Fig. 13.

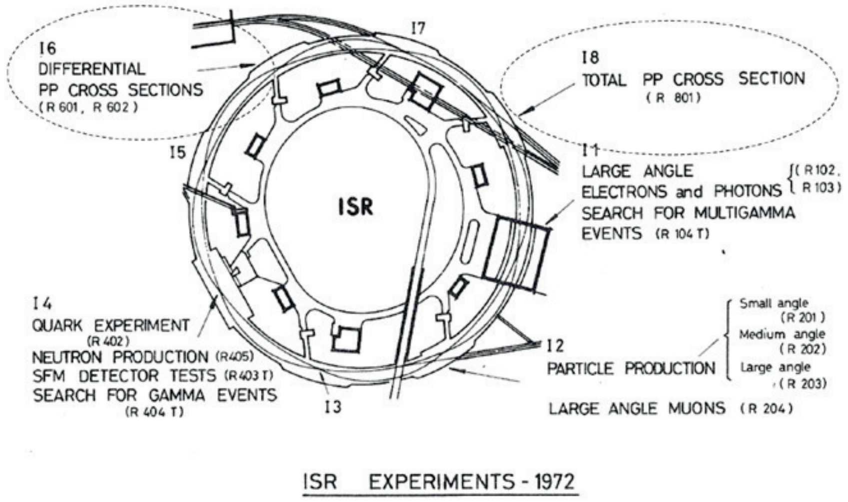

Fig. 13: ISR experiments in 1972: R601 = CERN–Rome, R602 = Aachen–CERN–Harvard–Genoa–Torino and R801 = Pisa–Stony Brook

A picture of the intersection region in which the ACHGT septum magnets and the Roman pots were installed is shown in Fig. 14.

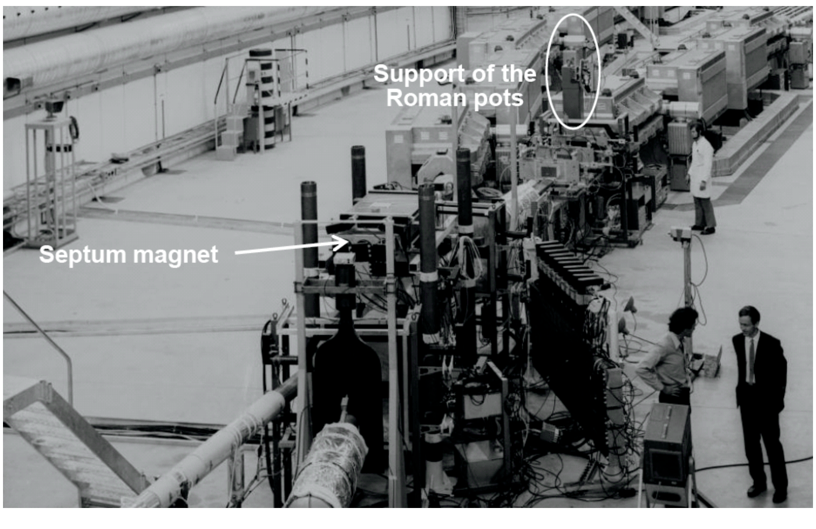

Fig. 14: Paolo Strolin describes to Alexander Skrinsky the ACHGT experiment, which measured with magnetostrictive spark chambers the momenta of the protons scattered between 30 and 100 mrad

4 First results on elastic scattering and total cross-sections

The slope of the forward elastic cross-section was the easiest measurement to perform. The 1971 results [25, 26], reported in Fig. 15, confirmed the behaviour found first at the PS and confirmed at Serpukhov: in the range $30 \le s \le 3000\ \mathrm{GeV}^2$, the increment of the forward elastic slope B is proportional to $\ln s$, in agreement with the description based on pomeron exchange.

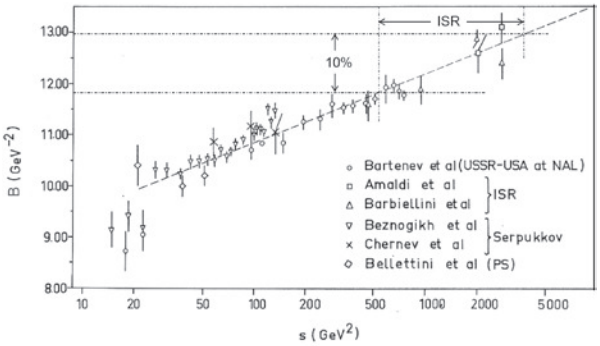

Fig. 15: The data available in 1971 for $-t \le 0.12\ \mathrm{GeV}^2$ and the results of the measurement performed in 1972 at NAL (Fermilab) [27]. The dashed line shows that, over a very large energy range, the t width (which is equal to $1/B$) of the forward elastic peak decreases as the inverse of $(a + b \ln s)$.

Taking into account all the data, the figure shows that, in the *full* ISR energy range ($23 \le \sqrt{s} \le 62$ GeV, i.e., $550 \le s \le 3800\ \mathrm{GeV}^2$), the slope parameter B increases by about 10% on passing from $11.9\ \mathrm{GeV}^{-2}$ to $13.0\ \mathrm{GeV}^{-2}$, which corresponds to a 5% increase of the proton–proton interaction radius.

In the Regge description, the energy variation of B is related to the slope of the pomeron trajectory at $t = 0$:

$$B = B_0 + 2\alpha'(0)\ln(s/s_0)$$

The dashed line of Fig. 15 corresponds to $\alpha'(0) = 0.28\ \mathrm{GeV}^{-2}$, confirming what was already known from lower-energy data: the pomeron slope at $t = 0$ is definitely smaller than the slope $\alpha_\rho'(0) \approx 1\ \mathrm{GeV}^{-2}$ of the ρ trajectory shown in Fig. 2.

In 1972 the ACHGT Collaboration reported two very interesting findings [28, 29]: (i) the forward elastic cross-section has a variation of slope at $|t| \approx 0.16\ \mathrm{GeV}^2$ (Fig. 16a) and (ii) the deep diffraction minimum located at $|t| \approx 1.4\ \mathrm{GeV}^2$ is the energy development of the structure observed at lower energies (Fig. 16b).

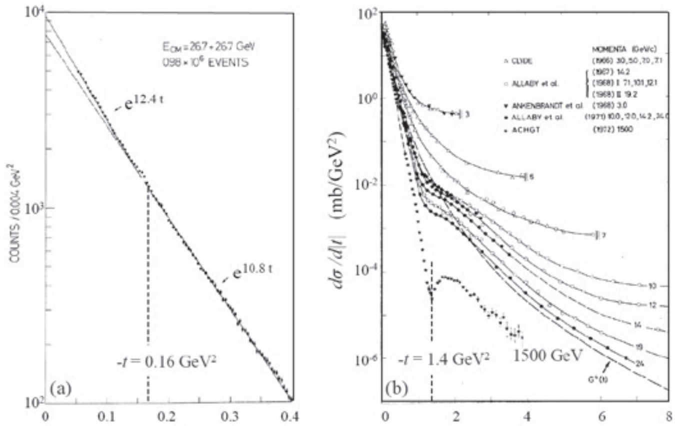

Fig. 16: First measurements by the ACHGT Collaboration of proton–proton elastic scattering (a) in the forward region and (b) at large momentum transfer

However, the real surprise came with the measurements of the total cross-section done by the Pisa–Stony Brook Collaboration, with the apparatus of Fig. 6, and by the ACHGT and the CERN–Rome Collaborations, using the forward elastic cross-section and the optical theorem.

This method, which, as far as I know, was not considered before the ISR start-up, was pioneered in 1971 by ACHGT [30]: the hadron–hadron forward elastic cross-section (measured outside the Coulomb peak with the Van der Meer method) is extrapolated to zero angle to obtain $(d\sigma/dt)_0$ and the optical theorem is applied to obtain

$$\sigma_{\rm tot} = \frac{\sqrt{16\pi\,(d\sigma/dt)_0}}{(1+\rho^2)}$$

It is worth remarking that the correction due to ρ^2 introduces a negligible error and that, because of the square root, the percentage error in $d\sigma/dt$ (due to the Van der Meer method and to the unavoidable errors in the measurement of the forward elastic rate) is reduced because of the square root in $\sigma_{\rm tot}$ by a (very helpful) factor of 2.

In the autumn of 1972 the three collaborations were competing to be the first to measure the total proton–proton cross-section. I remember very vividly that period, because I was the one performing the analysis of the CERN–Rome data. In the invited talk I gave in September 1973, i.e., one year later, at the Aix en Provence International Conference on Elementary Particles [31], I summarized with a figure the confusing status of the measurements in October 1972 (Fig. 17).

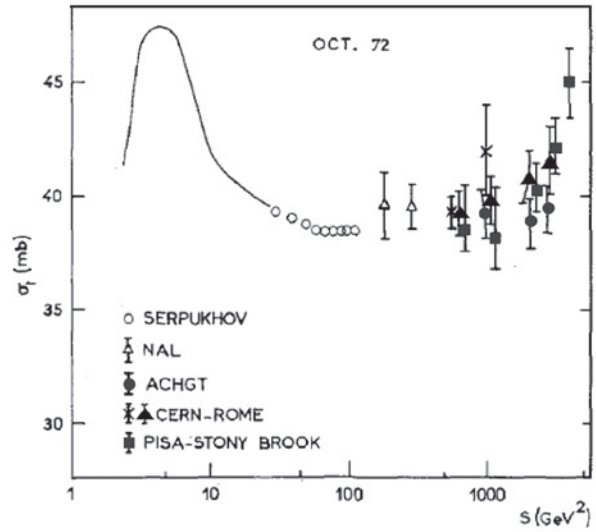

Fig. 17: Status of the total cross-section measurements in October 1972. The points by the CERN–Rome Collaboration were obtained with the luminosity measured with both the Van der Meer method and Coulomb scattering.

Figure 17 shows that, at that date, the Pisa–Stony Brook and CERN–Rome Collaborations had an indication of the rising cross-section, while AGHGT was finding no energy dependence. This much debated difference continued during the next months.

In February 1972 the CERN–Rome Collaboration published the first measurement of the ratio ρ between the real and imaginary parts of the forward scattering amplitude and of the total cross-section using Coulomb scattering as normalization [31]. The measurement could be performed only at the two lowest ISR energies because, with the apparatus of Fig. 18a, the minimum scattering angle was fixed at about 2.5 mrad by the background rate due to the beam halo. Thus at the highest ISR energies, after completion of the stacking process in the two ISR rings, the pots could not be moved close enough to the beams to reach the t range where the Coulomb scattering amplitude is as large as the nuclear one.

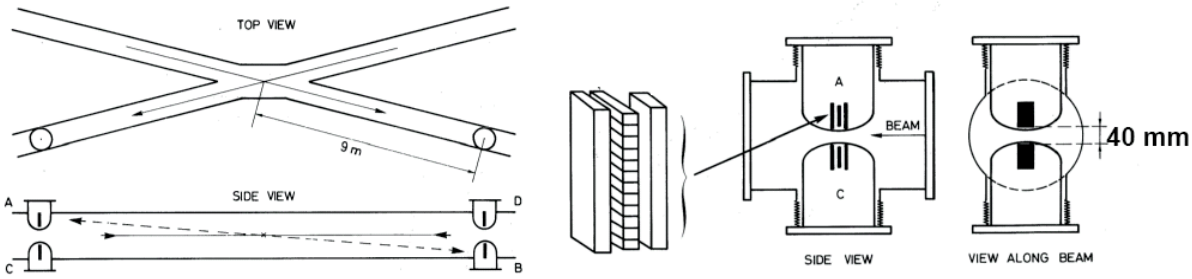

Fig. 18: The 1972 telescope system of the CERN–Rome Collaboration [32] was used (i) to obtain the ISR luminosity using the Coulomb scattering events and (ii) to measure ρ

The measured differential cross-sections are shown in Figs. 19a and 19b. The t dependence of the Coulomb amplitude is well known, because it is due to large-impact-parameter collisions of two point-like charges, is essentially real and decreases proportionally to $1/t^2$. In the t range indicated by the dashed ellipse, the nuclear amplitude varies little and its (small) real part interferes with the Coulomb amplitude, which is well known, being due to an electromagnetic phenomenon. The ratio ρ can thus be obtained by a fit to the very precise data. The results of this first experiment are shown as full dots in Fig. 19c.

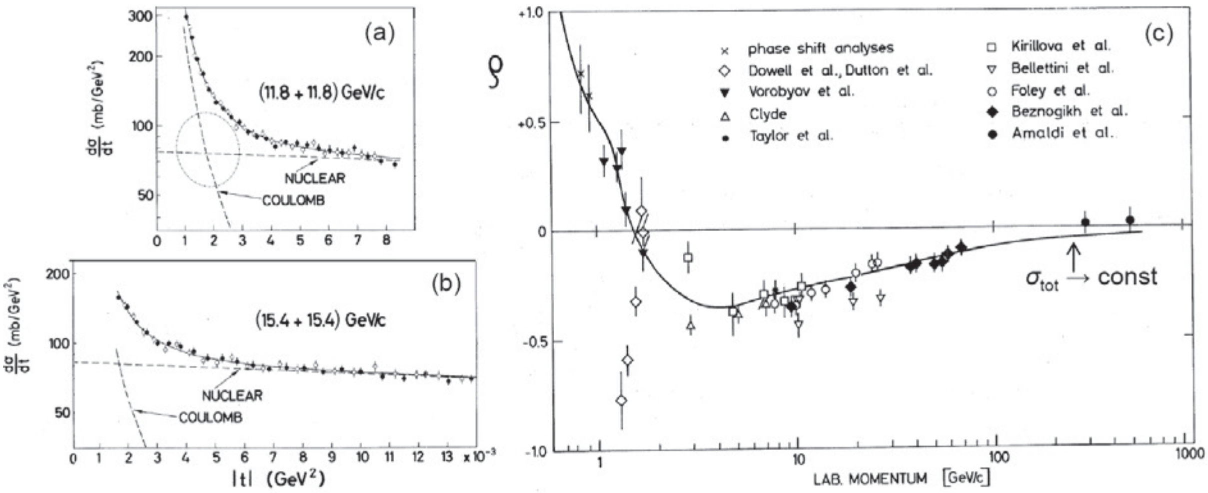

Fig. 19: The first measurements of the real part of the forward scattering amplitude were performed at the two lowest ISR energies [32]

The two data points indicated that ρ was becoming positive in the ISR energy range which, because of the Khuri–Kinoshita theorem, was a signal of the rise of the total proton–proton cross-section. The error bars are large, but within the Collaboration we knew that the indication was stronger than it appeared because, after many discussions, the errors were doubled to be on the safe side in the first paper reporting the result of a new delicate experiment.

The CERN–Rome and Pisa–Stony Brook data – presented at CERN in the already quoted March 1973 seminar and published in *Physics Letters* [33, 34] – definitely demonstrated that (i) the proton–proton total cross-section increases by about 10% in the ISR energy range (Fig. 20a) and (ii) the elastic cross-section (computed by integrating the measured differential cross-section) increases by the about same amount, so that in the full ISR energy range the ratio $\sigma_{el}/\sigma_{tot} \approx 0.17$, while it decreases monotonically at lower energies. This about constant ratio is definitely smaller than the value $\sigma_{el}/\sigma_{tot} = ½$ that would result from the scattering of a wave by a black disc.

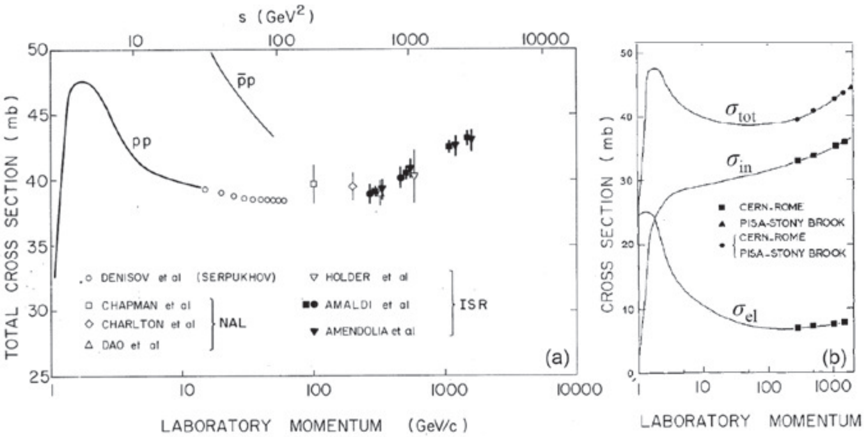

Fig. 20: (a) The proton–proton total cross-section increases for laboratory momenta larger than 300 GeV/c ($s > 500$ GeV^2). (b) The inelastic cross-section was computed by subtraction: $\sigma_{\text{in}} = \sigma_{\text{tot}} - \sigma_{\text{el}}$.

The inelastic cross-section is four times larger than the elastic cross-section and increases roughly proportionally to $s^{0.04}$ from about 50 MeV/c to the maximum ISR energy (Fig. 20b). Looking at the three curves of this figure, it appears that the shallow minimum of the total proton–proton cross-section $\sigma_{\text{tot}} = \sigma_{\text{in}} + \sigma_{\text{el}}$ around $s = 100$ GeV^2 is a consequence of the *continuously* rising inelastic cross-section which, through unitarity, drives the increase of the elastic cross-section.

If the energy dependence of the high-energy total cross-section is fitted with the formula of the Froissart–Martin bound, one obtains

$$\sigma_{\text{tot}} \simeq \left[\, 38.4 + 0.5 \ln\left(\frac{s}{s_{\text{o}}}\right)^2 \right] \text{ mb},$$

where $\sqrt{s_{\text{o}}} = 140$ GeV [33]. Since the coefficient 0.5 mb is much smaller than the limiting value predicted by the Froissart–Martin bound, the energy dependence measured at the ISR is most probably uncorrelated with the bound itself.

As I said, at the time, most experts were convinced of the constancy of the cross-sections at high energies, with two important exceptions. In 1952 Werner Heisenberg had published a paper that described pion production in proton–proton collisions as a shock wave problem governed by a non-linear equation and deduced a $\ln^2 s$ dependence of the cross-section [35]. The model proposed by H. Cheng and T.T. Wu [36] is much more sophisticated because it is based on quantum field theory, specifically on a massive version of quantum electrodynamics. After the announcement of the ISR results, the model was reconsidered and fitted to the experimental data by Cheng, Walker and Wu [37].

The CERN seminar and, soon after, the two publications made a certain impression also outside the physics community, so much so that I wrote an article for *Scientific American*. In spring and summer 1973 this took me a lot of time since the editor was following very closely the writing of the text and the production of the figures. The article was published in September 1973 [38] after a drastic cut of the part of the article containing the impact parameter description of the ISR collision. In substitution, I introduced the quantity 'average opaqueness' $O = 2\sigma_{\text{el}}/\sigma_{\text{tot}}$, which in wave mechanics is $O = 1$ for a black disc, and showed with a figure how O decreases at low energies and becomes roughly constant ($O \approx 0.35$) in the whole ISR energy range.

I also underlined that in 1972 the interest in models of rising cross-section [36] was raised when an analysis of high-energy cosmic data had indicated that the proton–proton cross-section is larger at $p \approx 10^4$ GeV/c than at the energies at the time available at particle accelerators [39]. However, one year later, from a different set of data, it was concluded that 'there is no evidence to suggest a change in the magnitude of the inelastic proton–proton cross-section up to 50 000 GeV' [40].

I may add that letters and telex exchanges were needed to convince the editor to insert the 29 names of the members of the CERN–Rome and Pisa–Stony Brook Collaborations, a request that in the past *Scientific American* – as they told me – had always refused because 'the readers are not interested'.

5 Second-generation experiments

In the years 1974–1978 three experiments brought more precise data.

The first one was performed by the Annecy–CERN–Hamburg–Heidelberg–Vienna Collaboration, which used the Split Field Magnet to accurately measure the elastic cross-section up to $q = 12$ GeV/c [41]. It was observed that the minimum at $q = 1.4$ GeV/c deepens around $E_{CM} = 30$ GeV and fills up at larger energies (Fig. 21a). It was interesting to remark that the deepest minimum happens at the same energies at which the forward real part is practically zero (Fig. 19c), possibly indicating that the fill-up at higher energy is due to a non-zero real part of the large-angle scattering amplitude.

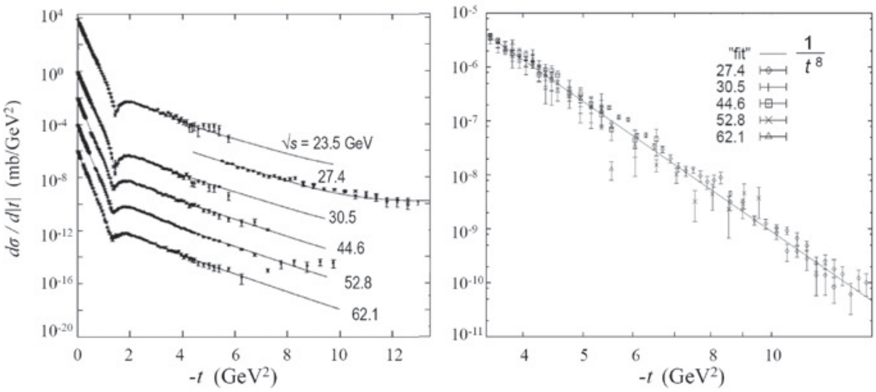

Fig. 21: (a) The elastic differential cross-sections at large momentum transfers plotted on different vertical scales [41]. (b) The elastic cross-section is energy independent and decreases as $1/t^8$ [42].

Figure 21b shows that the differential cross-section is energy independent when $-t$ varies in the range 3–10 GeV^2. The $1/t^8$ behaviour is predicted by the simple model in which the three quarks of the proton exchange a pomeron. The question [42] is this: Why does this lowest-order three-gluon exchange work so well?

Going back to 'small-angle physics', in 1973 the CERN–Rome and Pisa–Stony Brook Collaborations successfully tried a new method for measuring the total cross-section [43] and proposed to the ISR Committee a joint experiment that would have been done in new Roman pots installed – with more precise scintillator hodoscopes – in intersection region I2 where the Pisa–Stony Brook apparatus was located. Figure 22 shows the overall apparatus.

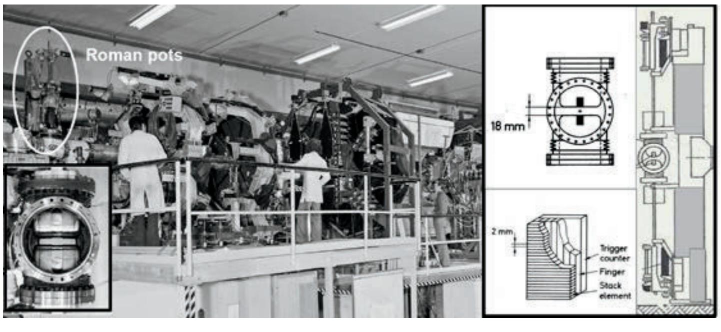

Fig. 22: The CERN–Rome–Pisa–Stony Brook experiment, which included two pairs of thin Roman pots (insets), was installed in I8

As the inset to Fig. 22 shows, the four pots – two per side – had very thin and flat windows, which allowed the pots – and the new systems of 'finger' scintillators they contained – to be moved much closer to the circulating proton beams, once the beam stacking process was completed. The set-up also allowed a much more accurate measurement of the distance between the edges of the two hodoscopes located one on top of the other. I well remember Giuseppe Cocconi and the NIKHEF PhD student Jheroen Dorenbosch spending long hours to improve – through accurate position measurements – the knowledge of the momentum transfer q.

The combination of the two detectors opened the way to the application of the new method for measuring total cross-sections. This is based on the measurement of (i) the total number of inelastic events N_{in}, measured by the Pisa–Stony Brook detector in a given run, which is, after small corrections due to the unavoidable losses, proportional to σ_{tot} and (ii) the extrapolated forward rate $(\mathrm{d}N/\mathrm{d}t)_0$, measured by the CERN–Rome hodoscopes, which is proportional to σ_{tot}^2. Because of the optical theorem, σ_{tot} is proportional to the ratio $(\mathrm{d}N_{\mathrm{el}}/\mathrm{d}t)_0/N_{\mathrm{tot}}$, where $(\mathrm{d}N/\mathrm{d}t)_0$ is the extrapolated forward number of events and $N_{\mathrm{tot}} = N_{\mathrm{in}} + N_{\mathrm{el}}$ is the total number of inelastic and elastic events, computed by integrating the differential rate $\mathrm{d}N_{\mathrm{el}}/\mathrm{d}t$:

$$\sigma_{\mathrm{tot}} = \frac{16\pi}{(1+\rho^2)} \; \frac{(\mathrm{d}N_{\mathrm{el}}/\mathrm{d}t)_0}{N_{\mathrm{el}} + N_{\mathrm{in}}}$$

The ratio ρ is small and contributes a negligible error to the overall uncertainty.

The combined results of the three methods are plotted in Fig. 23 [44] together with the CERN–Rome measurements of the real part of the forward amplitude [45, 46] obtained with the improved Roman pots of Fig. 22. The curves have been obtained by fitting all available data and taking into account the dispersion relation, which, by neglecting spin effects, connects the forward real parts (Fig. 23b) to energy integrals of the total cross-sections (Fig. 23a).

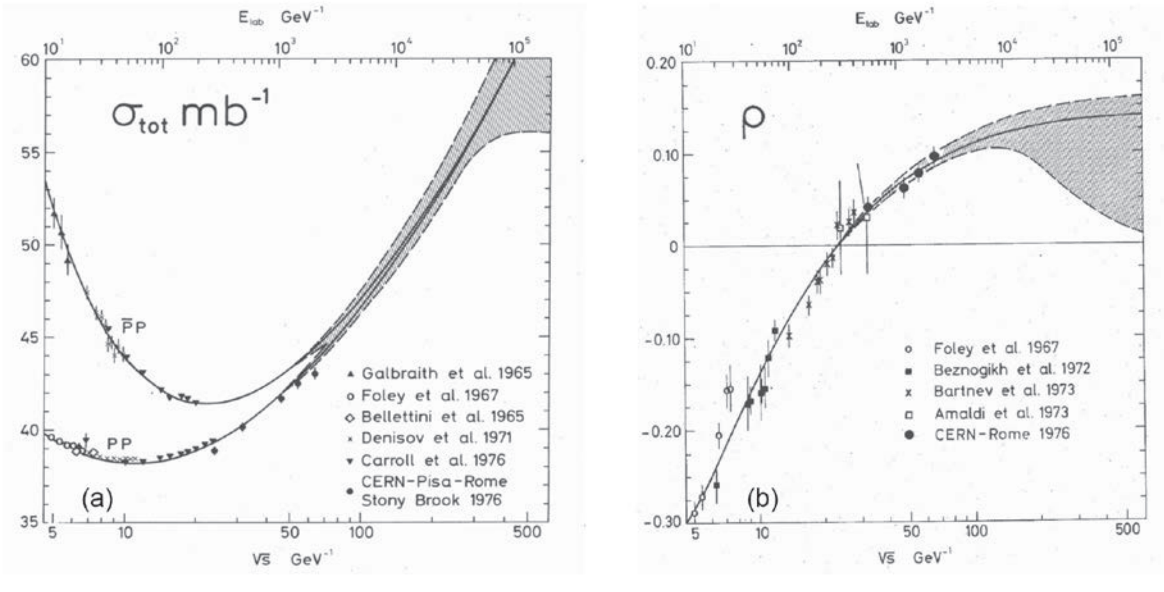

Fig. 23: The curves are fitted to the energy dependence of the total cross-sections and the forward real part, and are based on the analyticity properties of the scattering matrix [45, 46]

The physical content of the complicated mathematics can be understood by stating that, at high energies, ρ becomes roughly proportional to the *logarithmic* derivative of the total cross-section, $\mathrm{d}\sigma_{\mathrm{tot}}/\mathrm{d}(\ln s)$. This fits with the Khuri–Kinoshita theorem, which states that $\rho \rightarrow \pi \ln s$ for a cross-section that increases proportionally to $\ln^2 s$ – and explains why precise measurements of ρ at $\sqrt{s} \approx 50$ GeV determine the total cross-section up to about 500 GeV. (A rigorous discussion of this very rough argument can be found in Ref. [47].) It is worth underlining that this was the first experiment in which the measured ratio ρ was used to obtain information on the energy dependence of the total cross-section at energies much larger than those available in the laboratory.

The global CERN–Rome fit [45] gives a total cross-section that increases as $\ln(s/s_0)^\gamma$ with $\gamma = 2.1 \pm 0.1$ and $s_0 = 1$ GeV. The exponent coincides, within the error, with the limiting value of the Froissart–Martin bound. This fact was confirmed by a second experiment performed just before the demise of the ISR, when the availability of the CERN Antiproton Accumulator allowed a measurement of the real part of the antiproton–proton forward scattering amplitude. The CERN–Louvain-la-Neuve–Northwestern–Utrecht Collaboration used the apparatus of the CERN–Rome Collaboration and inherited most of the techniques: I remember Jheroen Dorenbosch and myself passing to Martin Bloch the codes we had developed over the years.

The experiment was a success and confirmed the proton–proton results reported in Fig. 23b [48]. More importantly, the antiproton–proton forward real part was measured to be positive, albeit with larger errors, as expected – due to the Pomeranchuk theorem – for a rising cross-section that becomes asymptotically equal to the proton–proton one. An overall fit with $s_0 = 1$ GeV, which included preliminary data obtained at the CERN proton–antiproton collider, gave $\gamma = 2.02 \pm 0.01$.

To understand the significance of these results, let us go a step backwards.

By applying to the scattering amplitude $f(t)$, which is a function of $q = (-t)^{1/2}$, the transformation written in Fig. 24, one can compute the 'profile function' $\Gamma(a)$ as a function of the impact parameter a in the plane perpendicular to the momenta of the colliding particles.

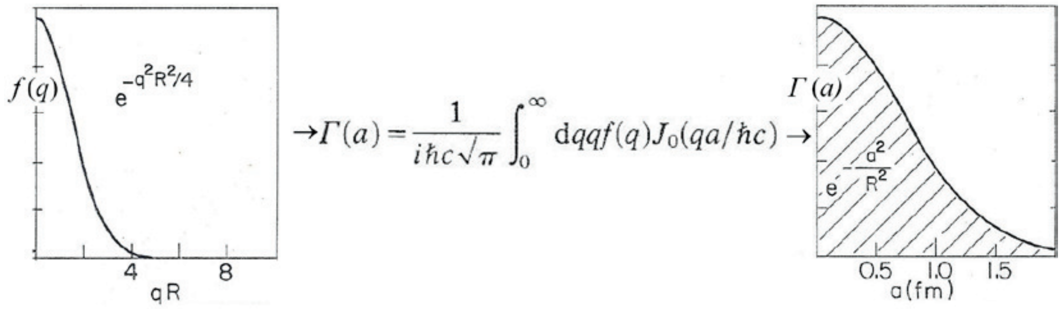

Fig. 24: A Gaussian elastic profile function corresponds to a scattering amplitude that decreases exponentially with $q^2 = |t|$. (In the integral, J_0 is the Bessel function of order zero.)

By applying the same transformation to the three terms of the unitarity relation, one obtains

$$2\,\mathrm{Re}\,\Gamma(a) = |\Gamma(a)|^2 + G_{\mathrm{in}}(a) \quad \text{with} \quad 0 \leq \Gamma(a) \leq 1 \quad 0 \leq G_{\mathrm{in}}(a) \leq 1$$

where the two inequalities express the limits imposed by unitarity. This equation shows how, in the diffraction limit, i.e., when $f(q)$ is essentially imaginary because ρ is small and $\Gamma(a)$ is practically real, the *inelastic overlap integral* $G_{\mathrm{in}}(a)$ determines the elastic profile function, $\Gamma(a) = 1 - \sqrt{[1 - G_{\mathrm{in}}(a)]}$, and vice versa, so that $\Gamma(a)$ and $G_{\mathrm{in}}(a)$ can be obtained by applying the Bessel transformation to the measured scattering amplitude $f(q)$.

If the inelastic overlap integral equals 1 up to an impact parameter $a = R$, the same happens to the profile function, which thus describes a black disc. In this case the elastic and inelastic cross-sections, given by the integrals of $|\Gamma(a)|^2$ and $G_{\mathrm{in}}(a)$, are equal ($\sigma_{\mathrm{el}} = \sigma_{\mathrm{in}}$) so that $\sigma_{\mathrm{tot}} = \sigma_{\mathrm{el}} + \sigma_{\mathrm{in}} = 2\sigma_{\mathrm{el}}$ and $\sigma_{\mathrm{el}}/\sigma_{\mathrm{tot}} = 0.5$, as mentioned above. In the ISR energy range, this ratio is $\sigma_{\mathrm{el}}/\sigma_{\mathrm{tot}} = 0.17$ and the colliding protons are not black but transparent to one another.

This statement can be made quantitative by computing $\Gamma(a)$ and $G_{\mathrm{in}}(a)$ from the measured elastic differential elastic cross-sections [49]. Figure 25a shows that the profile function is Gaussian-like and completely different from that of Fig. 25b, which describes a black disc having a radius proportional to $\ln(s/s_0)$ and a grey periphery of constant width, as needed to saturate the Froissart–Martin bound. (It can be noted that this is the high-energy behaviour predicted by the Cheng and Wu massive quantum electrodynamics model [36, 37].)

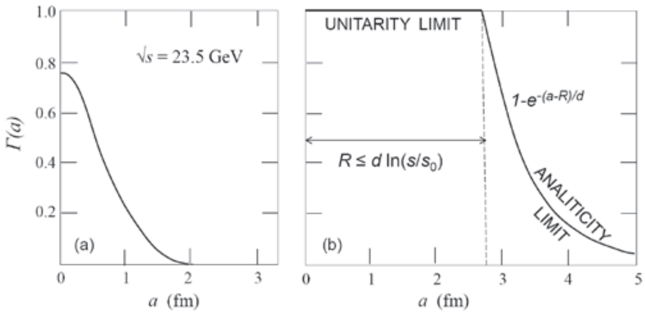

Fig. 25: At ISR energies the profile function [49] is far from saturating the unitarity and analyticity constraints that define the Froissart–Martin bound

Figure 25b is taken from Ref. [43], where the impact parameter descriptions of the analyticity limit and of the asymptotic behaviour of the forward real part are discussed in detail. In the simplified version depicted in Fig. 25b, the Froissart–Martin limiting profile function contains the length d, which is determined by the pion mass and fixes the maximum constant C that asymptotically multiplies $\ln^2(s/s_0)$. In the original works of the 1960s [6, 7], C was proven to be equal to $\pi(\hbar/m_\pi)^2 \approx 60$ mb, but in a 2009 paper [50] André Martin derived the new limit $C = \pi(\hbar/2m_\pi)^2$, which is four times smaller and corresponds to $d = \hbar/[(2\sqrt{2})m_\pi] \approx 0.5$ fm. It is worth noting that the new constant $C \approx 15$ mb is still thirty times larger than the best fit to the experimental data.

I now consider the measured *increase* $\Delta G_{\text{in}}(a)$ of the inelastic overlap integral over the ISR energy range. In 1973 I presented such an analysis in Aix en Provence, concluding that the increase of the proton–proton cross-section is a *peripheral* phenomenon [31], a conclusion reached at the same time by others [5051a, 51b].

This is confirmed by Fig. 26a, which is the result of an analysis performed in 1980 with Klaus Schubert on *all the data* collected at the ISR [49]. The novelties brought by this analysis were the direct calculation of $G_{\text{in}}(a)$ from the experimental data and a careful estimate of the effects of statistical and systematic errors. Figure 26b displays the results of the analysis by Henzi and Valin [52], who used a different approach by first fitting the differential cross-sections with analytical functions and then computing $G_{\text{in}}(a)$.

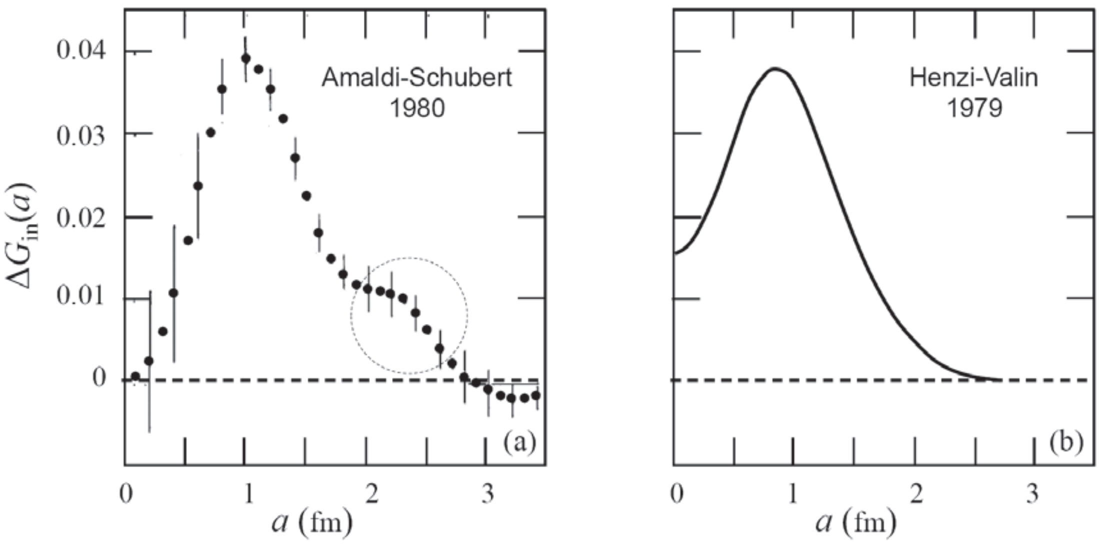

Fig. 26: The variation of the inelastic overlap integral in the ISR energy range (23 GeV ≤ $\sqrt{s}$ ≤ 62 Gev) as a function of the impact parameter a (expressed in fermis) is a good way to describe the physical significance of the phenomenon of the rising total proton–proton cross-section with energy

It is seen that the shadow of the inelastic channels increases by $\Delta G_{in} = 0.04$ at 1 fm, which confirms the peripheral nature of the phenomenon. At $a = 0$ the two analyses are compatible when the errors are properly taken into account and indicate that $\Delta G_{in}(0)$ is less than three times smaller than $\Delta G_{in}(1 \text{ fm})$. It could even be zero, since small impact parameters imply large moment transfers, and in this region the analytical fits to the cross-section [52] are not perfect, a problem that is not encountered when the experimental data are used directly [49]. It is also worth mentioning that the physical origin of the bump of $\Delta G_{in}(a)$ in Fig. 26a at $a = 2.3$ fm is not known.

As mentioned above, the fitted exponent of the logarithmic increase of σ_{tot} is 2, with a very small error. We can now answer the question: Is this fact connected with the exponent 2 predicted by the Froissart–Martin bound? The answer must be negative, because the overlap integral of Fig. 25a is very different from that of Fig. 25b, but the coincidence is so puzzling that, without understanding, the expression 'qualitative saturation of the Froissart–Martin bound' was introduced and much used.

As the last argument of this section, let us consider the *t*-channel description of diffractive scattering from the impact parameter point of view. By applying the Bessel transformation to the pomeron amplitude with $\alpha(0) = 1$, one obtains a profile function $\Gamma(a)$ that has a radius R that *increases* with energy as $\ln(s/s_0)$ and a central value that decreases. Thus in the Regge model with pomeron intercept $\alpha(0) = 1$, the forward peak *shrinks* as $\ln(s/s_0)$ while the central value *decreases* as $\ln(s/s_0)$, so that the total cross-section remains *constant*. This is certainly not in agreement with the measurements summarized by the function $\Delta G_{in}(a)$ represented in Fig. 26.

In synthesis, the 1973 ISR measurements of elastic scattering and total cross-section highlighted an unexpected state of affairs: with increasing collision energy, the proton–proton 'opacity' at zero impact parameter does not decrease – as predicted by the 'classical' pomeron exchange model – but remains about constant.

6 Particle production and diffraction dissociation

The first experiments performed at the ISR on particle production observed the two main properties well known at lower energies: the transverse momenta were small and about half of the total energy $\sqrt{s}$ was going, on average, in the forward direction, giving rise to what was called the 'leading particle effect'.

The two variables used to describe the inclusive production of single particles are the fractional momentum $x = 2p_L/\sqrt{s}$ (where p_L is the longitudinal momentum in the centre-of-mass system) and the rapidity $y = \frac{1}{2}\ln[(E + p_L)/(E - p_L)]$, where E is the total energy of the particle. The importance of the variable 'rapidity' stems from the fact that, in non-relativistic kinematics, the rapidity of a particle coincides with its velocity and, in the relativistic regime, rapidities add linearly – as do non-relativistic velocities – while velocities do not.

When the production angle of a relativistic particle in the centre-of-mass system is $\theta = 0$, so that $p_L = p = \sqrt{(E^2 - m^2)}$, the two variables vary within the ranges

$$-1 \le x \le 1 \qquad \text{and} \qquad -y_{max} \le y \le y_{max} \qquad \text{with} \qquad y_{max} = \tfrac{1}{2}\ln(s/m^2)$$

Thus the maximum rapidity in a proton–proton collision is $\ln[(\sqrt{s})/m_p]$: it was 2 at the PS ($\sqrt{s} = 6.8$ GeV) and became 4.2 at the maximum ISR energy ($\sqrt{s} = 63$ GeV).

At the Aix en Provence Conference of September 1973, Giorgio Bellettini and Lorenzo Foà presented the most recent data obtained by the Pisa–Stony Brook Collaboration by showing, among other results, the plots reproduced here as Fig. 27a [53]. Since the hodoscopes of Fig. 8 measured the angles θ of the outgoing particles with respect to the beam direction, and not the energy, the pseudorapidity $\eta = -\ln\tan\theta/2$ was used. (Note that $y = \eta$ for massless particles and that, for particle with mass, $y \to \eta$ at high energies and for most angles, but not in the very forward region, since for $\theta \to 0$ the pseudorapidity increases without limit.)

After subtracting the two tracks having maximum and minimum pseudorapidity, each recorded event was plotted (for a given multiplicity n_{ch} of the observed charged tracks) as a point having coordinates η_{av} and $\delta(\eta_{av})$, which are the *average* pseudorapidity of the remaining tracks and the *dispersion around* the average. The surfaces were drawn as smooth interpolations of the data.

The events clearly subdivide in two classes: (i) the 'central' inelastic events, which dominate for large multiplicities and cluster around $\eta_{av} = 0$ with large dispersion $\delta(\eta_{av})$, and (ii) the 'forward' inelastic events, which dominate at low multiplicities, have an average pseudorapidity close to the maximum (and the minimum) and a small dispersion.

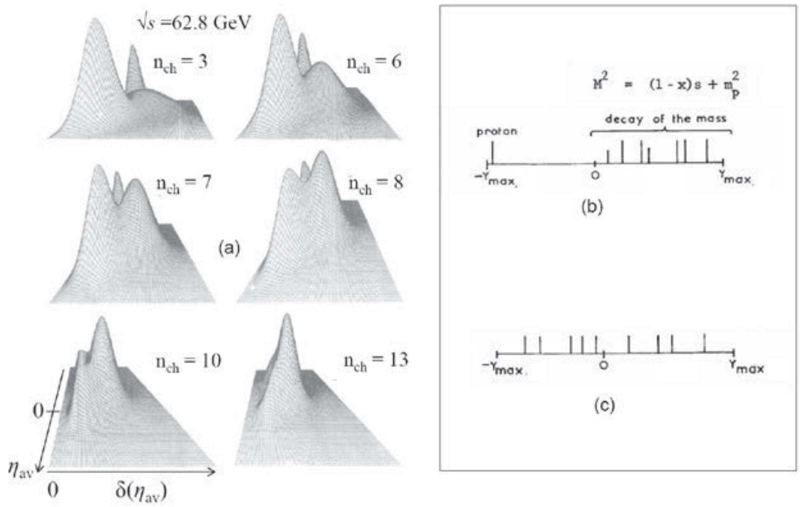

Fig. 27: (a) Distribution of the events measured by the Pisa–Stony Brook Collaboration at the maximum ISR energy as a function of the charge multiplicity n_{ch} [51]. The coordinates represent the average pseudorapidity and the dispersion around the average. (b,c) Rapidity distributions of the particles (b) in a diffraction dissociation event and (c) in a central inelastic event.

The second class is dominated by *single diffraction dissociation* events of the type represented along the y-axis of Fig. 27b: on one side there is the proton, which has a large fractional momentum x, and on the opposite side there are a few particles, which have an invariant mass M such that $M^2 = (1 - x)s + m^2$, where m is the proton mass.

At PS energies the phenomenon of single diffraction dissociation with production of the first excited states of the proton had been well measured [54]. The new features, discovered at the ISR by the CERN–Holland–Lancaster–Manchester (CHLM) Collaboration with the detector shown in Fig. 28, was a highlight of ISR small-angle physics.

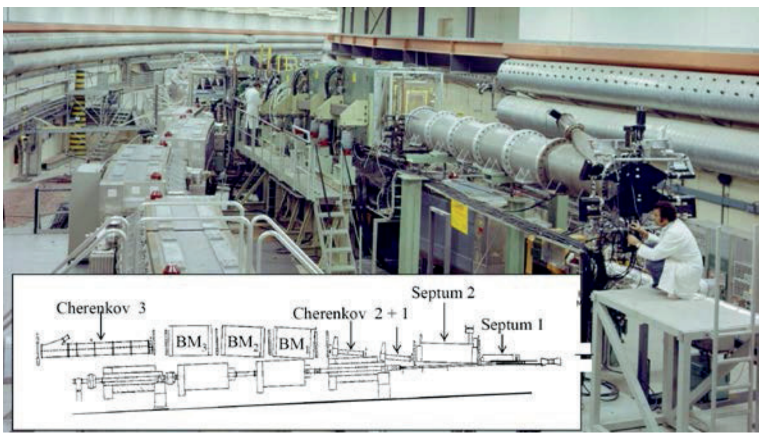

Fig. 28: As shown in Fig. 13, the apparatus of experiment R201 by the CERN–Holland–Lancaster–Manchester Collaboration was mounted in intersection region I2

By accurately measuring the momentum p of the forward-going proton, the mass M of the system moving in the opposite hemisphere and the momentum transfer t could be computed. As early as 1973 the CHLM Collaboration concluded [55] that the *invariant* cross-section shows a peak for $x \approx 1$ that *does not* change when the collision energy increases (Fig. 29a). (Note that most of the events belonging to the quasi-elastic peak ($0.95 \leq x \leq 1$) correspond to excitation of states with large masses: up to $M = 10$ GeV for the top ISR energy.) Figures 29b and 29c give other important properties of large-mass diffraction dissociation discovered by the CHLM Collaboration in the following two years [56, 57].

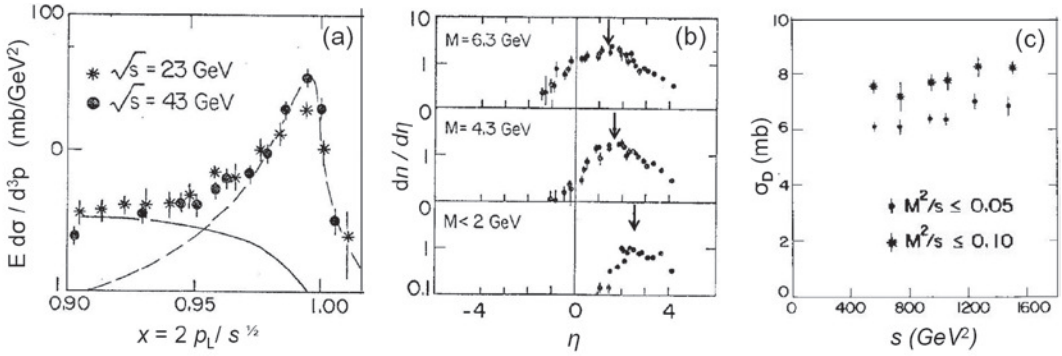

Fig. 29: (a) The high-mass peak of the invariant single diffraction cross-section, for a transverse momentum equal to 0.525 GeV/c, is energy independent [55]. (b) For all masses the pseudorapidity distributions peak around the arrows, which indicate the centre of the distribution expected from kinematics [56]. (c) The integrated single diffraction dissociation cross-section σ_D has a slight energy dependence in the range $550\ \text{GeV}^2 \leq s \leq 1500\ \text{GeV}^2$ [57].

In the t-channel approach, this phenomenon is interpreted by drawing a pomeron exchange graph (Fig. 30a′) similar to the one describing diffractive elastic scattering. This justifies the name 'single diffraction dissociation' of one of the incoming protons into a system of mass M. The rapidity span is $\ln(s/mM)$ (Fig. 30a) and M must have the same quantum numbers as the incoming proton, while spin and parity may be different because orbital angular momentum can be transferred by the exchanged pomeron. The three phenomena depicted in the figure are characterized by large 'rapidity gaps' and are particularly interesting when systems of large mass ($M > 2.5$ GeV) are produced.

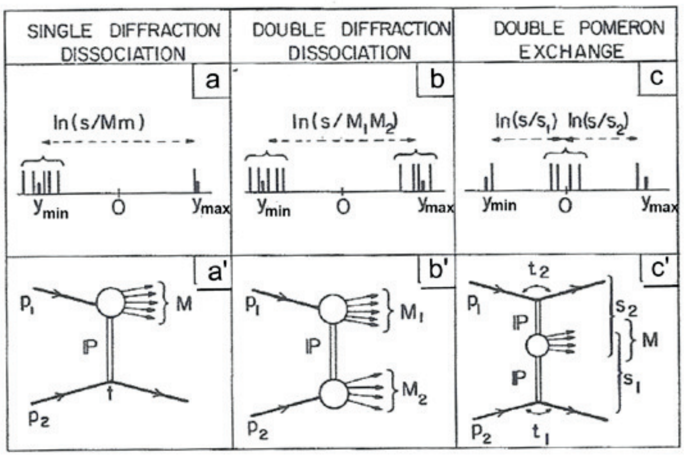

Fig. 30: Typical rapidity configurations of (a,a′) single diffraction dissociation, (b,b′) double diffraction dissociation and (c,c′) double pomeron exchange [58]

In the following years, the phenomenon was further studied, and in 1976 the CHLM Collaboration published other results, the most important being the measurements of the single diffraction cross-section σ_D [57], reproduced in Fig. 29c, which shows that its value (7–8 mb) is similar to that of the elastic cross-section.

The data were not sufficiently precise to decide whether the single diffraction cross-section also increases in the ISR energy range. However, the experimental fact [59] that (at fixed s and t) the invariant cross-section $d\sigma_D/dM^2$ *decreases* as $1/M^2$ indicates that its integral *increases* as $\ln s$, since it has to be computed for $0.95 \leq x \leq 1$, i.e., up to a maximum value of $M^2 = 0.05s$, which increases linearly with s. This and other interesting aspects of diffraction dissociation are discussed in two review papers published in 1976 and 1981 [58, 60].

Experimentally, *double* diffraction dissociation (Fig. 30b′) is much more difficult to study than single diffraction because the reconstruction of the two masses M_1 and M_2 requires both a large enough total rapidity span and the measurement of charged and neutral particles in the two forward cones. These conditions were not quite satisfied at the ISR.

Still, an estimate of the double diffractive cross-section could be made using ISR and Fermilab data, so much so that K. Goulianos, in the section 'Elastic and total cross-sections – Are they related through diffraction dissociation?' of a very often quoted review paper published in the closing year of the ISR [61], argued that the 'peripheral' rise of the total cross-section discovered at the ISR could be driven exclusively by the rapid increase of the sum of single and double diffraction dissociation.

The focus of ISR small-angle physics on the pomeron brought to light the very important phenomenon of Fig. 30c′, the so-called 'double pomeron exchange', which deserves a short discussion even if it is not really 'small-angle physics'.

In this reaction – even to produce a low-mass state having the quantum numbers of the vacuum – the two rapidity gaps have to be larger than $\Delta y = 3$ and the two final protons must have $x > 0.95$, conditions that are satisfied only at the largest ISR energies. In the last days of the ISR, forward drift chambers were added to the Axial Field Spectrometer (AFS) and the AFS Collaboration collected high-statistics data on the production of pion pairs in pomeron–pomeron collisions, as well as observing two kaons, four pions and proton–antiproton central states [62].

In a recent review paper on double pomeron exchange, Albrow, Coughlin and Forshaw [63] discussed the evolution of the field from the ISR times to the expectation that a single Higgs particle could be produced in Large Hadron Collider (LHC) pomeron–pomeron collisions. Such a discovery would be the last pillar of a long bridge whose first pillar was built forty years ago on the ISR shore.

Multiparticle production is the final subject to be discussed with reference to the very interesting results of the long-standing activity of the CERN–Bologna–Frascati (CBF) Collaboration working at the Split Field Magnet. The presentation will be short because, on the occasion of the ISR fortieth anniversary, the subject has been well covered by Antonino Zichichi [64, 65]. More details can be found in Ref. [66].

As already mentioned, at the ISR the bulk of the particles created in the collisions have small transverse momenta (of the order of 200 MeV/c, which correspond to a source having a radius of about 1 fm) and also a uniform rapidity distribution. The mean multiplicity of the events was expected to increase almost logarithmically with energy, a feature that was duly confirmed in the first months of running.

At the time, this mean multiplicity, when plotted as a function of the centre-of-mass energy $\sqrt{s}$, was different from that measured in electron–positron collisions, and nobody had thought to look for a correlation. Years later, the detailed study of thousands of such events guided the CBF Collaboration to the definition of an 'effective energy', which takes into account the fact that in the ISR events a large fraction of the energy of the colliding protons is taken away by the leading baryons, as shown in Fig. 31a. The situation is very different in electron–positron annihilations (Fig. 31b) and in deep inelastic scattering (DIS) induced by either charged leptons or neutrinos (Fig. 31c).

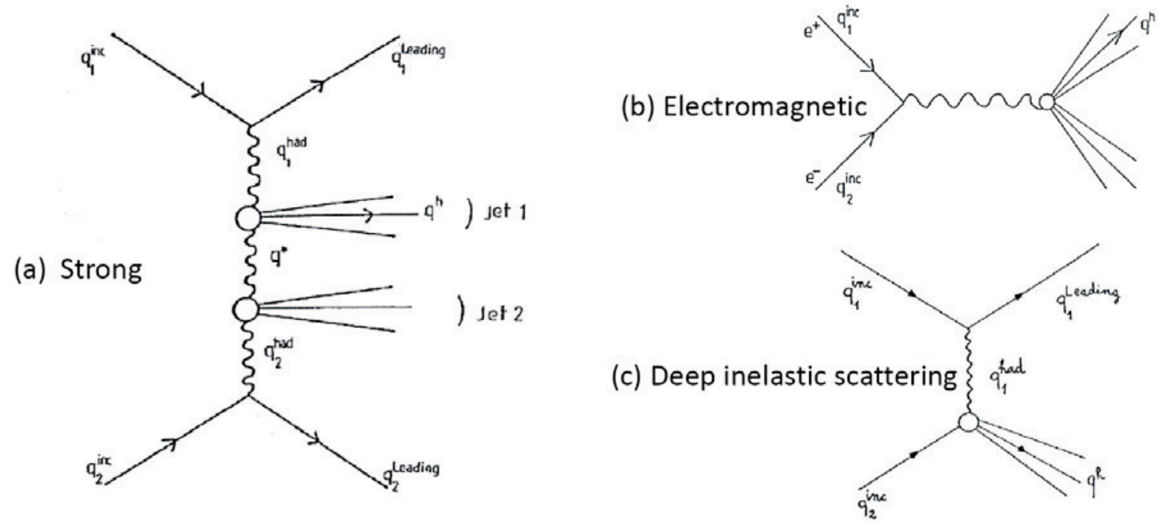

Fig. 31: In these kinematical graphs the quantities q are four-vectors. The final hadron jets are due to (a) the strong interaction, (b) the electromagnetic interaction in the time-like region and (c) either the electromagnetic or the weak interaction in the space-like region.

On subtracting the leading particles, the effective energy in the centre-of-mass system (indicated by the authors with the symbol $2E_{\mathrm{had}}$) is determined by the four-vectors $q_{1,2}{}^{\mathrm{had}}$, so taking into account the leading particle effect. In the same reference system, one can also compute the x variable of a hadron which (as shown in Fig. 31a) has momentum q^{h}. As shown in Fig. 32, a continuum of effective energies contribute to the distributions measured in collisions that happen at a given 'nominal' proton–proton energy (for instance $\sqrt{s}$ = 62 GeV).

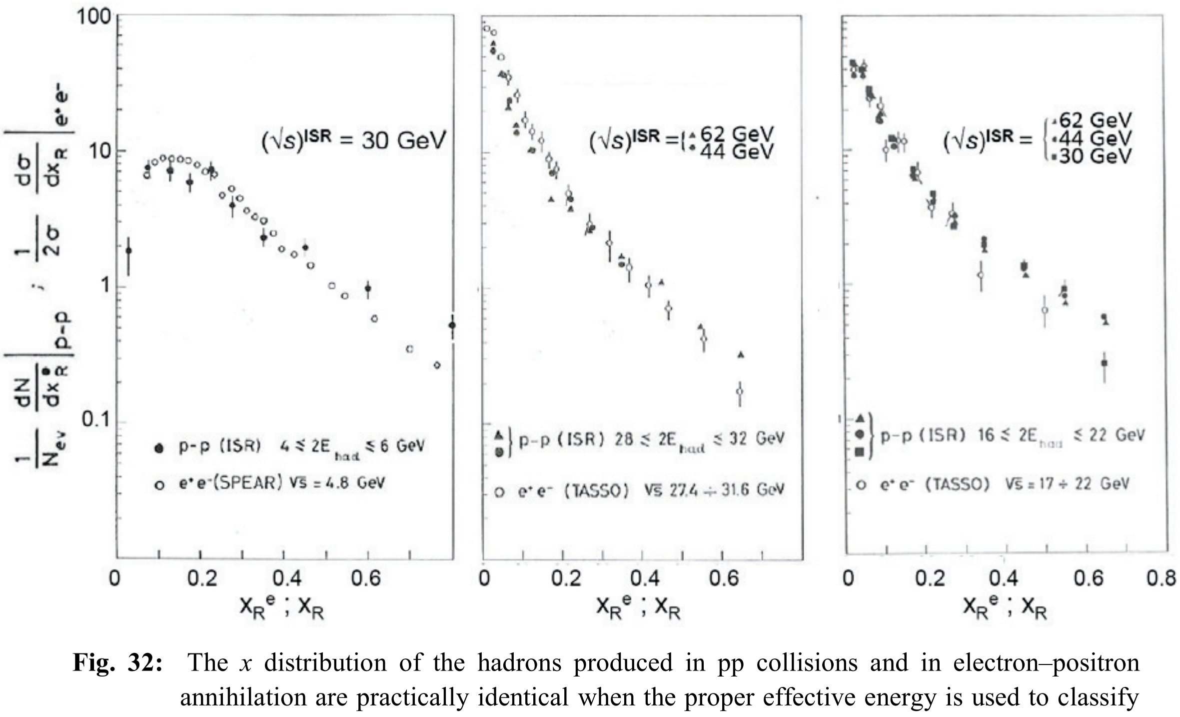

Fig. 32: The x distribution of the hadrons produced in pp collisions and in electron–positron annihilation are practically identical when the proper effective energy is used to classify the events

In Fig. 32 the x distributions of the single hadrons produced at the ISR – subdivided into three energy bands of effective energy – are compared with the results obtained in electron–positron collisions at the corresponding total energies.

Since the single-particle x distributions are similar, as shown in Fig. 32, the mean multiplicities in proton–proton and electron–positron collisions have the same energy dependence when the effective energy is used as independent variable.

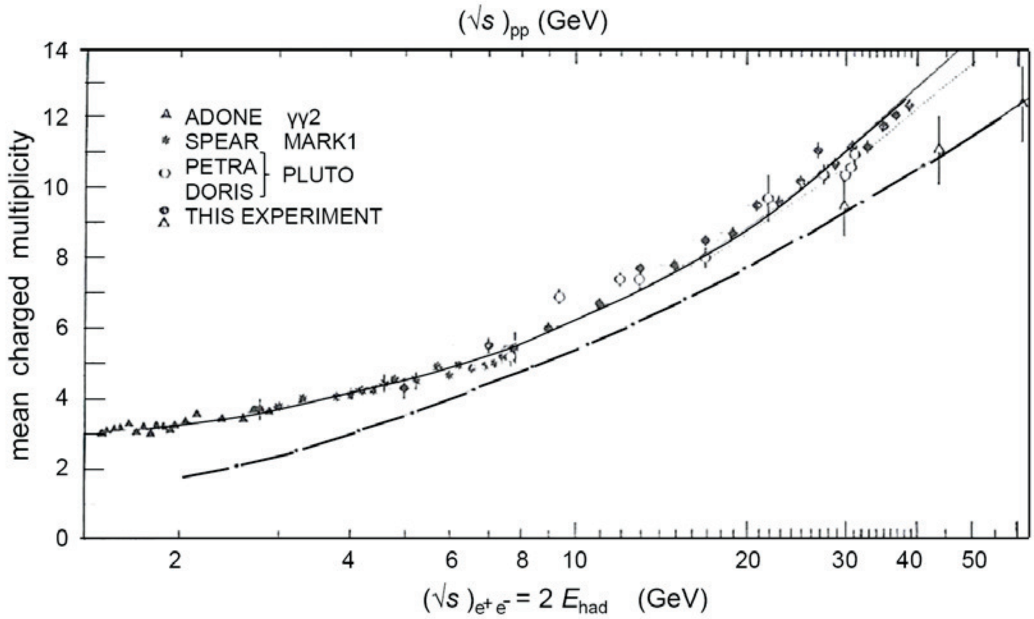

Fig. 33: As discovered by the CERN–Bologna–Frascati Collaboration, the mean multiplicities of electron–positron and proton–proton events cluster around the same continuous line when plotted versus the effective energy. The dash-dotted line represents proton–proton mean multiplicity plotted versus the collision energy $\sqrt{s}$.

Similar 'universality features' have been found by the CBF Collaboration when comparing, as a function of the effective energy, experimental data concerning the average charged-particle distributions in pp and νp collisions, the transverse momentum distributions and even scale breaking effects in pp and e^+e^- collisions. Moreover, when a hadron is present in the initial state, the leading effect is also universal and is determined by the 'flow' of quarks from the initial to the final state.

7 The ISR 'small-angle physics' seen from higher energies

In forty years, the energy of hadron–hadron colliders has passed from $\sqrt{s}$ = 30 GeV, the ISR minimum value, to the $\sqrt{s}$ = 7000 GeV available at the LHC starting in 2009. A review of the first results from this high-energy frontier is beyond the scope of the present paper, which however closes with some remarks concerning the energy evolution of the main phenomena discussed in the previous sections.

As a first point, let me consider multiple particle production and the physical quantities discussed at the end of the last section: it will be most interesting to compare the distributions of the many quantities studied at the ISR with the data collected at the LHC (pp collisions) and the Large Electron–Positron (LEP) collider (electron–positron annihilation). A confirmation of the universality features observed at energies that are ten times larger would give even more weight to the concepts of 'effective energy' and of 'quantum number flow'.

Going back to total cross-sections and real parts of the forward scattering amplitude, Fig. 34 reproduces the data obtained at the CERN antiproton–proton collider and at the Tevatron. The LHC total cross-section measurement published in 2011 by the TOTEM Collaboration [67] has been added to the summary figures, which describe all the data up to the Tevatron energy [68]. The best fit passes through the LHC point and gives $\gamma = 2.2 \pm 0.3$ as the exponent of the $\ln s$ term, in good agreement with what was found at the ISR [45].

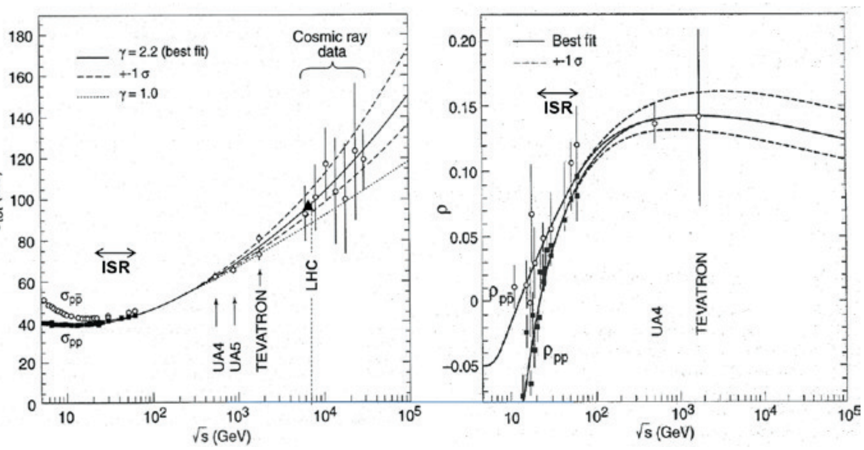

Fig. 34: The continuous lines represent the best fits to all the data, excluding the total cross-section measured in 2011 at the LHC: ($98.3 \pm 0.2 \pm 2.8$) mb [65]

Also, the slope of the forward elastic cross-section continues the trend measured at lower energies (Fig. 35), so that, by interpreting it as due to the slope of the pomeron trajectory, one still obtains $\alpha'(0) = 0.25$ GeV^{-2}.

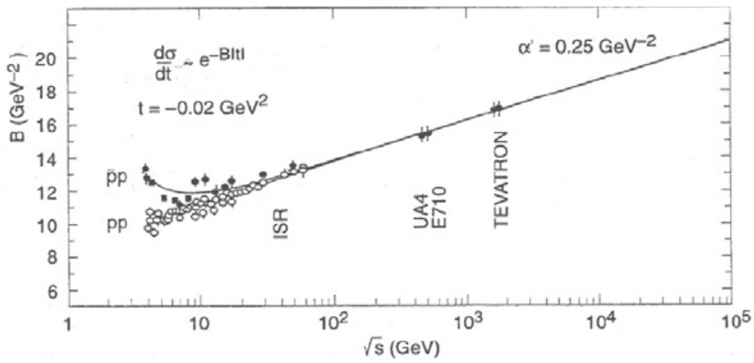

Fig. 35: The forward elastic cross-section shrinks as ln s in an enormous energy range: $30 \le \sqrt{s} \le 2000$ GeV

As far as the elastic and single diffraction dissociation cross-sections are concerned, Fig. 36 (taken from the review paper by Giorgio Matthiae [69]) shows that the single diffraction cross-section rises with energy in the same energy range (30–2000 GeV) and that the ratios σ_{el}/σ_{tot} and σ_D/σ_{tot}, which are equal and constant in the ISR energy range, diverge at larger energies.

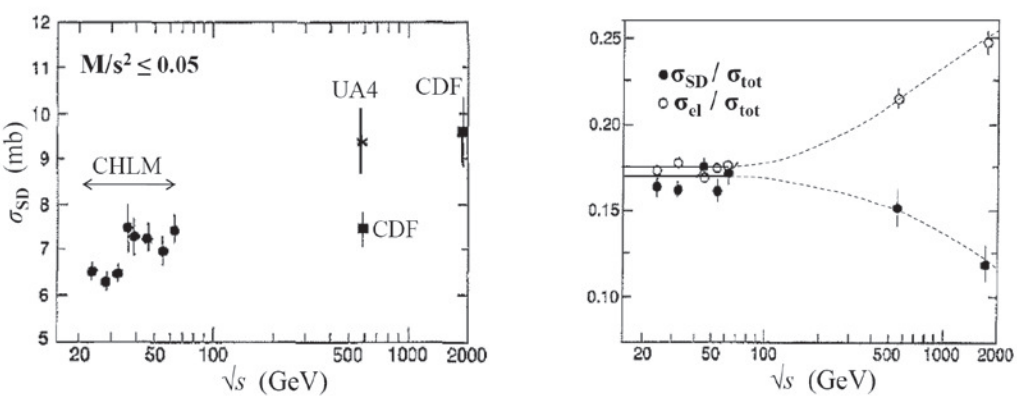

Fig. 36: The energy dependence of the cross-section for single diffraction dissociation σ_D seems to increase with energy (a) but the ratio σ_D/σ_{tot} definitely decreases (b), so that the importance of the phenomenon reduces at high energies

Figure 35b clearly indicates that the ISR energy range, in which masses larger than about 2.5 GeV can be produced in single diffractive dissociation, is a *transition region* and that the constancy of the ratio σ_{el}/σ_{tot} with energy is not an asymptotic behaviour.

Nevertheless, the scaling with $1/M^2$ of the single diffractive cross-section, found at the ISR, still holds at 500 GeV, as shown in Fig. 37, in agreement with the prediction of the triple pomeron exchange model.

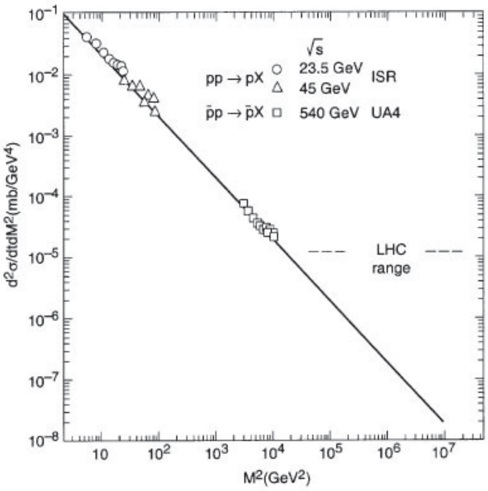

Fig. 37: The invariant single diffraction cross-section at a fixed t value ($-t = 0.5\ \mathrm{GeV}^{-2}$) measured at the CERN antiproton collider scales as $1/M^2$ as found at the ISR [69]

It is clear that the LHC, with its very large centre-of-mass energy, opens new possibilities because systems with very large masses can be excited by single (and also double) diffraction dissociation; for $M^2 \leq 0.05s$, the mass M of a singly diffracted system can be as large as 1.6 TeV!

Let us now consider elastic and total cross-sections. In the ISR energy range, the almost constant ratio $\sigma_{el}/\sigma_{tot} \approx 0.17$ (Fig. 36b) was an indication of an energy-independent value of the central inelastic overlap function $G_{in}(a = 0)$, even if this is not a rigorous conclusion, as shown by the analysis reported in Fig. 26b. Since the ratio σ_{el}/σ_{tot} increases at higher energies, as shown in the same figure, it does not come as a surprise that the behaviour of $\Delta G_{in}(a)$, in passing from the ISR to the CERN proton–antiproton collider, definitely increases with energy as shown by Henzi and Valin [70].

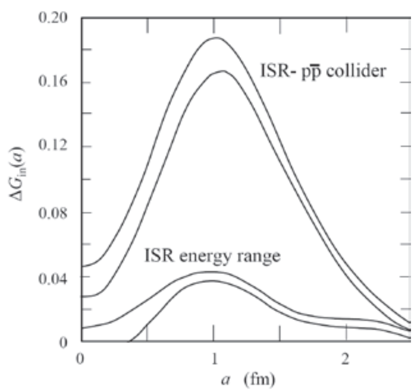

Fig. 38: (a) In the energy range that goes from the ISR to the CERN proton–antiproton collider (i.e., from 53 to 550 GeV), the central inelastic overlap integral increases [70]. (b) In the ISR energy range (i.e., from 23 to 62 GeV), the errors are such that no definite conclusion can be drawn on $G_{in}(0)$ [49]. The bands represent the estimated errors.

In summary, the s-channel description based on a *purely peripheral* increase of the inelastic overlap integral (sometimes called 'geometrical scaling') may be valid, but it is not certain, in the ISR energy range. This, together with the decreasing importance of single diffraction dissociation (Fig. 36b), implies that the rise with energy of the total cross-section may be driven by single and double diffraction up to $\sqrt{s} \approx 100$ GeV, but this is not the case at higher energies.

I conclude this discussion of the s-channel description of high-energy scattering by recalling that Henzi and Valin gave to their 1983 paper [70] a well-chosen title: 'Towards a blacker, edgier and larger proton'.

As a final argument, I consider the complementary, t-channel description of the energy dependence of hadron–hadron cross-sections.

In 1992 Donnachie and Landshoff wrote all the hadron–hadron total cross-sections as the sum $\sigma_{\text{tot}} = Xs^{\varepsilon} + Ys^{-\eta}$ of two powers, the first being due to pomeron exchange and the second to the exchange of the trajectory of Fig. 2 [3]. Figure 39 shows the experimental points and the fitted curves for the four best-measured channels. Of course, all known channels were included in the fit and the model contains 15 free parameters, most of which describe the low-energy behaviour of the cross-sections. It has to be stressed that the intercept of the reggeon trajectory ($\alpha_R(0) = 0.45$) is in good agreement with the value derived from the masses of the particles belonging to it (Fig. 2).

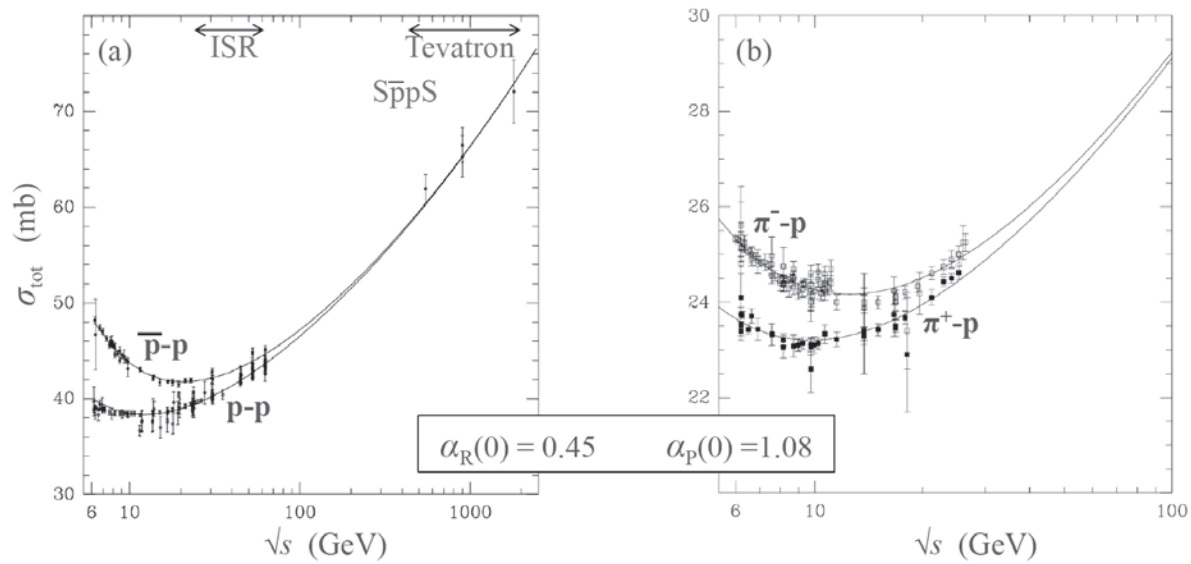

Fig. 39: The figure shows the fits obtained by A. Donnachie and P. Landshoff to the best-measured total cross-sections [3]

In the fit, the standard pomeron intercept is at $\alpha(0) = 1.08$ but the authors warn the reader that the exponent $\varepsilon = 0.08$ (appearing in the energy dependence s^{ε} of the total cross-sections) is a little less than $\alpha(0) - 1$ because of multiple pomeron exchange.

They state their conclusion in the following terms: 'The fact that all cross-sections rise with energy at the same rate s^{ε} makes it unnatural to attribute the rise to some intrinsic property of the hadrons involved. It is unhelpful to adopt a geometrical approach and to talk of hadrons becoming bigger and blacker as the energy increases. Rather the rise is a property of something that is exchanged, the pomeron, and this is why the rise is universal. … Our conclusions are in accord with the recent important results from UA8 at the CERN collider, which indicate that the pomeron does have a rather real existence: it can hit hadrons hard, break them up and knock most of their fragments sharply forward.'

This shows that twenty years ago the debate between the followers of the s-channel and the t-channel approaches to high-energy scattering phenomena was going on. And it is still alive, as indicated by a recent paper by Donnachie and Landshoff [69] who, forty years after the first ISR physics run, have analysed the data produced at the LHC by the TOTEM Collaboration [72] coming to the conclusion that their picture is still valid but a term has to be added due to the ‘hard pomeron’ already seen in electron–proton collisions at HERA.

8 Conclusions

It is often said that the ISR did not have the detectors needed to discover fundamental phenomena made accessible by its large and new energy range. This is certainly true for ‘high-momentum-transfer physics’, which, since the end of the 1960s, became a main focus of research, but the statement does not apply to the field that is the subject of this paper.

In fact, looking back to the results obtained at the ISR by the experiments that were programmed to study ‘small-angle physics’, one can safely say that the detectors were very well suited to the tasks and performed much better than foreseen.

As far as the results are concerned, in this particular corner of hadron–hadron physics, new phenomena were discovered, unexpected scaling laws were found and the first detailed studies of that elusive concept, which goes under the name ‘pomeron’, were performed, opening the way to phenomena that we hope will be observed at the LHC.

Moreover, some techniques and methods have had a lasting influence: all colliders had and have their Roman pots, and the different methods developed at the ISR for measuring the luminosity are still in use.

‘Small-angle physics’ is not very fashionable today but gave a lot of satisfaction to those who laboured around it and, in addition, has a great merit: it requires a very close collaboration among machine physicists and experimentalists, an invaluable gift that we enjoyed at the time of the ISR and for which we experimentalists are still grateful forty years later.

I am grateful to Mike Albrow, Luigi Di Lella and Kurt Hübner for suggestions and corrections to the first version of this report.

References

[1] A.N. Diddens *et al.*, *Phys. Rev. Lett.* **9** (1962) 108.

[2] S.P. Denisov *et al.*, *Phys. Lett.* **B36** (1971) 415.

[3] A. Donnachie and P.V. Landshoff, *Phys. Lett.* **B296** (1992) 227.

[4] V.N. Bolotov *et al.*, *Nucl. Phys.* **B73** (1974) 365

[5] I.Ya. Pomeranchuk, *Zh. Ehksp. Teor. Fiz.* **30** (1956) 423 [*Sov. Phys. JETP* **3** (1956) 306].

[6] M. Froissart, *Phys. Rev.* **123** (1961) 1053.

[7] A. Martin, *Phys. Rev.* **129** (1963) 1432.

[8] N.N. Khuri and T. Kinoshita, *Phys. Rev.* **B137** (1965) 720; *Phys. Rev.* **B140** (1965) 706.

[9] G. Bellettini *et al.*, Measurement of the p–p total cross section, CERN/ISRC/69-12, 14 March 1969.

[10] (a) P. Darriulat and C. Rubbia, CERN Int. Rep 68/340/5 SIS/si, 28 February 1968.

(b) P. Darriulat and C. Rubbia, On beam monitoring for ISR experiments, ISR User's Meeting, CERN, 10–11 June 1968.

[11] C. Rubbia, Report to the ISR user's meeting, CERN, ISR User's Meeting, 10–11 June 1968.

[12] W. Schnell, A mechanical beam profile monitor for the ISR, CERN, ISR User's Meeting, CERN Int. Rep., ISR-RF/68-19, 22 April 1968.

[13] J. Steinberger, Suggestions for the luminosity measurement of the ISR, CERN, ISR User's Meeting, 10–11 June 1968.

[14] A.P. Onuchin, Suggestions for the luminosity measurements at the ISR, CERN Int. Rep., NP/68/26.

[15] G. Cocconi, An absolute calibration of the ISR luminosity, CERN. Int. Rep., NP/67/436, 1967.

[16] L. Di Lella, Elastic proton–proton scattering with the ISR, CERN, ISR User's Meeting, 10–11 June 1968.

[17] C. Rubbia and P. Darriulat, High beta interaction region: a magnifying lens for very small angle proton–proton scattering, 1968.

[18] S. Van der Meer, Calibration of the effective beam height in the ISR, CERN Int. Rep., ISR-PO/68-31, 18 June 1968.

[19] K. Potter, Luminosity measurements and calculations, CERN Accelerator School 1992, CERN Yellow Report 94-01.

[20] U. Amaldi *et al.*, The measurement of proton–proton differential cross-section in the angular region of Coulomb scattering at the ISR, CERN/ISRC/69-20, 24 March 1969.

[21] L. Jones, Int. Conf. on High Energy Accelerators, Dubna, Eds. A.A. Kolomensky, A.B. Kusnetsov and A.N. Lebedev, JINR, 1964, p. 1232.

[22] B.D. Hyams and V. Agoritsas, Background in the ISR, CERN Int. Rep., AR/Int. SG/65-29.

[23] U. Amaldi, R. Biancastelli, C. Bosio, G. Matthiae, E. Jones and P. Strolin, Report on background measurements at the PS in preparation of the small angle ISR elastic scattering experiment, ISRC 70-25.

[24] P. Darriulat *et al.*, Measurement of the elastic scattering cross-section at the ISR, CERN/ISRC/69-19, 16 March 1969.

[25] M. Holder *et al.* (ACHGT Collaboration), *Phys. Lett.* **B35** (1971) 355.

[26] U. Amaldi *et al.* (CERN–Rome Collaboration), *Phys. Lett.* **B36** (1971) 504.

[27] V. Bartenev *et al.*, *Phys. Rev. Lett.* **31** (1973) 1088, 1367.

[28] G. Barbiellini *et al.* (ACHGT Collaboration), *Phys. Lett.* **B39** (1972) 663.

[29] A. Boehm *et al.* (ACHGT Collaboration), *Phys. Lett.* **B49** (1974) 491.

[30] M. Holder *et al.* (ACHGT Collaboration), *Phys. Lett.* **B36** (1971) 400.

[31] U. Amaldi, Elastic scattering and low multiplicities, Proc. Aix en Provence Int. Conf. on Elementary Particles, 6–12 September 1973 [*J. Phys. (Paris), Suppl. 10*, **34** (1973) C1-241].

[32] U. Amaldi *et al.* (CERN–Rome Collaboration), *Phys. Lett.* **B43** (1973) 231.

[33] U. Amaldi *et al.* (CERN–Rome Collaboration), *Phys. Lett.* **B44** (1973) 112.

[34] R. Amendolia *et al.* (Pisa–Stony Brook Collaboration), *Phys. Lett.* **B44** (1973) 119.

[35] W. Heisenberg, *Z. Phys.* **133** (1952) 65.

[36] H. Cheng and T.T. Wu, *Phys. Rev. Lett.* **24** (1970) 1456.

[37] H. Cheng, J.K. Walker and T.T. Wu, *Phys. Lett.* **B44** (1974) 283.

[38] U. Amaldi, Proton interactions at high energies, *Sci. Am.* **299** (1973) 36.

[39] G.B. Yodth, Y. Pal and J.S. Trefil, *Phys. Rev. Lett.* **28** (1972) 1005.

[40] J. Wdowczyk and E. Zujewska, *J. Phys.* **A6** (1973) L9.

[41] E. Nagy *et al.* (Annecy–Bonn–CERN–Hamburg–Heidelberg–Wien Collaboration), *Nucl. Phys.* **B150** (1979) 221.

[42] A. Donnachie and P.V. Landshoff, *Phys. Lett.* **B387** (1996) 637.

[43] U. Amaldi, Laws of hadronic matter, Proc. Erice School 1973, Ed. A. Zichichi (Academic Press, New York, 1974), p. 673.

[44] U. Amaldi *et al.* (CERN–Rome–Pisa–Stony Brook Collaboration), *Phys. Lett.* **B62** (1976) 460.

[45] U. Amaldi *et al.* (CERN–Rome Collaboration), *Phys. Lett.* **B66** (1976) 390.

[46] J. Dorenbosch, The real part of the forward proton–proton scattering amplitude measured at the CERN intersecting storage rings, Ph.D. thesis, University of Amsterdam, 1977.

[47] J.B. Bronzan, G.K. Jane and U.P. Sukhatme, *Phys. Lett.* **B49** (1974) 272.

[48] N. Amos *et al.* (CERN–Louvain-la-Neuve–Northwestern–Utrecht Collaboration), *Nucl. Phys.* **262** (1985) 689.

[49] U. Amaldi and K. Schubert, *Nucl. Phys.* **B166** (1980) 301.

[50] A. Martin, *Phys. Rev.* **D80** (2009) 065013.

[51] (a) H.I. Miettinen, s-channel phenomenology of diffraction scattering, Proc. Aix en Provence Int. Conf. on Elementary Particles, 6–12 September 1973 [*J. Phys. (Paris), Suppl. 10*, **34** (1973) C1-263].

(b) R. Henzi, B. Margolis and P. Valin, *Phys. Rev. Lett.* **32** (1974) 1077.

[52] R. Henzi, and P. Valin, *Nucl. Phys.* **B148** (1979) 513.

[53] L. Foà, High multiplicities, Proc. Aix en Provence Int. Conf. on Elementary Particles, 6–12 September 1973 [*J. Phys. (Paris), Suppl. 10*, **34** (1973) C1-241].

[54] J.V. Allaby *et al.* (CERN–Rome Collaboration), *Nucl. Phys.* **B52** (1973) 316.

[55] M.G. Albrow *et al.* (CHLM Collaboration), *Nucl. Phys.* **B72** (1973) 376.

[56] M.G. Albrow *et al.* (CHLM Collaboration), *Phys. Lett.* **B51** (1974) 424.

[57] M.G. Albrow *et al.* (CHLM Collaboration), *Nucl. Phys.* **B108** (1976) 1.

[58] U. Amaldi, M. Jacob and G. Matthiae, Diffraction of hadronic waves, *Annu. Rev. Nucl. Sci.* **26** (1976) 385.

[59] Y. Akimov *et al.* (The Axial Field Spectrometer Collaboration), *Phys. Rev.* **D14** (1976) 57.

[60] G. Alberi and G. Goggi, Diffraction of subnuclear waves, *Phys. Rep.* **74** (1981) 1.

[61] K. Goulianos, Diffraction interactions of hadrons at high energies, *Phys. Rep.* **101** (1983) 169.

[62] T. Åkesson *et al.* (The Axial Field Spectrometer Collaboration), *Nucl. Phys.* **B264** (1986) 154.

[63] M.G. Albrow, T.D. Coughlin and J.R. Forshaw, Central exclusive particle production in hadron colliders, *Prog. Part. Nucl. Phys.* **65** (2010) 149.

[64] A. Zichichi, Totally unexpected results from the ISR, *Nuovo Saggiatore* **27** (2011) 48.

[65] A. Zichichi, The ISR's totally unexpected results, *CERN Courier*, July 2011.

[66] V.N. Gribov, G. 't Hooft, G. Veneziano, V.F. Weisskopf and L.N. Lipatov (Eds.), *The Creation of Quantum Chromodynamics and the Effective Energy: In Honour of A. Zichichi on the Occasion of the Galvani Bicentenary Celebrations* (World Scientific Series in 20th Century Physics, Vol. 25, World Scientific, Singapore, 2000), p. 343.

[67] G. Antchev *et al.* (TOTEM Collaboration), *Europhys. Lett.* **96** (2011) 21002.

[68] C. Augier *et al.*, *Phys. Lett.* **B315** (1993) 503.

[69] G. Matthiae, Diffractive physics at the LHC, *Braz. J. Phys.* **30** (2000) 244.

[70] R. Henzi and P. Valin, *Phys. Lett.* **B132** (1983) 443.

[71] A. Donnachie and P.V. Landshoff, arXiv: 1112.2485 [hep-ph], 12 December 2011.

[72] G. Antchev *et al.* (TOTEM Collaboration), *Europhys. Lett.* **95** (2011) 41001.

Large-transverse-momentum processes: the ISR as a gluon collider

P. Darriulat

Abstract
It is argued that, contrary to what is often said, large-transverse-momentum hadronic processes studied at the ISR have made a significant contribution to the understanding of the strong interaction and, in particular, to the development of quantum chromodynamics. In their unique role as a gluon collider the ISR have provided information that no other accelerator could have directly offered. They allowed one to probe high values of the centre-of-mass energy that were not available to fixed-target experiments. The latter, however, were more flexible and, together, they allowed for powerful explorations of the hadron structure and of the relevant dynamics in sectors such as inclusive particle production, direct photon production, and jet structure studies. It remains true that, rightly so, the ISR will be mostly remembered as the founders of a lineage that includes the proton–antiproton colliders and, today, the LHC.

1 Introduction

It so happens that the lifetime of the Intersecting Storage Rings (ISR), roughly speaking the 1970s, coincides with a giant leap in our understanding of particle physics. However, it is honest to say that, to first order, there is no causal relation between the two. Yet, those of us who have worked at the ISR remember these times with the conviction that we were not merely spectators of the ongoing progress, but also — admittedly modest — actors. The ISR contribution, it seems to us, is too often unjustly forgotten in the accounts that are commonly given of the progress of particle physics during this period. In the present article, I try to present arguments of relevance to this issue in what I hope to be as neutral and unbiased a way as possible. I restrict the scope of my presentation to large-transverse-momentum processes, or equivalently to the probing of the proton structure at short distances. This, however, is not much of a limitation, as the ISR did not significantly contribute to the progress achieved in the weak sector.

Anyone trying to reconstruct history is prompt to learn that each individual has his own vision of what has happened in the past and that history can merely be an attempt at collecting all such visions into as coherent as possible a story. As David Gross reminds us [1], quoting Emerson, *"There is properly no history; only biography"*. In physics, this is particularly true when discoveries and new ideas occur at a rapid pace, as was the case in the 1970s. Each of us remembers a seminar, a discussion at coffee, the reading of a particular article, or another event of this kind as a milestone in his own understanding of the new ideas. For most of us, it has no incidence on the history of physics: I understood superconductivity 40 years after BCS and general relativity 90 years after Einstein... But for those having played a major role in the blooming of the new ideas, it has. For example, reading accounts by Steve Weinberg [2], David Gross [1], Gerard 't Hooft [3] or Jerry Friedman [4] of how they remember this period is particularly instructive in this respect.

The same kind of disparity that exists between the visions of different individuals also occurs between the visions of different communities. In particular, during the 1970s, the e^+-e^- community, the neutrino community, the fixed-target community, and the ISR community have all had quite different perceptions of the progress that was being achieved. It is therefore useful to recall briefly the main events in this period.

2 The main milestones

When Vicky Weisskopf, in December 1965, in his last Council session as Director-General obtained approval for the construction of the ISR, there was no specific physics issue at stake, which the machine was supposed to address; its only justification was to explore the *terra incognita* of higher-centre-of-mass-energy collisions (to my knowledge, since then, all new machines have been proposed and approved with a specific physics question in mind, which they were supposed to answer). The strong interaction was perceived as a complete mystery. The eightfold way, today understood as the approximate *SU(3)* flavour symmetry associated with interchanges of *u, d* and *s* quarks, was not believed to have significant consequences in the dynamics of the strong interaction. The fact that no free quark had been found in spite of intensive searches, and that states such as Δ^{++}, with spin-parity $3/2^{+}$, could not be made of three identical spin-½ *u* quarks without violating Fermi statistics, were discouraging such interpretations.

The first hint to the contrary came in 1968–1969 at SLAC [4] with the discovery of an important continuum in the deep-inelastic region of electron proton scattering. The 2-mile linear accelerator had started operation the preceding year and the experimental programme, using large spectrometers, extended over several years. From the very beginning, experimenters and theorists were in close contact, feeding each other with new data and new ideas, starting with Bjorken's ideas on scaling [5] and Feynman's ideas on partons [6], both early advocates of a proton structure consisting of point-like constituents. However, one had to wait until 1972 for the case for a quark model to become strong: by then, scaling had been established; the measurement of a small *R* value (the ratio of the absorption cross-sections of transverse and longitudinal virtual photons) had eliminated competitors such as the then popular Vector Dominance Model; deuterium data had been collected allowing for a comparison between the proton and neutron structure functions; a number of sum rules had been tested; evidence for the quarks to carry but a part of the proton longitudinal momentum had been obtained; the first neutrino deep-inelastic data from Gargamelle had become available [7]. By the end of 1972, the way was traced for Gross, Wilczek, and Politzer [8] to conceive the idea of asymptotic freedom and its corollary, infrared slavery, explaining why one could not see free quarks. By the end of 1973, the connection with non-Abelian gauge theories had been established and the "advantages of the colour-octet gluon picture", including the solution of the Fermi statistics puzzle, had been presented by Fritzsch, Gell-Mann, and Leutwyler [9]. QCD was born and, by 1974, was starting to be accepted by the whole community as ***the*** theory of the strong interaction. It took another three to four years for it to come of age.

By mid 1972, SPEAR, the Stanford electron–positron collider, had begun operation. In November 1974, it shook the physics community with what has since been referred to as a Revolution: the discovery of the Ψ going hand in hand with the simultaneous discovery of the *J* at Brookhaven. It immediately exploited its ability to produce pure quark–antiquark final states to measure the number of colours. However, there were so many things happening in the newly available energy domain (opening of the naked charm channels, crowded charmonium spectroscopy, production of the τ lepton) that it took some time to disentangle their effects and to understand what was going on. By the end of the decade, scaling violations had been studied both in neutrino interactions and in electron–proton annihilations (DORIS had started operation in Hamburg two years after SPEAR). QCD had reached maturity and the only puzzling questions that remained unanswered, the absence of a CP-violating phase and our inability to handle the theory at large distances, are still with us today.

3 What about the ISR?

The above account of the progress of particle physics in the 1970s, while following the standard folklore, does not even mention the name of the ISR. I remember having asked David Gross whether he was aware of the results obtained at the ISR and whether they had an impact on the development of QCD. His answer [10] was: *"Every one was aware of the qualitative phenomena observed in hadronic physics at large* p_T*, which were totally consistent with simple scattering ideas and parton* *model ideas [...] The tests were not as clean as in deep inelastic scattering, the analysis was more difficult and deep inelastic scattering was much cleaner in the beginning of perturbative QCD [...] Parton ideas did not test QCD at all, they simply tested the idea that there were point-like constituents but not the dynamics."* Alvaro de Rujula, who witnessed from Boston "the maiden years of QCD", being asked the same question, simply answered [10]: *"I do not know the answer to this question, I am not an historian"*. Such answers illustrate well the way in which the ISR were generally perceived: a collider that was shooting Swiss watches against each other, as Feynman once jokingly described. Yet, some theorists followed closely what the ISR were producing; paradoxically, Feynman was one of them, Bjorken was another.

David Gross could have returned the question to me: *"How aware were you, the ISR community, of the experimental progress at SLAC and of the new ideas in theory?"* The first name that comes to mind in answer to this question is that of Maurice Jacob. Maurice had spent a sabbatical at Stanford where, together with Sam Berman, he had written a seminal paper on point-like constituents and large-transverse-momentum production [11]. Back at CERN, he organized a lively series of discussions between ISR experimenters and theorists that proved to be extremely successful in permeating our community with the progress in deep-inelastic scattering and, later, in electron–positron collisions. At that time, our community was small enough to fit in the ISR auditorium. Maurice was gifted with an unusual talent to make theoretical ideas accessible to us. We all remember these seminars as a most profitable experience that brought coherence and unity in our community. For this reason, it makes sense to talk about a common ISR culture. In particular, by 1972, we were aware of the basic parton ideas and of the picture of large-transverse-momentum production factorized in three steps (Fig. 1): singling out a parton in each proton, making them interact (how, was not clear) in a binary collision and letting the final-state partons fragment into hadrons. There were a few papers [6, 11–16] in support of such a picture which most of us had read and which were our basic reference. Yet, in these early days, there was a typical delay of at least six months between SLAC and us for a new idea to be digested. There was even more delay, for most of us, to digest the more subtle development of non-Abelian gauge theories: we only knew about it from our theorist friends.

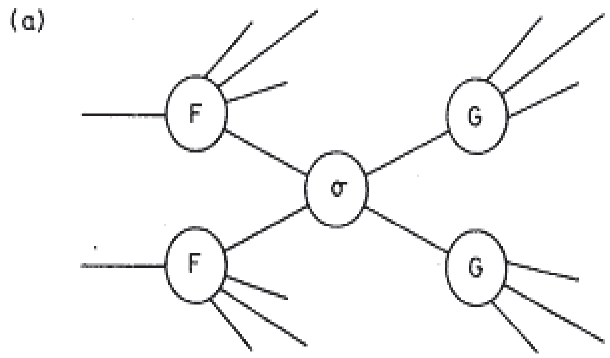

Fig. 1: Parton model picture of high-p_T hadron interactions. One parton of each of the incident hadrons (structure function F) experiences a binary collision (σ) and the outcoming partons fragment into hadrons (fragmentation function G)

Table 1 lists leading-order diagrams involving quarks or gluons. A simple glance at it illustrates the originality of the ISR: gluons contribute to leading order. In electron–proton annihilations and deep-inelastic scattering, gluons contribute to next-to-leading order only, in the form of radiative corrections associated with a bremsstrahlung gluon radiated from a quark line. This does not mean that such gluon contributions are unimportant: the scaling violations which they induce have been one of the most powerful tool in the development of our understanding of QCD. But, at the ISR, gluons not only contribute to leading order but indeed dominate the scene: in the low x regime characteristic of the ISR, collisions involving gluons, either gluon–gluon or quark–gluon, account for most of the high-p_T cross-section. Gluon interactions being a privileged domain of the ISR, and gluons having been the last component of the theory to be understood and digested, it seems difficult to argue that the ISR have played but a minor role. The more so when one considers that the ISR had exclusive access to the three- and four-gluon vertices, which are a specific expression of QCD as a non-Abelian gauge theory.

Table 1: Leading order processes involving quarks or gluons

Electron–positron annihilations			
1		$e^+e^- >\gamma< q^+q^-$	α^2G^2
Deep-inelastic electron scattering			
2		$eq]\gamma[eq$	α^2FG
Deep-inelastic neutrino scattering			
3	Neutral currents	$vq]Z[vq$	$\alpha_n{}^2FG$
4	Charged currents	$vq]W[lq$	$\alpha_{ch}{}^2FG$
Proton–proton collisions (ISR)			
5	Drell–Yan	$q^+q^- >\gamma< l^+l^-$	α^2F^2
6	Direct photons	$q^+q^-]q[\gamma g$	$\alpha\alpha_sF^2G$
7		$gq]q[\gamma q$	
8	Large p$_T$ hadrons	$qq]g[qq$	$\alpha_s{}^2F^2G^2$
9		$qq]q[gg$	
10		$q^+q^- >g< gg$	
11		$q^+q^- >g< q^+q^-$	
12		$gq]q[qg$	
13		$gq]g[qg$	
14		$qg >q< qg$	
15		$gg >g< q^+q^-$	
16		$gg >g< gg$	
17		$gg]q[qq$	
18		$gg]g[gg$	
19		$gg >< gg$	

We note s channel exchange as >< and t channel exchange as][. When necessary, quarks are written q^+ and antiquarks q^-. The last column gives the coupling constants, the number of structure functions (F), and the number of fragmentation functions (G) taking part in the cross section. The couplings are written α_n for $\alpha/(\sin\theta_W \cos\theta_W)^2$ and α_{ch} for $\alpha/\sin\theta_W{}^2$ with θ_W being the Weinberg angle. Processes involving gluons in the initial state are shaded.

4 Large transverse momentum: inclusive production data

In 1972–1973, three ISR teams [17–19] announced the observation of an unexpectedly copious pion yield at large transverse momenta (Fig. 2), orders of magnitude above a (traditionally called naïve) extrapolation of the exponential distribution observed at low-p_T values, ~exp$(-6p_T)$. "Unexpectedly" is an understatement. The whole ISR experimental programme had been designed under the assumption that all hadrons would be forward-produced. The best illustration was the Split Field Magnet, meant to be the general multipurpose detector at the ISR. No experiment was equipped with very large solid angle good-quality detectors at large angle. This first discovery was opening the ISR to the study of large-transverse-momentum production and was providing a new probe of the proton structure at short distances. That

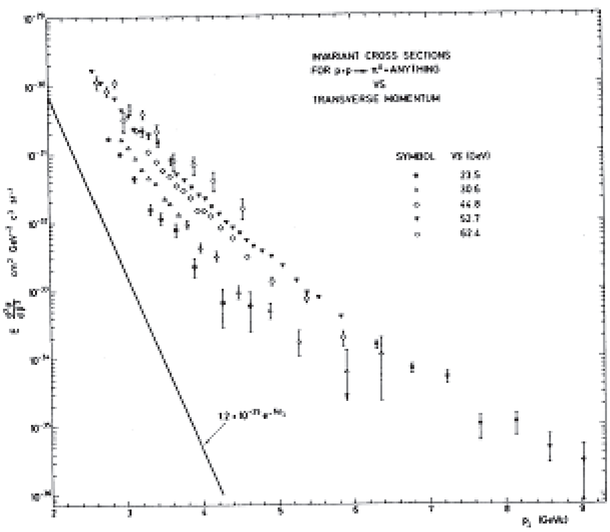

Fig. 2: Early inclusive π^0 cross-section [20] giving evidence for copious production at high p_T well above the exponential extrapolation of lower energy data

was the good side of it. But it also had a bad side: the background that had been anticipated in the search for new particles had been strongly underestimated and such searches were now becoming much more difficult than had been hoped for.

Bjorken scaling was found to apply, in support of the parton picture, but the index of the p_T power law was twice as high as the value expected from point-like constituents, 8 rather than 4. Precisely, the π^0 inclusive invariant cross-section was of the form $p_T^{-n}\exp(-kx_T)$ where $x_T = 2p_T/\sqrt{s}$, $n = 8.24 \pm 0.05$ and $k = 26.1 \pm 0.5$. The impact of this result was quite strong and brought into fashion the so-called constituent interchange model [20]. The idea was to include mesons in addition to quarks among the parton constituents of protons: deep-inelastic scattering would be blind to such mesons because of their form factor but hadron interactions would allow for quark rearrangements such as $\pi^+ + d \rightarrow \pi^0 + u$. At large values of x_T, the cross section was then predicted to be of the form $p_T^{-2(n-2)}(1-x_T)^{2m-1}$ where n stands for the number of "active quark lines" taking part in the hard scattering and m stands for the number of "passive" quark lines wasting momentum in the transitions between hadrons and quarks. The model, that correctly predicted the power 8 measured at the ISR, had many successes but did not stand the competition with early QCD models that were starting to be developed. Such an example is illustrated in Fig. 3, giving evidence for important quark–gluon and gluon–gluon contributions [21] beside the quark–quark term. By then, the inclusive production of charged pions, kaons, protons, and antiprotons as well as η mesons had been studied at the ISR, and at Fermilab where a π^- beam had also been used, providing decisive evidence in favour of QCD. It was then understood that the p_T power law was indeed evolving to p_T^{-4} at high values of x_T, which, however, were only accessible, in practice, to larger-centre-of-mass-energy collisions. The successes of the constituent interchange models were then relegated to the rank of "higher twist corrections" to the leading-order perturbative regime.

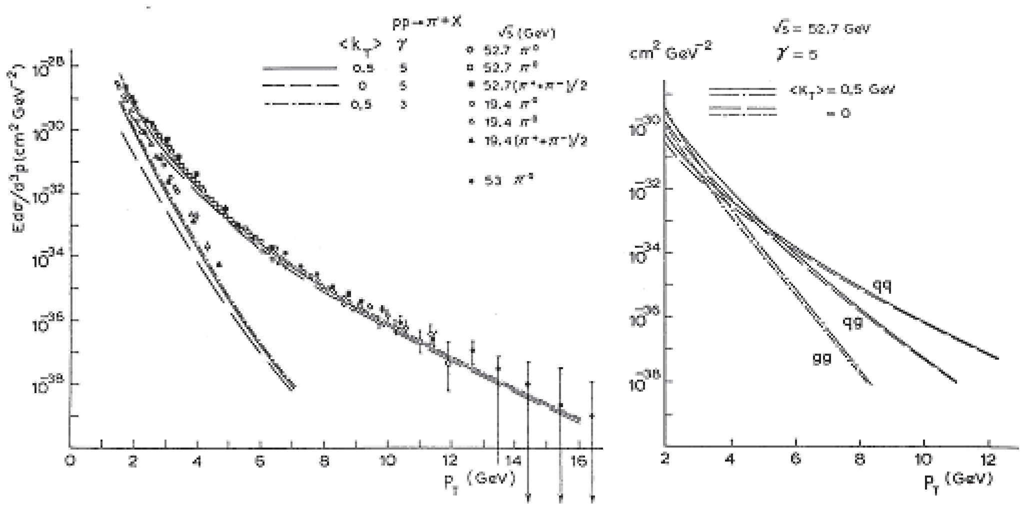

Fig. 3: A typical QCD fit [21] to inclusive pion data (left) and the relative contributions of quark–quark, quark–gluon and gluon–gluon diagrams (right)

Between 1973 and 1978, inclusive high-p_T single-hadron production in hadron collisions had given exclusive contributions to the establishment of QCD as the theory of the strong interaction in a domain where other experiments — deep-inelastic scattering and electron–positron annihilations — could not contribute: that of short-distance collisions involving gluons to leading order of the perturbative expansion. In this domain, the data collected at the CERN ISR — at the higher-centre-of-mass energies — and at Fermilab — with a variety of beams and targets — nicely complemented each other. As the results were confirming the validity of QCD, and as there were so many important events happening elsewhere in physics, people tended to neglect or forget these important contributions.

5 Event structure and jets

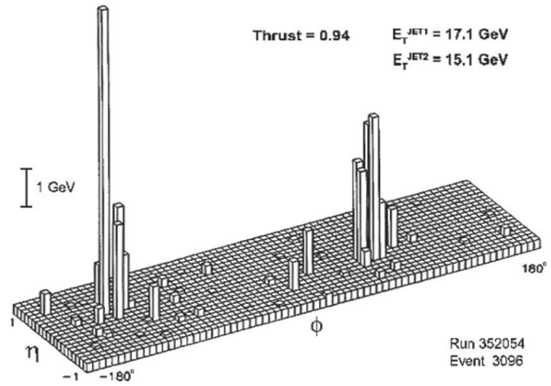

Fig. 4: A lego plot from the AFS experiment showing the two-jet structure that dominates at larger transverse energies. (from Ref. [23])

The early evidence in favour of the parton picture encouraged studies of the global event structure and, in particular, experiments aiming at the detection of the hadron jets into which the hard-scattered partons were supposed to fragment. Unfortunately, none of the existing ISR detectors was matched to the task. In March 1975, a large magnetic detector serving precisely this purpose had been proposed to the ISR Committee by a collaboration of British, Scandinavian, and US physicists but had been rejected in October of the same year. The proposal had been reiterated with various amendments. It was enjoying the support of the ISR community, of a Working Party that had been appointed to assess "the need for a new magnetic facility at the ISR", with Nino Zichichi in the chair, and of the ISR Committee (69th meeting, November 10th, 1976). It was definitively turned down two weeks later by the Research Board. Meanwhile, step by step, the existing ISR experiments had upgraded their set-ups as well as they could but one had to wait until 1982, with the Axial Field Spectrometer in I8 and the Superconducting Solenoid in I1 to see detectors having large calorimeter coverage (electromagnetic and hadronic for the former but only electromagnetic for the latter). When the ISR closed down in 1984, a rich set of important results had been obtained by these two groups [22], with two-jet events (Fig. 4) dominating the scene for transverse energies in excess of 35 GeV [23]; but the CERN proton–antiproton collider, which had published its first jets in 1982 [24], had already taken the limelight away from the ISR.

There is no doubt that the lack of proper instrumentation has been a major handicap for the ISR in their contribution to the physics of hard collisions. More support from the management would probably have made it possible to gain two precious years. Retrospectively, it is difficult to estimate how much of a negative impact the approval of a new large facility at the ISR would have had on the high-priority CERN programmes, LEP and the proton–antiproton collider. There is no doubt that these were the machines where quark and gluon jets could be studied in optimal conditions: in comparison, the ISR were quite marginal. Moreover, the ISR beam geometry, with a crossing angle of 15° and the need for large vacuum chambers, was making the design of a 4π detector difficult. Seen from today, thirty years later, our frustration was certainly understandable and legitimate, but the decision of the management sounds now more reasonable than it then did.

Between 1973 and 1978, several ISR experiments had completed studies of the event structure and the evidence for hard jets in the final state, already clear in 1976 [25], had become very strong. Figure 5 shows the longitudinal phase-space density of charged particles produced in a hard-scattering collision. It is an average of data collected by the British–French Collaboration using a charged-particle trigger at 90° and momentum analysing in the Split Field Magnet the charged particles produced in association. Particle densities are normalized to those obtained in minimum-bias collisions. Particle densities are normalized to those obtained in minimum-bias collisions. Several features are visible: diffraction is suppressed at large rapidities, a ‘same-side’ jet is present alongside the trigger and ‘away-side jets’, at opposite azimuth to the trigger, cover a broad rapidity range.

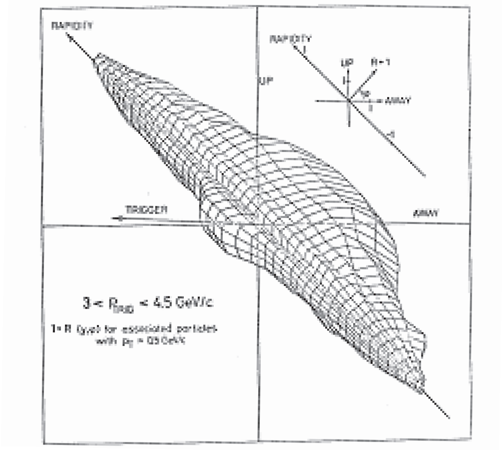

Fig. 5: Longitudinal phase-space density (relative to minimum-bias events) associated with a single particle trigger at 90° (see text)

A difficulty inherent to the study of hard hadron collisions is the presence of a so-called ‘underlying event’ which contains the fragments of the spectator partons that do not take part in the hard collision. This is at variance with electron–positron annihilations where all hadrons are fragments of the hard scattered partons and, to a lesser extent, with deep-inelastic scattering where most of the information is carried by the structure functions. It implies a transverse momentum threshold, half a GeV to one GeV, below which a particle cannot be unambiguously identified as being a fragment of a hard scattered parton. At ISR energies, it is a serious limitation.

A second difficulty, resulting from the lack of proper calorimeter coverage in the first decade of ISR operation, was the so-called ‘trigger bias’. Since the hard parton scattering cross-section has a much steeper p_T dependence than has the fragmentation process, it is very likely for a particle of a given p_T to be the leading fragment of a rather soft jet. This distortion of the ‘same-side’ jet fragmentation creates an asymmetry between it and the ‘away-side’ jet, which makes it more difficult to compare their properties. For this reason, an ideal experiment should trigger on the total transverse energy E_T using calorimetric devices. Numerous studies of the ‘same-side’ correlations have been performed at the ISR, establishing early that they were not the result of resonance production but of a jet fragmentation characterized by a limited transverse momentum around the jet axis.

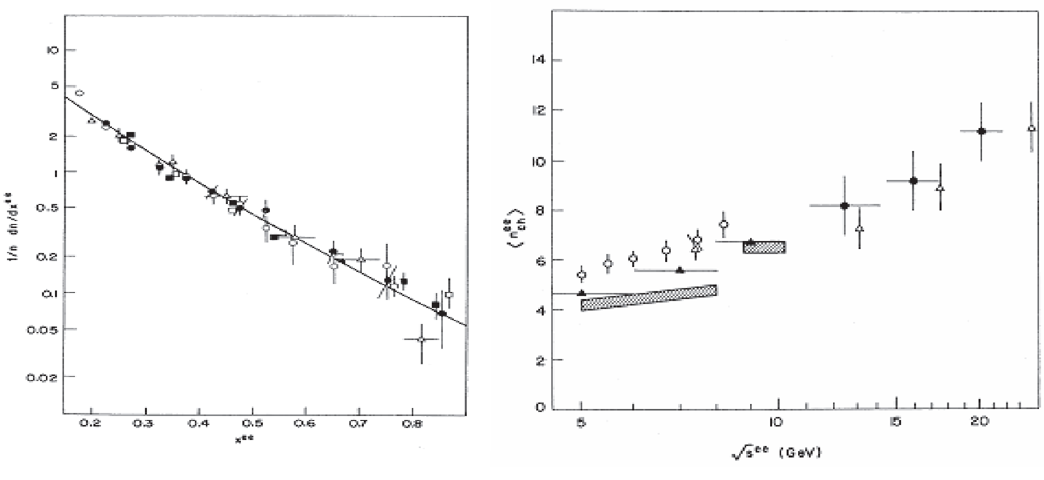

Fig. 6: Left: Jet fragmentation functions measured in different processes (triangles are for neutrino deep-inelastic, circles for high-p_T hadronic interactions at the ISR and the solid line for e^+e^- annihilations). Right: Mean charge multiplicity of hadron jets as a function of the equivalent e^+e^- energy as measured at SPEAR and DORIS (cross-hatched rectangles), at PETRA (open triangles), in neutrino deep-inelastic

Evidence for an excess of particles at opposite azimuth to the trigger had been obtained very early and it had soon been recognized that it was due to a collimated jet produced at a rapidity which was different from event to event. The away-side jet multiplicity could then be measured and compared to that of quark jets observed in deep inelastic and electron–positron annihilations (Fig. 6 right). ISR jets being dominantly gluon jets, one could expect to see a difference but the p_T range accessible to the ISR was still too low to reveal significant differences in the fragmentation functions of quark and gluon jets (Fig. 6 left).

In electron–positron collisions, the first evidence for quark jets came from SPEAR in 1975 [26] and the first evidence for gluon jets came from PETRA in 1979–1980 [27]. The former were 4 GeV quark jets, PETRA's gluon jets were typically 6 GeV, ISR jets — mostly gluon jets — were at least 10 GeV. The e^+e^- data were analysed in terms of event shapes: sphericity, oblateness, thrust, triplicity, etc. There was no doubt that, without any theoretical preconception, the evidence for ISR jets was stronger than the evidence for quark jets at SPEAR in 1975 and the evidence for gluon jets at PETRA in 1979–1980; the ISR physicists who studied large-transverse-momentum production were rightly feeling frustrated with the relative lack of public recognition given to their data compared with the enthusiasm generated by the SPEAR and PETRA results. The worst sceptics were to be found in the fixed-target community where too low values of the centre-of-mass energy prevented jets from being revealed. There were exceptions, however. I remember Walter Selove spending the Summer months at CERN and scanning with us our streamer chamber data collected with a high-p_T π^0 trigger at 90°: each time he would see some kind of a jet, he would exult and copy its configuration in a notebook.

Part of the imbalance in the reception given to ISR data compared with SPEAR and PETRA data was subjective: the analysis of ISR data was too complicated, which for many meant "was not clean". But, one must recognize that a good part was objective. First because the SPEAR and PETRA detectors were better fitted to these kinds of studies and second, more importantly, because good physics is done with, rather than without, theoretical preconception. In the SPEAR case, the beauty of their results came from two important features which gave strong support to the quark jet hypothesis: the azimuthal distribution of the jet axis displayed the behaviour expected from the known beam polarization and its polar angle distribution obeyed the $1 + \cos^2\theta$ law expected in the case of spin -½ partons. In the PETRA case, by mid-1980, all four experiments had presented clear evidence for gluon bremsstrahlung, including convincing comparisons with QCD predictions.

At the ISR, the complexity of the physics processes at stake was undoubtedly much larger than at electron–positron colliders, making it difficult to devise decisive QCD tests independent from what had been learned at other accelerators. But, once again, ISR data were exploring elementary processes which were not accessible to other accelerators and were shown to nicely fit in a coherent QCD picture embedding deep-inelastic as well as e^+e^- annihilation results. This was clearly an independent and essential contribution to the validation of QCD.

6 Photons and leptons

Leptons were produced at the ISR either as decay products of other particles or as a continuum of opposite-charge pairs coupled to a quark–antiquark pair in the initial state via a virtual photon in the s channel, the so-called Drell–Yan process. In the first half of the decade, the e/π ratio had been measured by several experiments to be of the order of 10^{-4} over a broad range of transverse momenta and was understood as being the result of a 'cocktail' of different sources, including, among others, open charm and charmonium. By the end of the decade, the J/Ψ and the Υ had been detected and their production cross-section had been measured. Moreover, a clear evidence for D production [28] had been obtained at the Split Field Magnet — for the first time in hadron interactions. Dilepton masses up to 20 GeV have been ultimately studied, giving evidence for strong next-to-leading-order corrections to the Drell–Yan leading-order diagram.

The production of direct photons was soon recognized to be a particularly simple process: its comparison with QCD predictions could be expected to be instructive. It proceeds either by a quark–antiquark pair in the initial state radiating a photon and a gluon in the final state or by a Compton-like interaction between a quark and a gluon producing a quark and a photon. In both cases, the photon is produced alone, without high-p_T companions, and its transverse momentum is balanced by a hadron jet. At the ISR, the Compton diagram dominates: the study of direct photon production should provide information on the gluon structure function as well as a measurement of α_s, the quark fragmentation being borrowed from e^+e^- data. In the first half of the decade, pioneering measurements established the existence of a signal and identified backgrounds, the main source being π^0 and η decays sending one of the two decay photons alongside their own momentum. At the end of the decade, clear signals were observed [29, 30] and a series of measurements followed, which, together with fixed-target data, provided a very successful laboratory for QCD (Fig. 7). Once again, hadronic interactions, both on fixed-target machines and at the ISR, had made use of their unique ability to study gluon collisions and to give essential contributions to the study of the strong interaction in the QCD perturbative regime [31].

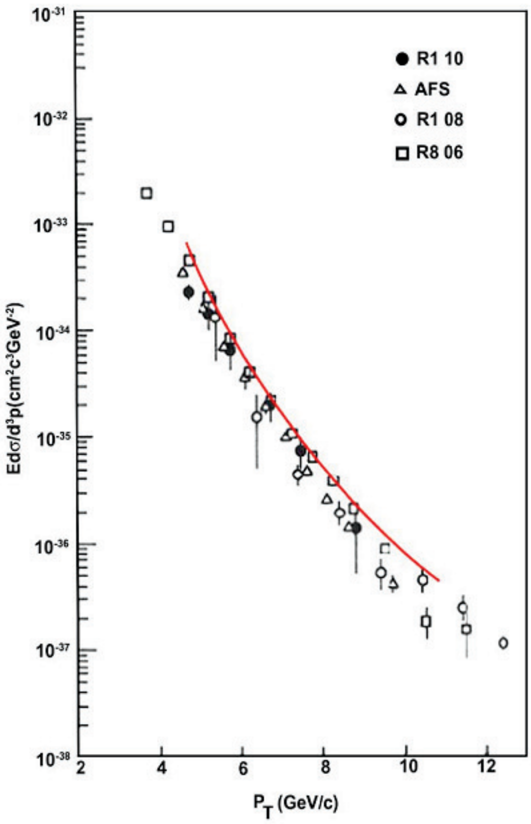

Fig. 7: Experimental invariant cross-sections for direct photon production (compilation by L. Camilleri) are compared with a next to leading order QCD calculation (by P. Aurenche and M. Werlen), from Ref 24.

7 The ISR legacy

I hope that this brief review of ISR contributions to the new physics that was born in the 1970s, and specifically to QCD becoming the theory of the strong interaction, has convinced the reader that they were more than a mere test of the idea that there were point-like constituents inside the proton. Together with hard hadron interactions on fixed-target machines, they made optimal use of their exclusive property to study the gluon sector of QCD to leading order. The ISR had the privilege of a higher centre-of-mass energy, fixed-target machines had the privilege of versatility, their respective virtues nicely complemented each other. Many factors have contributed to the relative lack of recognition which has been given to ISR physics results: the absence, for many years, of detectors optimized for the study of hard processes, the fact that the weak sector, which during the decade was the scene of as big a revolution as the strong sector, was completely absent from the ISR landscape and, may be most importantly, the fact that hard hadron collisions imply complex processes which may seem ‘dirty’ to those who do not make the effort to study them in detail.

We, who worked at the ISR, tend not to attach much importance to this relative lack of recognition because for us, their main legacy has been to have taught us how to make optimal use of the proton–antiproton collider, which was soon to come up. They had given us a vision of the new physics and of the methods to be used for its study which turned out to be extremely profitable. They had played a seminal role in the conception of the proton–antiproton collider experiments, they were the first hadron collider ever built in the world, they were the machine where a generation of physicists learned how to design experiments on hadron colliders. We tend to see the ISR and the proton–antiproton colliders, both at CERN and at the Tevatron, as a lineage, father and sons, the success of the latter being indissociable from the achievements of the former.

We were young then, this may be another reason why we remember these times with affection. With the LHC coming up, the lineage has now extended to a third generation and we look at the future with the eyes of grandparents, full of tenderness and admiration for their grandson whom we wish fame and glory.

Acknowledgements

It is a pleasure to thank the Director-General and the organizers of the Colloquium for their very successful initiative and for having invited me to give this brief recollection. I am deeply grateful to Luigi Di Lella, Antonino Zichichi and Giorgio Bellettini for pertinent comments on the manuscript and at the end of the oral presentation.

References

General reviews, such as those listed below, are an important source of references:
Giorgio M. Giacomelli and Maurice Jacob, *Physics at the CERN-ISR*, Phys. Rep. 55 (1979) 1–132.
Léon van Hove and Maurice Jacob, *Highlights of 25 years of physics at CERN*, Phys. Rep. 62 (1980) 1–86.
Maurice Jacob, *History of ISR physics* in: *A Review of Accelerator and Particle Physics at the CERN Intersecting Storage Rings: Invited Talks at the Last Meeting of the ISR Committee*, 27 January 1984, CERN 84-13 (1984), pp. 21–81.

[1] David J. Gross, *Asymptotic freedom, confinement and QCD*, History of Original Ideas and Basic Discoveries in Particle Physics, Erice, Italy, 1994, H. B. Newman and T. Ypsilantis editors, NATO ASI series, B352 (Plenum, New York, 1996), p. 75.

[2] Steven Weinberg, *Electroweak reminiscences*, History of Original Ideas and Basic Discoveries in Particle Physics, Erice, Italy, 1994, H. B. Newman and T. Ypsilantis editors, NATO ASI series, B352 (Plenum, New York, 1996), p. 27; *The making of the Standard Model*, Symposium on Prestigious Discoveries at CERN, CERN, Geneva, 2003, R. Cashmore, L. Maiani, and J.-P. Revol editors, Eur. Phys. J. C34 (2004) 5–13.

[3] Gerard ‘t Hooft, *Gauge theory and renormalization*, History of Original Ideas and Basic Discoveries in Particle Physics, Erice, Italy, 1994, H. B. Newman and T. Ypsilantis editors, NATO ASI series, B352 (Plenum, New York, 1996), p. 37; *The creation of quantum chromodynamics,* The Creation of Quantum Chromodynamics and the Effective Energy, Festschrift in Honour of A. Zichichi on the Occasion of the Galvani Bicentenary Celebrations, 1998, L. N. Lipatov editor, World Scientific Series in XXth Century Physics, Volume 25 (World Scientific, Singapore, 2001).

[4] Jerome I. Friedman, *Deep inelastic scattering evidence for the reality of quarks*, History of Original Ideas and Basic Discoveries in Particle Physics, Erice, Italy, 1994, H. B. Newman and T. Ypsilantis editors, NATO ASI series, B352 (Plenum, New York, 1996), p. 725.

[5] James D. Bjorken, private communication to the MIT–SLAC group, 1968, and Phys. Rev. 179 (1969) 1547.

[6] Richard P. Feynman, Phys. Rev. Lett. 23 (1969) 1415; Proceedings of the IIIrd International Conference on High Energy Collisions, Stony Brook, NY, 1969 (Gordon and Breach, New York, 1969).

[7] Donald H. Perkins, *in* Proceedings of the XVIth International Conference on High Energy Physics, Batavia, IL, 1972, D. J. Jackson, A. Roberts, and R. Donaldson editors (NAL, Batavia, IL, 1973), vol. 4, p. 189.

[8] David J. Gross and Frank Wilczek, Phys. Rev. Lett. 30 (1973) 1343; Phys. Rev. D8 (1973) 3633 and Phys. Rev. D9 (1974) 980.

[9] H. Fritzsch, Murray Gell-Mann, and H. Leutwyler, Phys. Lett. 47B (1973) 368.

[10] Alvaro De Rújula, *QCD in "her" maiden years*, History of Original Ideas and Basic Discoveries in Particle Physics, Erice, Italy, 1994, H. B. Newman and T. Ypsilantis editors, NATO ASI series, B352 (Plenum, New York, 1996), p. 123.

[11] S. M. Berman and M. Jacob, Phys. Rev. Lett. 25 (1970) 1683.

[12] J. D. Bjorken and E. A. Paschos, Phys. Rev. 185 (1968) 1975.

[13] S. D. Drell, D. J. Levy, and T. M. Yan, Phys. Rev. 187 (1969) 2159.

[14] S. M. Berman, J. D. Bjorken, and J. Kogut, Phys. Rev. D4 (1971) 3388.

[15] J. Kuti and V. F. Weisskopf, Phys. Rev. D4 (1971) 3418.

[16] S. D. Drell and T. M. Yan, Phys. Rev. Lett. 25 (1970) 316.

[17] B. Alper *et al.*, Phys. Lett. B44 (1973) 521.

[18] M. Banner *et al.*, Phys. Lett. B44 (1973) 537.

[19] F. W. Büsser *et al.*, Phys. Lett. B46 (1973) 471 and Proceedings of the XVIth International Conference on High Energy Physics, Batavia, IL, 1972, D. J. Jackson, A. Roberts, and R. Donaldson editors (NAL, Batavia, IL, 1973).

[20] For a review, see D. Sivers, R. Blankenbecler, and S. J. Brodsky, Phys. Rep. C23 (1976) 1.

[21] A. P. Contogouris, R. Gaskell and S. Papadopoulos, Phys. Rev. D17 (1978) 2314.

[22] T. Akesson *et al.*, Phys. Lett. B118 (1982) 185 and 193; Phys. Lett. B123 (1983) 133; Phys. Lett. B128 (1983) 354; Z. Phys. C25 (1984) 13; Z. Phys. C30 (1986) 27; Z. Phys. C32 (1986) 317; Z. Phys. C34 (1987) 163.

A. L. S. Angelis *et al.*, Phys. Lett. B126 (1983) 132; Nucl. Phys. B244 (1984) 1; Nucl. Phys. B303 (1988) 569.

[23] Christian W. Fabjan and Norman McCubbin, *Physics at the CERN Intersecting Storage Rings (ISR) 1978–1983*, Phys. Rep. 403–404 (2004) 165–175.

[24] M. Banner *et al.*, Phys. Lett. B118 (1982) 203.

[25] P. Darriulat, Proceedings of the XVIIIth International Conference on High Energy Physics, Tbilisi, USSR, 1976, N. N. Bogolioubov *et al.* editors (JINR, Dubna, 1976); *Large transverse momentum hadronic processes,* Annu. Rev. Nucl. Part. Sci. 30 (1980) 159.

[26] G. Hanson *et al.*, Phys. Rev. Lett. 35 (1975) 1609.

[27] James G. Branson, *Gluon jets*, History of Original Ideas and Basic Discoveries in Particle Physics, Erice, Italy, 1994, H. B. Newman and T. Ypsilantis editors, NATO ASI series, B352 (Plenum, New York, 1996), p. 101.

[28] D. Drijard *et al.*, Phys. Lett. B81 (1979) 250 and B85 (1979) 452.

[29] M. Diakonou *et al.*, Phys. Lett. B87 (1979) 292.

[30] A. L. S. Angelis *et al.*, Phys. Lett. B94 (1980) 106.

[31] T. Ferbel and W. M. Molzon, Rev. Mod. Phys. 56 (1984) 181; L. F. Owens, Rev. Mod. Phys. 59 (1987) 485; P. Aurenche *et al.*, Nucl. Phys. B297 (1988) 661 and Eur. Phys. J. C9 (1999) 107.